

## 2023 European School on Magnetism

ESM 2023 will be held from 4 to 15 Sep 2023, in mixed format, both onsite in Madrid, Spain, and online. The topic is *Nanomagnetism for emerging technologies*. Activities consist of lectures (36h), question sessions (6h), practicals and tutorials (14h), team work (4h), access to a Library on Magnetism.

[Subscribe to the mailing list](#) to stay tuned. Request for participation is open from 1st March to 15th April 2023.



**Oxitronics, VdW and beyond.....**

Jacobo Santamaria

Universidad Complutense de Madrid

# Outline

- Interest of TM oxides. **GFMC**
- PART I. ferromagnetic superconducting proximity effect: **Long range Josephson effect.**
- PART II. 3d/5d oxide heterostructures. **Topological spin textures.**
- PART III. 2D freestanding oxides: **oxide twistrionics.**

Laboratory for materials and heterostructures for spintronics



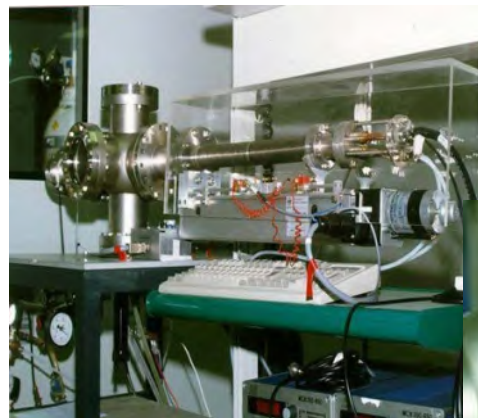
GFMC 

# What we can do

Oxide heterostructures with atomically sharp oxide interfaces .  
quantum matter, spintronics, magnetism superconductivity

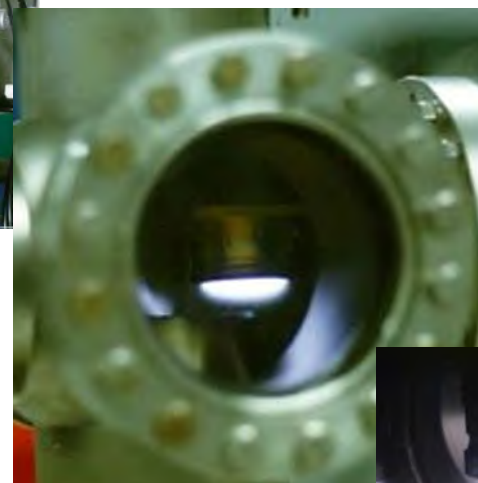


3- high pressure O sputtering system  
in a clean room environment

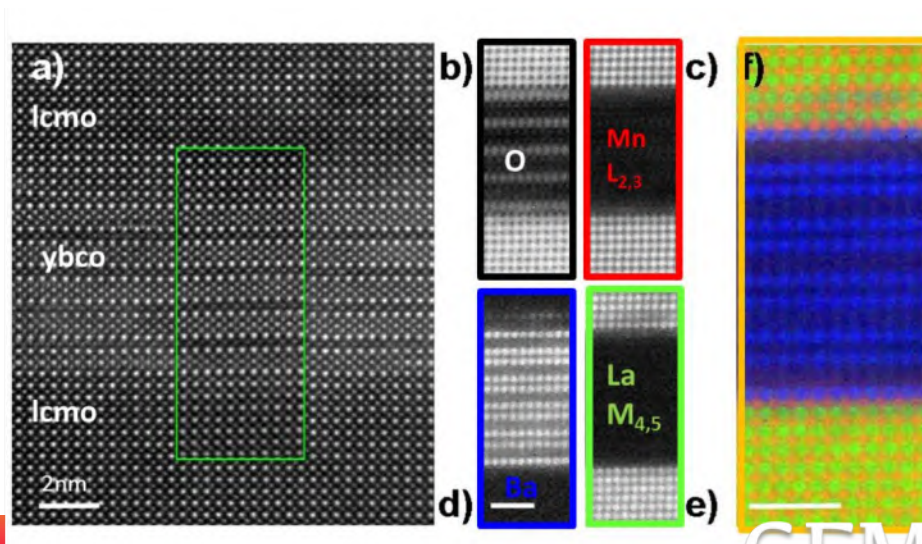


$T_s = 900 \text{ }^\circ\text{C}$

$P = 3 \text{ mbar oxygen plasma}$



State of the art HRTEM-EELS



Phys. Rev. Lett. **113**, 189902 (2014)

**Oxides have always been there....**



**But are they interesting??**

- L. de Broglie –  
Nature 112, 540 (1923).



- E. Schrodinger – 1925, ....



- Pauli exclusion Principle - 1925
- Fermi statistics - 1926
- Thomas-Fermi approximation – 1927
- Dirac equation – relativistic quantum mechanics - 1928





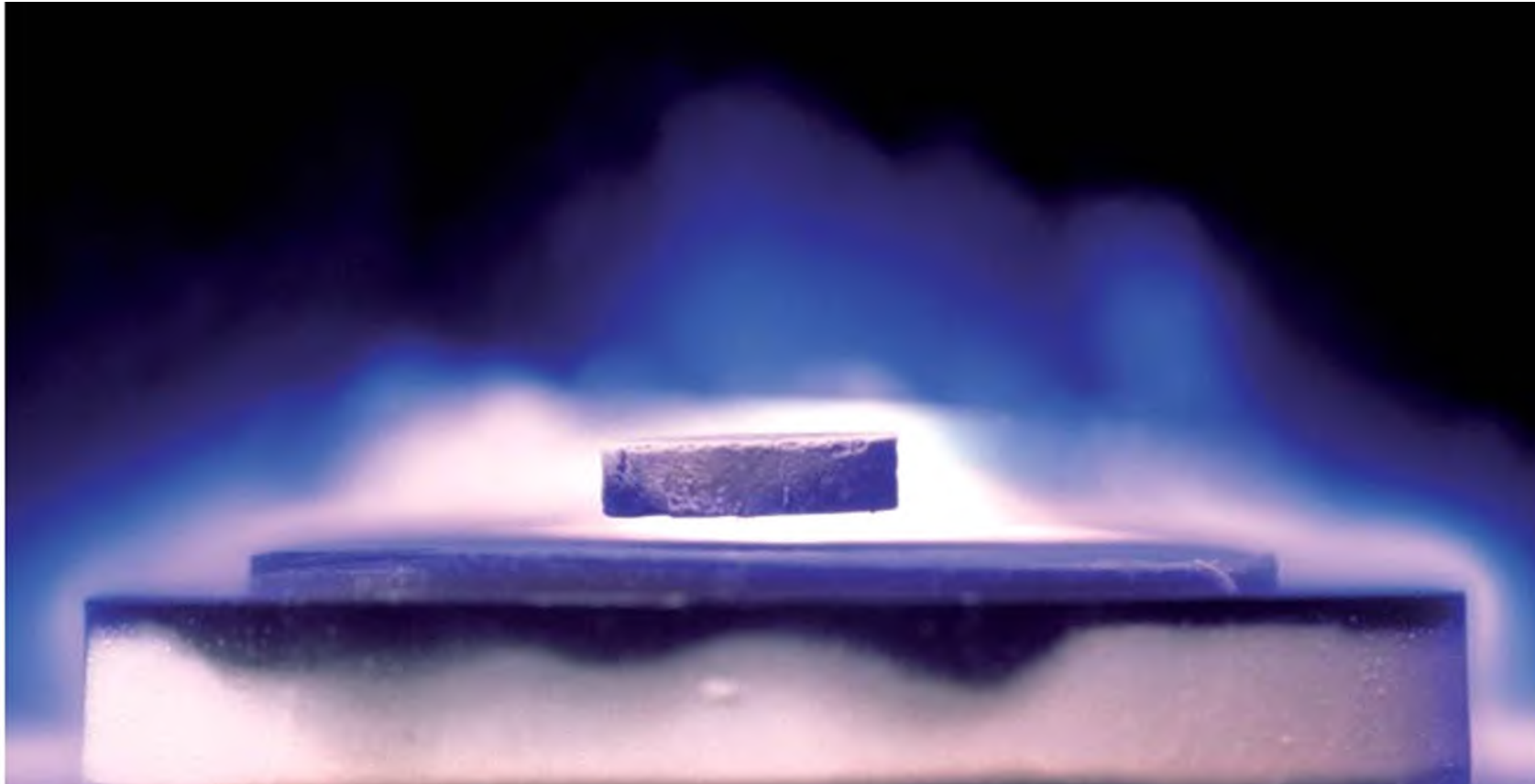
**1987 J. G. Bednorz and K. A. Mueller (High Tc)**

**2010 Andre Geim, Konstantin Novoselov (GRAPHENE)**

**2016 David J. Thouless, F. Duncan M. Haldane and J. Michael Kosterlitz  
"topological phases of matter".**

# Focus point 1.....

correlated electrons feel each other: **Tunability**



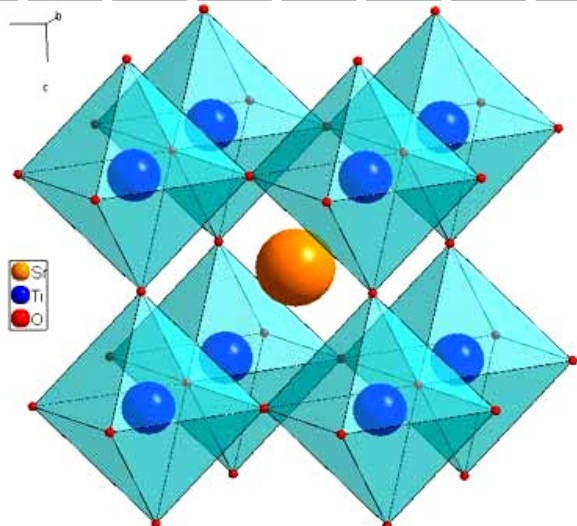
# 3d TRANSITION METAL OXIDES: correlated electrons

Los Alamos National Laboratory Chemistry Division

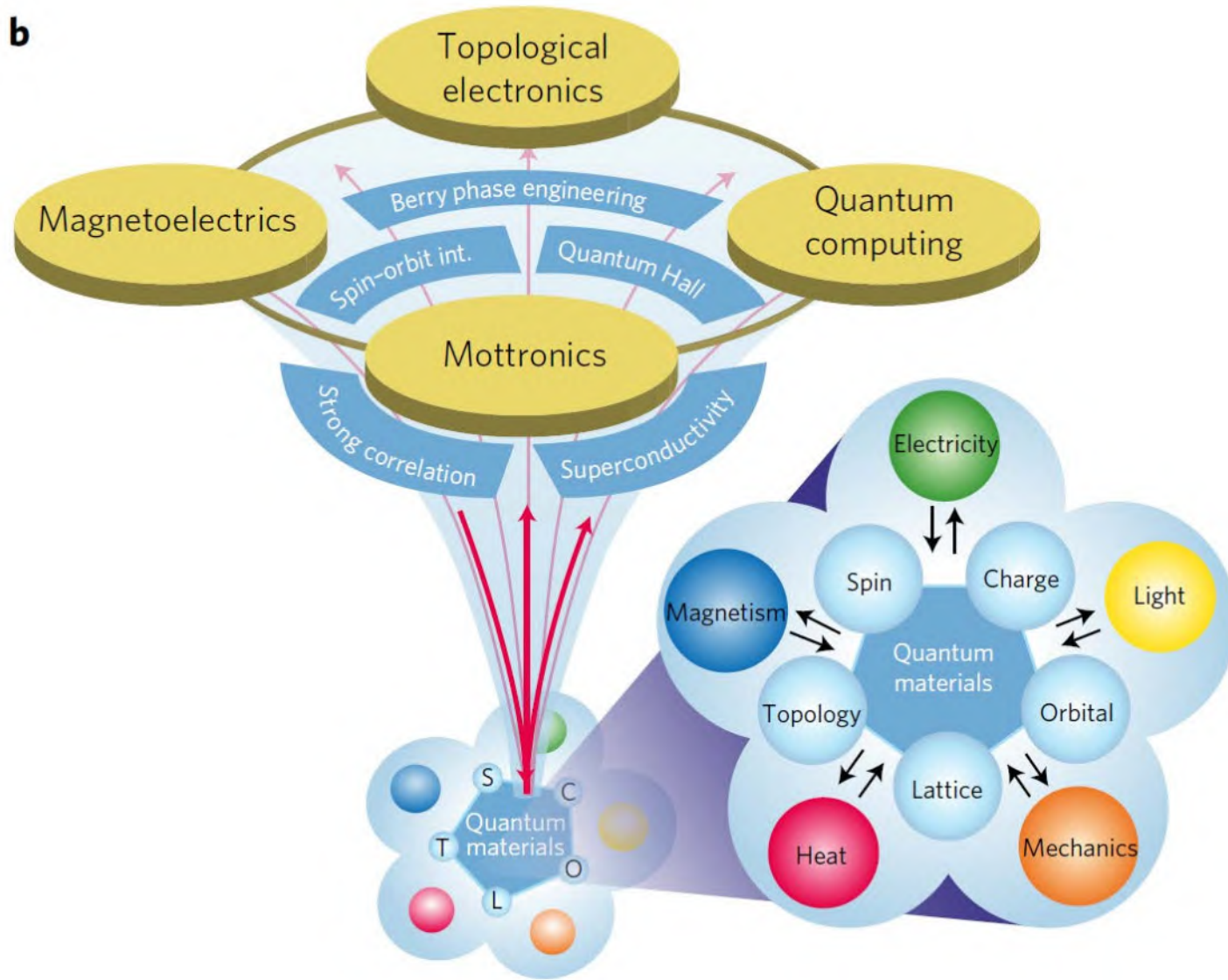
Periodic Table of the Elements

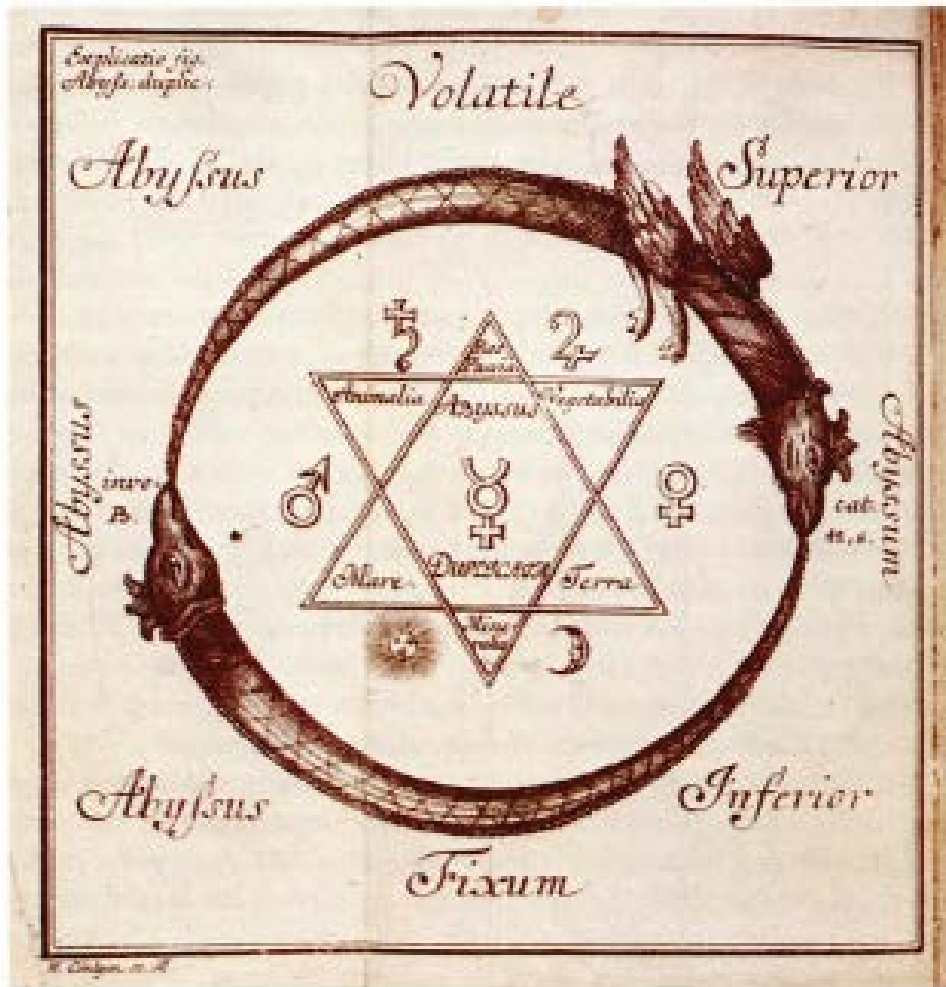
3d

1A 1 <b>H</b> hydrogen 1.008	2A 4 <b>Be</b> beryllium 9.012											3A 5 <b>B</b> boron 10.81	4A 6 <b>C</b> carbon 12.01	5A 7 <b>N</b> nitrogen 14.01	6A 8 <b>O</b> oxygen 16.00	7A 9 <b>F</b> fluorine 19.00	8A 2 <b>He</b> helium 4.003	
3 <b>Li</b> lithium 6.941	11 <b>Na</b> sodium 22.99	12 <b>Mg</b> magnesium 24.31	21 <b>Sc</b> scandium 44.96	22 <b>Ti</b> titanium 47.88	23 <b>V</b> vanadium 50.94	24 <b>Cr</b> chromium 52.00	25 <b>Mn</b> manganese 54.94	26 <b>Fe</b> iron 55.85	27 <b>Co</b> cobalt 58.93	28 <b>Ni</b> nickel 58.69	29 <b>Cu</b> copper 63.55	30 <b>Zn</b> zinc 65.39	31 <b>Ga</b> gallium 69.72	32 <b>Ge</b> germanium 72.58	33 <b>As</b> arsenic 74.92	34 <b>Se</b> selenium 78.96	35 <b>Br</b> bromine 79.90	36 <b>Kr</b> krypton 83.80
19 <b>K</b> potassium 39.10	37 <b>Rb</b> rubidium 85.47	38 <b>Sr</b> strontium 87.62	39 <b>Y</b> yttrium 88.91	40 <b>Zr</b> zirconium 91.22	41 <b>Nb</b> niobium 92.91	42 <b>Mo</b> molybdenum 95.94	43 <b>Tc</b> technetium (98)	44 <b>Ru</b> ruthenium 101.1	45 <b>Rh</b> rhodium 102.9	46 <b>Pd</b> palladium 106.4	47 <b>Ag</b> silver 107.9	48 <b>Cd</b> cadmium 112.4	49 <b>In</b> indium 114.8	50 <b>Sn</b> tin 118.7	51 <b>Sb</b> antimony 121.8	52 <b>Te</b> tellurium 127.6	53 <b>I</b> iodine 126.9	54 <b>Xe</b> xenon 131.3
55 <b>Cs</b> cesium 132.9	87 <b>Fr</b> francium (223)	56 <b>Ba</b> barium 137.3	57 <b>La*</b> lanthanum 138.9	72 <b>Hf</b> hafnium 178.5	73 <b>Ta</b> tantalum 180.9	74 <b>W</b> tungsten 183.9	75 <b>Re</b> rhenium 186.2	76 <b>Os</b> osmium 190.2	77 <b>Ir</b> iridium 190.2	78 <b>Pt</b> platinum 195.1	79 <b>Au</b> gold 197.0	80 <b>Hg</b> mercury 200.5	81 <b>Tl</b> thallium 204.4	82 <b>Pb</b> lead 207.2	83 <b>Bi</b> bismuth 208.9	84 <b>Po</b> polonium (209)	85 <b>At</b> astatine (210)	86 <b>Rn</b> radon (222)
		88 <b>Ra</b> radium (226)	89 <b>Ac~</b> actinium (227)	10 <b>R<sup>a</sup></b> rutherfordium (261)							1 <b>Lu</b> lutetium (175)	112 <b>Uub</b> unbinilium (277)		114 <b>Uuq</b> ununquadium (296)		116 <b>Uuh</b> ununhexium (298)		118 <b>Uuo</b> ununoctium (?)



**b**





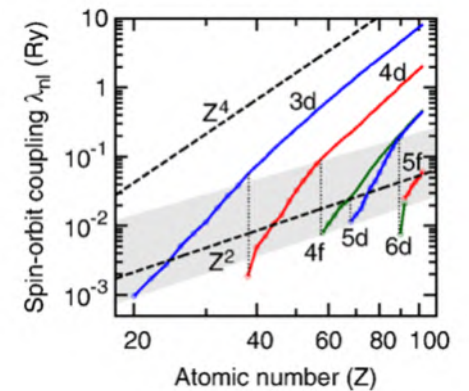
# Focus point 2.....



spin orbit int.: Topology **Robustness**

$$\mathcal{H}_{SO} = \frac{\xi}{\hbar} \hat{\sigma} (\nabla \phi \times \mathbf{p})$$

$$\mathbf{B} = -\frac{\mathbf{v} \times \mathbf{E}}{c^2}$$



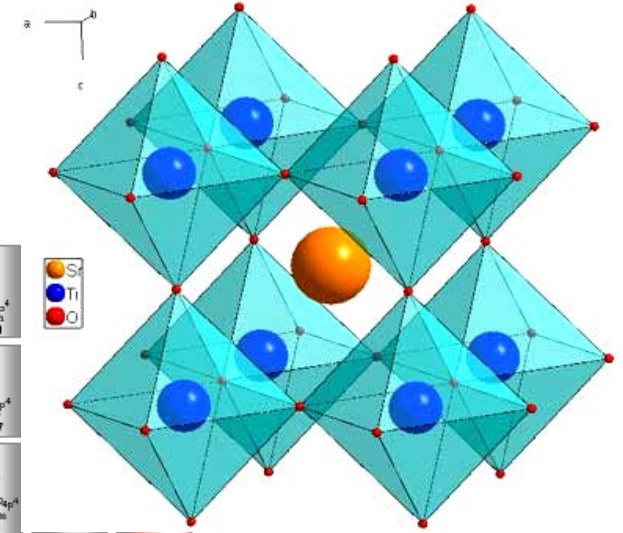
# 5d TRANSITION METAL OXIDES: strong spin orbit

Los Alamos National Laboratory Chemistry Division

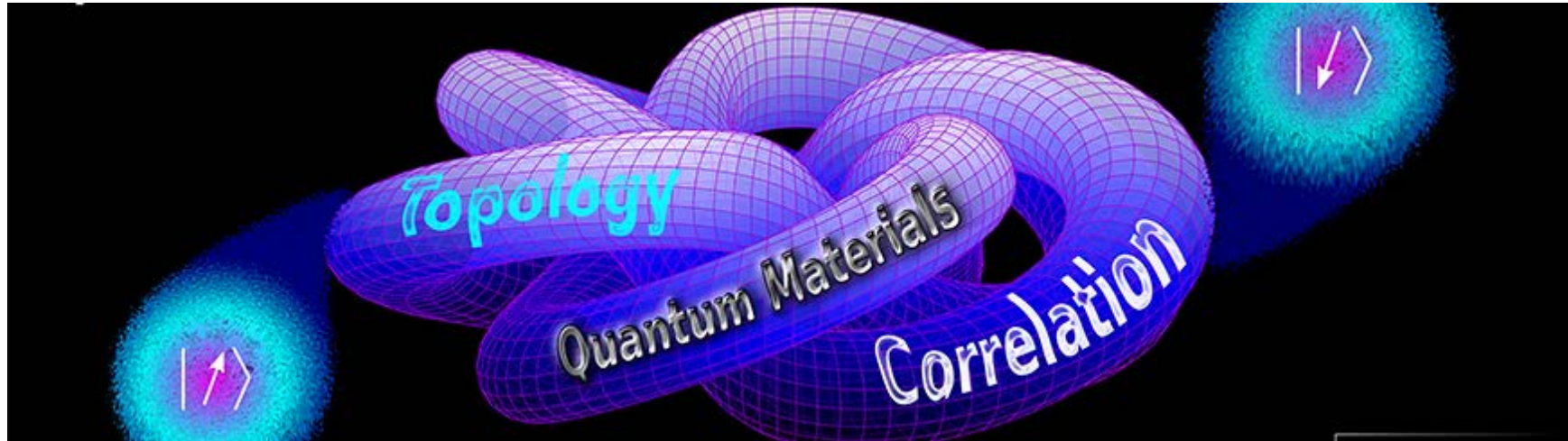
Periodic Table of the Elements

5d

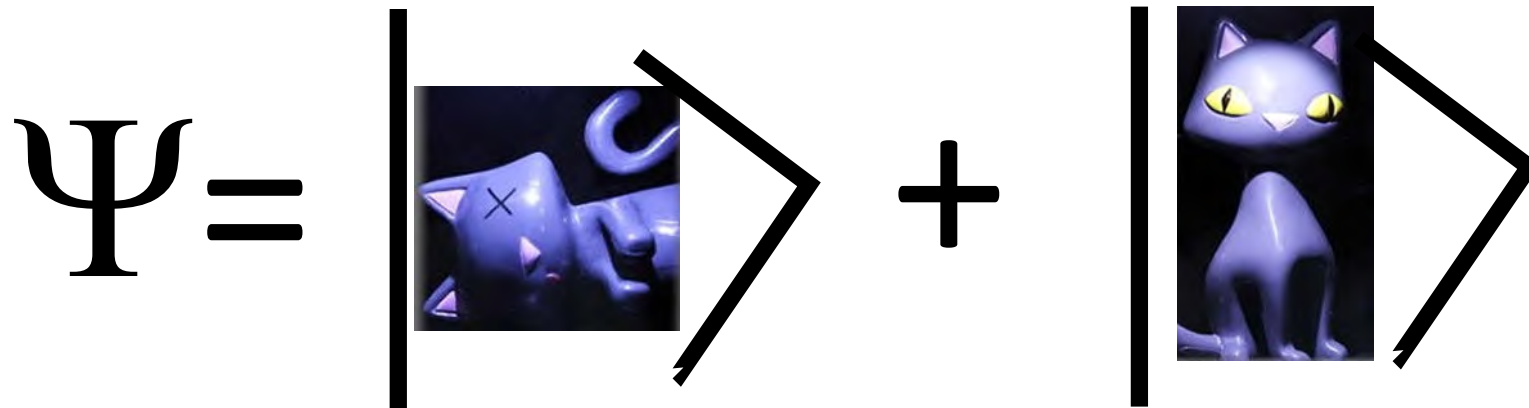
1A 1 <b>H</b> hydrogen 1.008	2A 4 <b>Be</b> beryllium 9.012											3A 5 <b>B</b> boron 10.81	4A 6 <b>C</b> carbon 12.01	5A 7 <b>N</b> nitrogen 14.01	6A 8 <b>O</b> oxygen 16.00																																								
3 <b>Li</b> lithium 6.941	11 <b>Na</b> sodium 22.99	19 <b>K</b> potassium 39.10	37 <b>Rb</b> rubidium 85.47	55 <b>Cs</b> cesium 132.9	87 <b>Fr</b> francium (223)	2A 12 <b>Mg</b> magnesium 24.31	20 <b>Ca</b> calcium 40.08	38 <b>Sr</b> strontium 87.62	56 <b>Ba</b> barium 137.3	88 <b>Ra</b> radium (226)	3B 21 <b>Sc</b> scandium 44.96	39 <b>Y</b> yttrium 88.91	4B 22 <b>Ti</b> titanium 47.88	40 <b>Zr</b> zirconium 91.22	57 <b>La*</b> lanthanum 138.9	89 <b>Ac~</b> actinium (227)	5B 23 <b>V</b> vanadium 50.94	41 <b>Nb</b> niobium 92.91	104 <b>Rf</b> rutherfordium (257)	6B 24 <b>Cr</b> chromium 52.00	42 <b>Mo</b> molybdenum 95.94	105 <b>Db</b> dubnium (260)	7B 25 <b>Mn</b> manganese 54.94	43 <b>Tc</b> technetium (98)	106 <b>Sg</b> seaborgium (263)	8B 26 <b>Fe</b> iron 55.85	44 <b>Ru</b> ruthenium 101.1	107 <b>Bh</b> bohrium (262)	9B 27 <b>Co</b> cobalt 58.93	45 <b>Rh</b> rhodium 102.9	108 <b>Hs</b> hassium (265)	10B 28 <b>Ni</b> nickel 58.69	46 <b>Pd</b> palladium 106.4	109 <b>Mt</b> meitnerium (266)	11B 29 <b>Cu</b> copper 63.55	47 <b>Ag</b> silver 107.9	110 <b>Ds</b> darmstadtium (271)	12B 30 <b>Zn</b> zinc 65.39	48 <b>Cd</b> cadmium 112.4	111 <b>Uuu</b> (272)	3A 13 <b>Al</b> aluminum 26.98	49 <b>In</b> indium 114.8	81 <b>Tl</b> thallium 204.4	5A 15 <b>P</b> phosphorus 30.97	51 <b>Sb</b> antimony 121.8	83 <b>Bi</b> bismuth 208.9	6A 16 <b>S</b> sulfur 32.07	52 <b>Te</b> tellurium 127.6	84 <b>Po</b> polonium (209)	7A 17 <b>Cl</b> chlorine 35.45	53 <b>I</b> iodine 126.9	85 <b>At</b> astatine (210)	8A 18 <b>Ar</b> argon 39.95	54 <b>Xe</b> xenon 131.3	86 <b>Rn</b> radon (222)



# Why do we care?.....



# ENTANGLEMENT: quantum state of a system expressed in terms of the states of its parts

$$\Psi = \left| \begin{array}{c} \text{cat with X} \end{array} \right\rangle + \left| \begin{array}{c} \text{cat with yellow eyes} \end{array} \right\rangle$$


- 1) Knowledge of the system does not imply knowledge of its parts
- 2) Trivial entanglement can be smoothly transformed in a product state. Independent parts.
- 3) Non trivial entanglement resulting from manybody effects driven by Coulomb interaction

# The Quantum Revolution



## Alain ASPECT

Professor at Institut d'Optique Graduate School and Ecole Polytechnique, France

Member of the French Academy of Science and Academy of Technologies

Member of several Science and Technology Academies

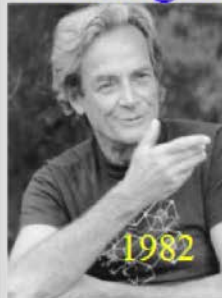
### Wave-particle duality: single particle interference



- A **particle** (an electron) also behaves as a **wave**
- A **wave** (light) can also behave as a **particle** (single photon effects)

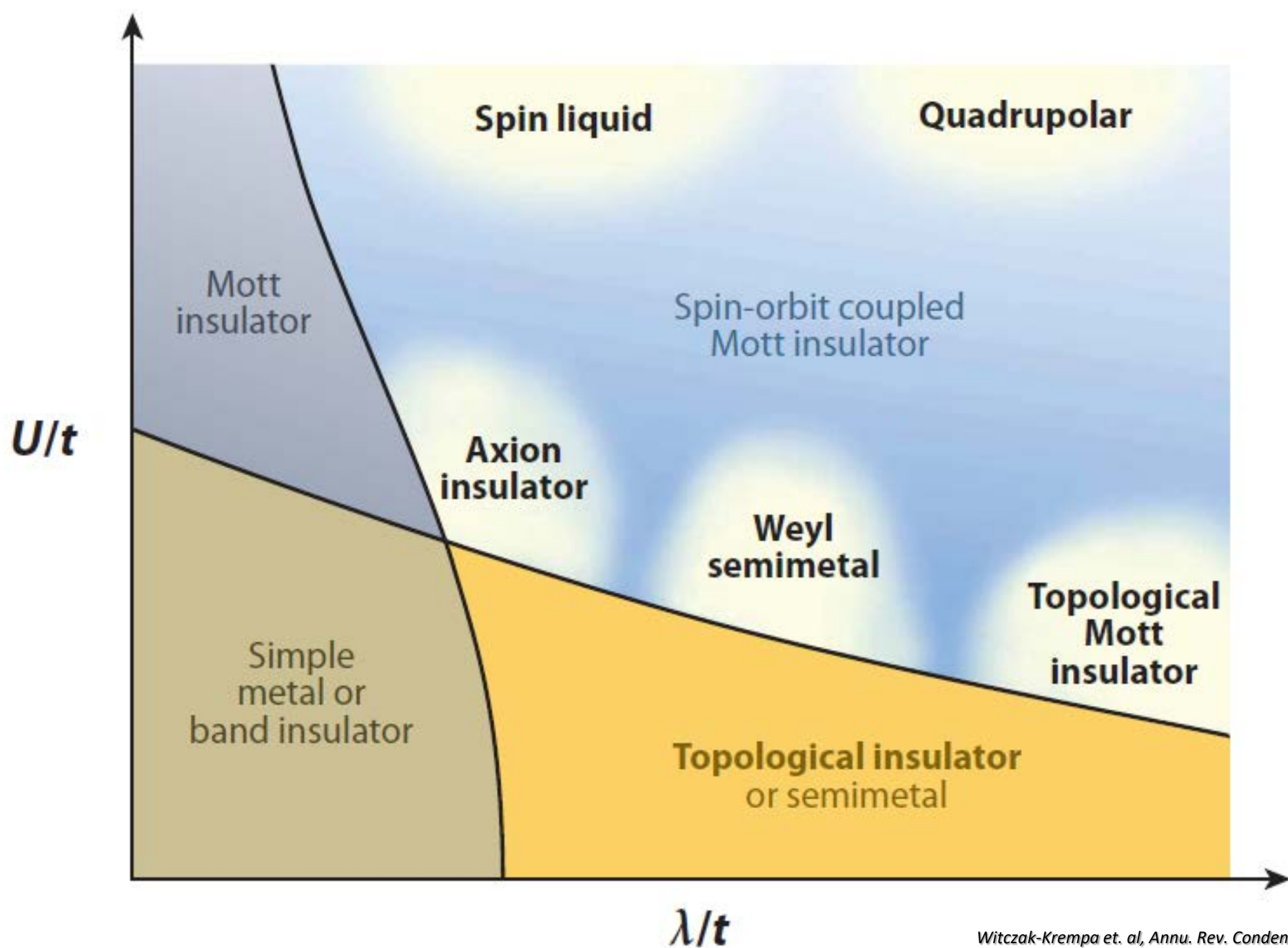
Classical models, (local realism *à la* Einstein) in ordinary space-time

### Entanglement: interference between two-particles amplitudes

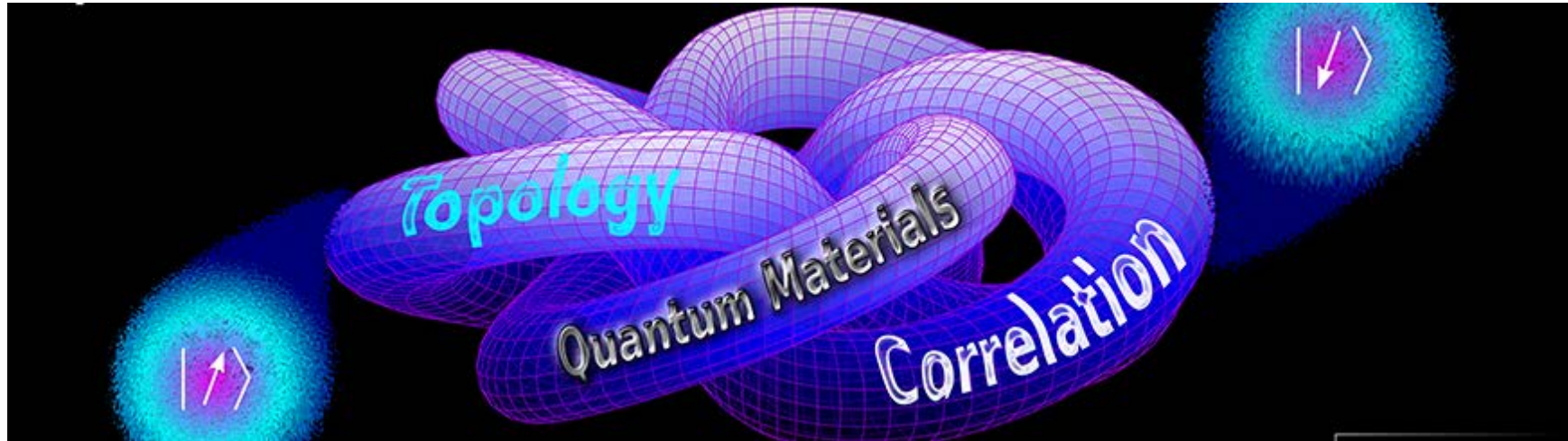


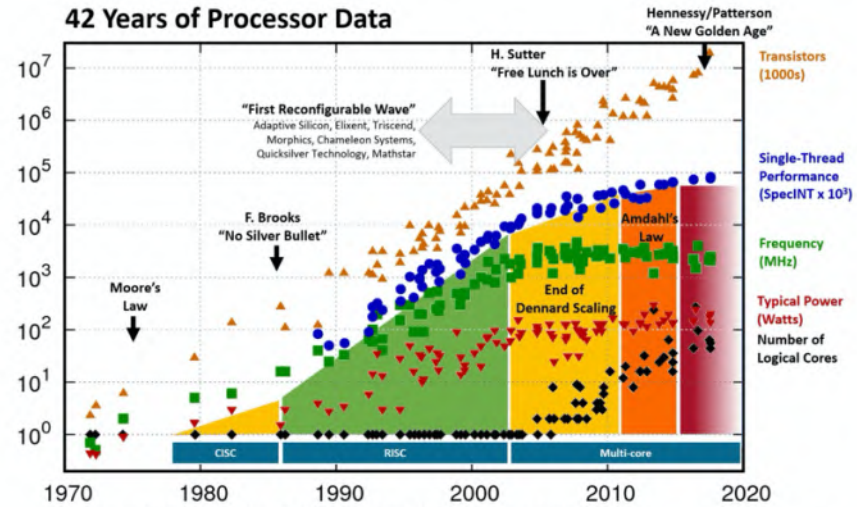
- Hanbury Brown-Twiss effect for particles
- **Hong-Ou-Mandel effect**
- **Bell's inequalities violation**

Interference in Hilbert space. No classical model in ordinary space-time

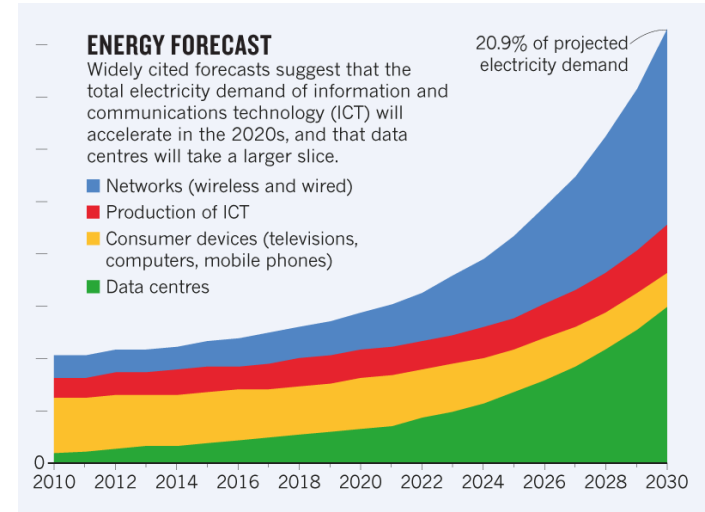


# Why do we care?.....





Hennessy and Patterson, Turing Lecture 2018, overlaid over "42 Years of Processors Data"  
<https://www.karlsruhp.net/2018/02/42-years-of-microprocessor-trend-data/>; "First Wave" added by Les Wilson, Frank Schirrmeyer  
 Original data up to the year 2010 collected and plotted by M. Horowitz, F. Labonte, O. Shacham, K. Olukotun, L. Hammond, and C. Batten  
 New plot and data collected for 2010-2017 by K. Rupp



N. Jones, Nature 561, 163 (2018)



Nature 24 October 2019



# Focus point 3.....

## “graphene-like oxides”, we call them oxide-membranes

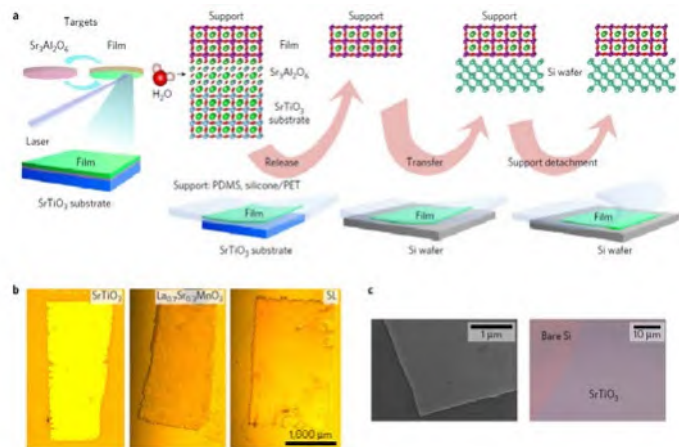
nature  
materials

LETTERS

PUBLISHED ONLINE: 12 SEPTEMBER 2016 | DOI: 10.1038/NMAT4749

### Synthesis of freestanding single-crystal perovskite films and heterostructures by etching of sacrificial water-soluble layers

Di Lu<sup>1,2</sup>, David J. Baek<sup>3</sup>, Seung Sae Hong<sup>2,4</sup>, Lena F. Kourkoutis<sup>5,6</sup>, Yasuyuki Hikita<sup>2\*</sup> and Harold Y. Hwang<sup>2,4\*</sup>

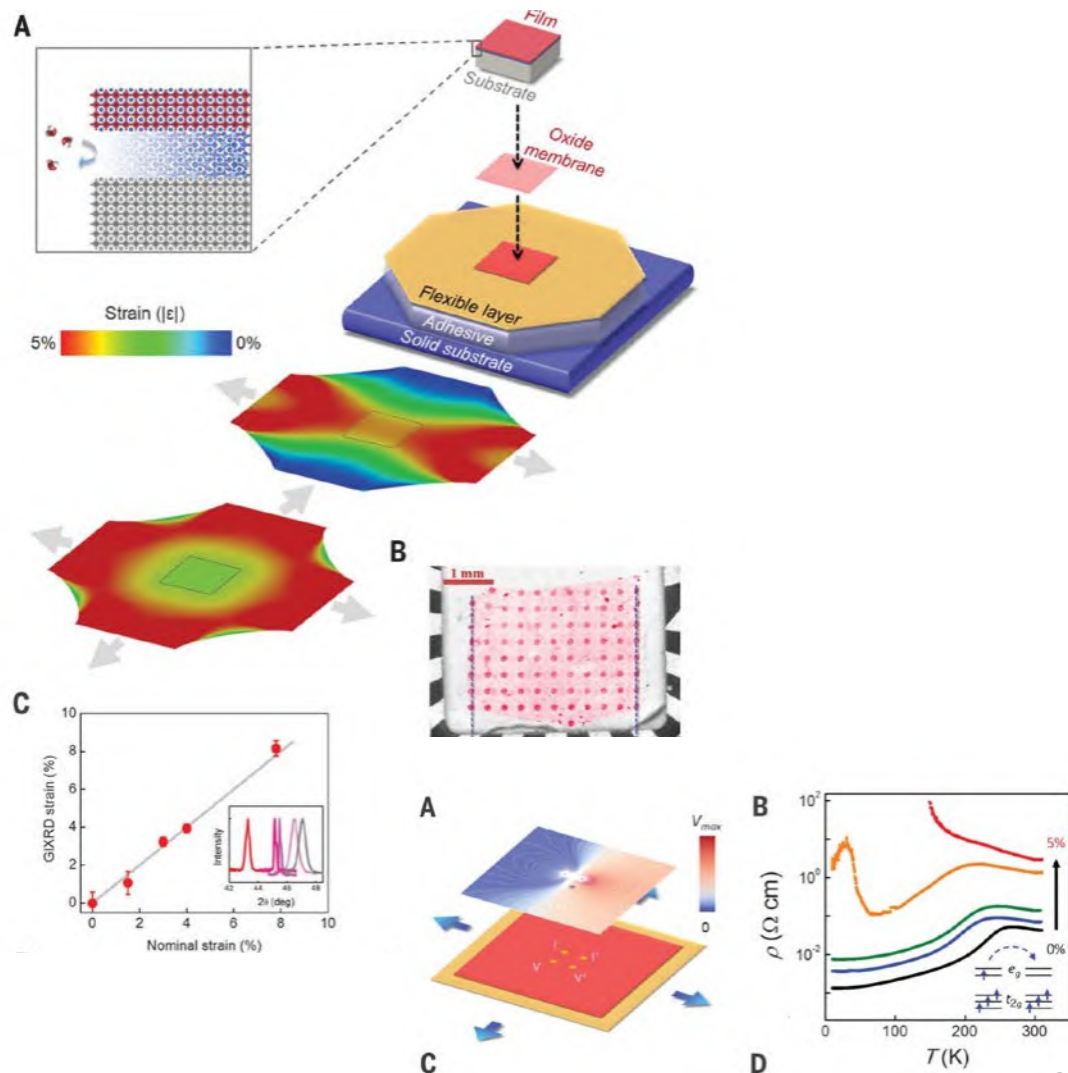


Lu et al. Nature Mater 15, 1255 (2016).

COMPLEX OXIDES

### Extreme tensile strain states in $\text{La}_{0.7}\text{Ca}_{0.3}\text{MnO}_3$ membranes

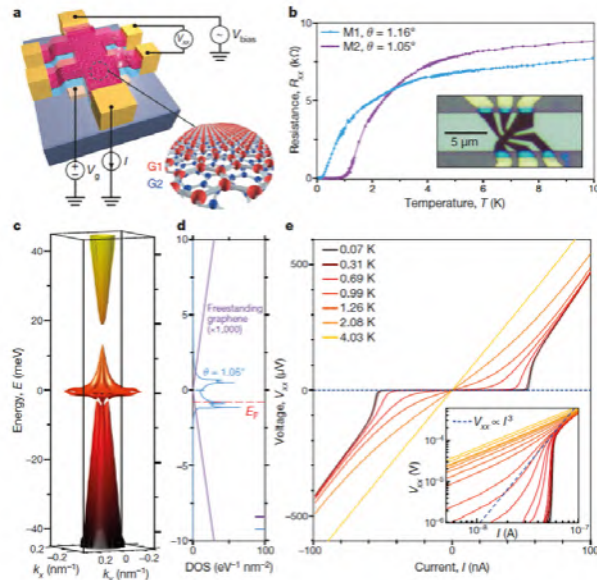
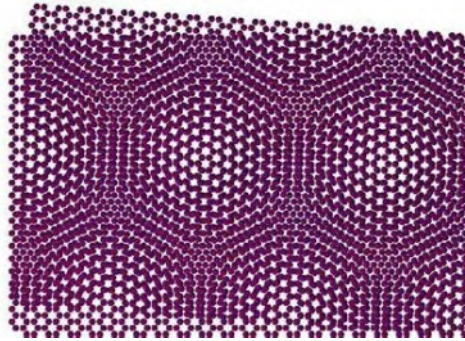
Seung Sae Hong<sup>1,2,3\*</sup>, Mingqiang Gu<sup>4,5</sup>, Manish Verma<sup>6</sup>, Varun Harbola<sup>2,7</sup>, Bai Yang Wang<sup>2,7</sup>, Di Lu<sup>2,4,7</sup>, Arturas Vailionis<sup>8,9</sup>, Yasuyuki Hikita<sup>2</sup>, Rossitza Pentcheva<sup>6</sup>, James M. Rondinelli<sup>4</sup>, Harold Y. Hwang<sup>1,2</sup>



Lu et al. Science 368, 71 (2020).

# Unconventional superconductivity in magic-angle graphene superlattices

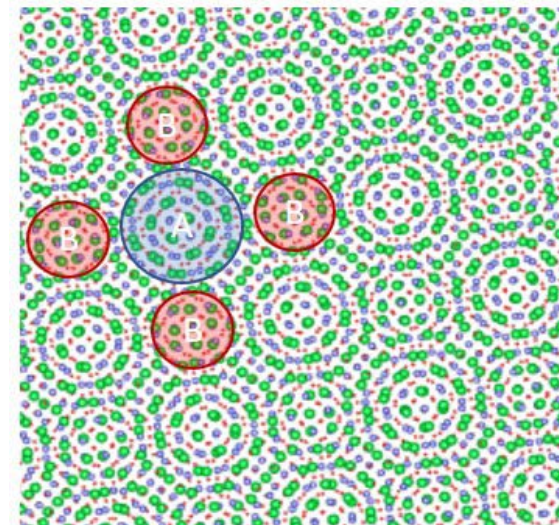
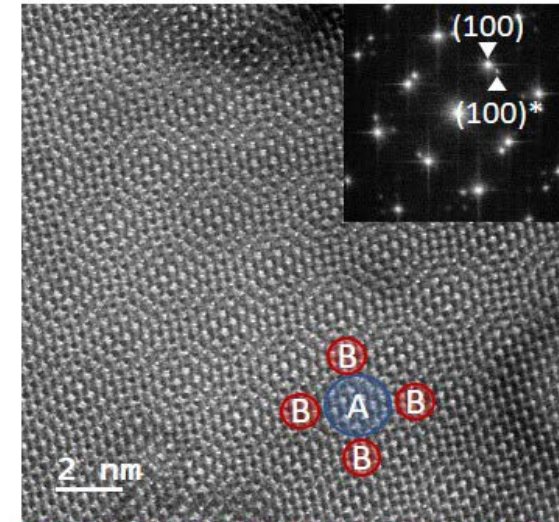
Yuan Cao<sup>1</sup>, Valla Fatemi<sup>1</sup>, Shiang Fang<sup>2</sup>, Kenji Watanabe<sup>3</sup>, Takashi Taniguchi<sup>3</sup>, Efthimos Kaxiras<sup>2,4</sup> & Pablo Jarillo-Herrero<sup>1</sup>



Y. Cao, Nature 556, 43 (2018).

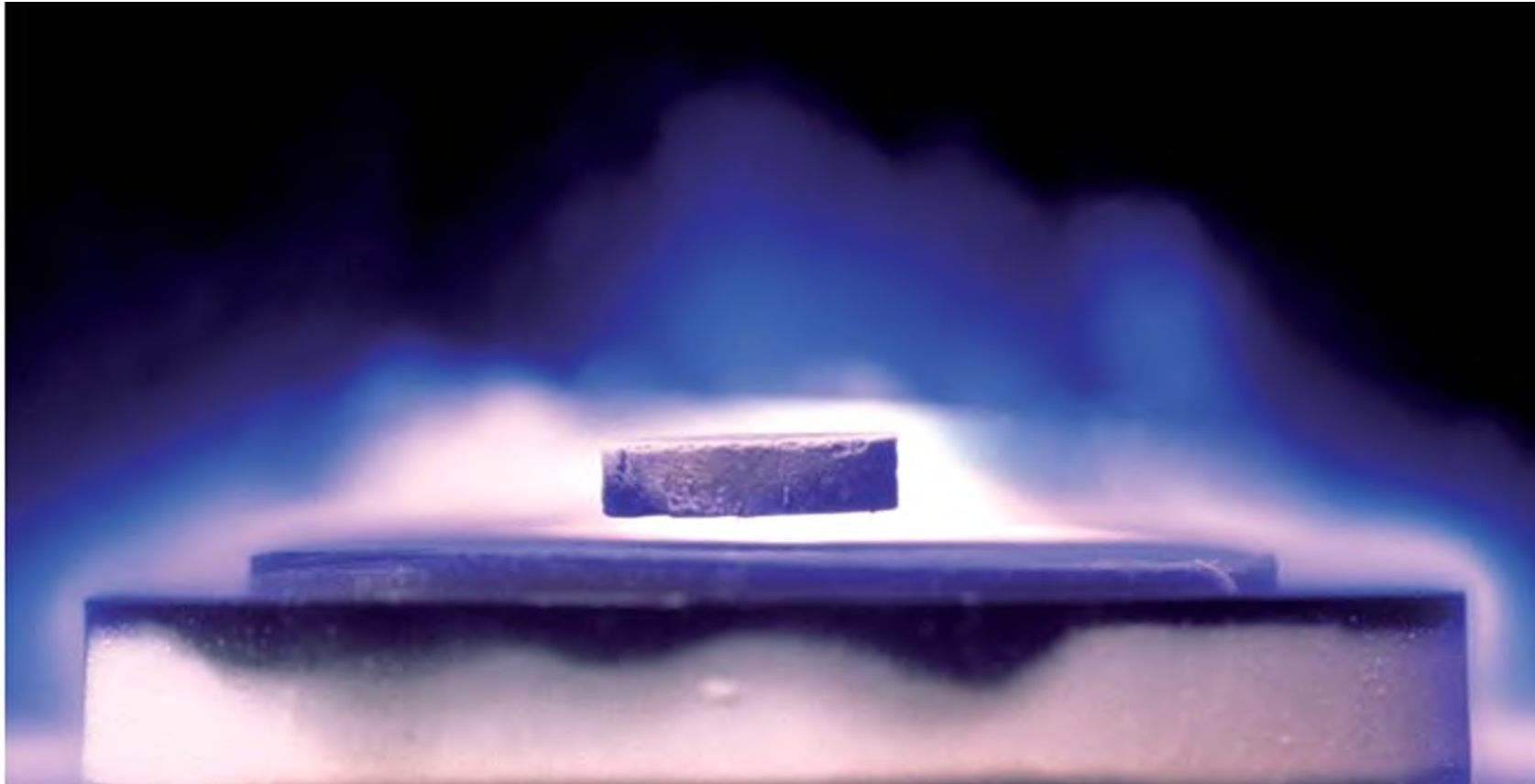
# We aim at ...oxide twistrionics

Freestanding BaTiO<sub>3</sub> twisted bilayers .



# Focus point 1.....

correlated electrons feel each other: **Tunability**

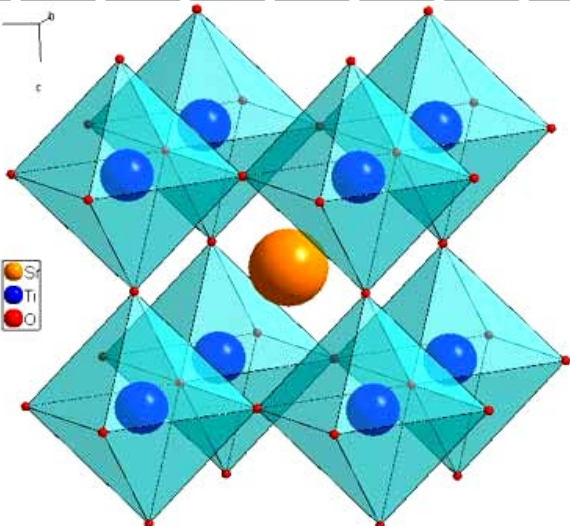


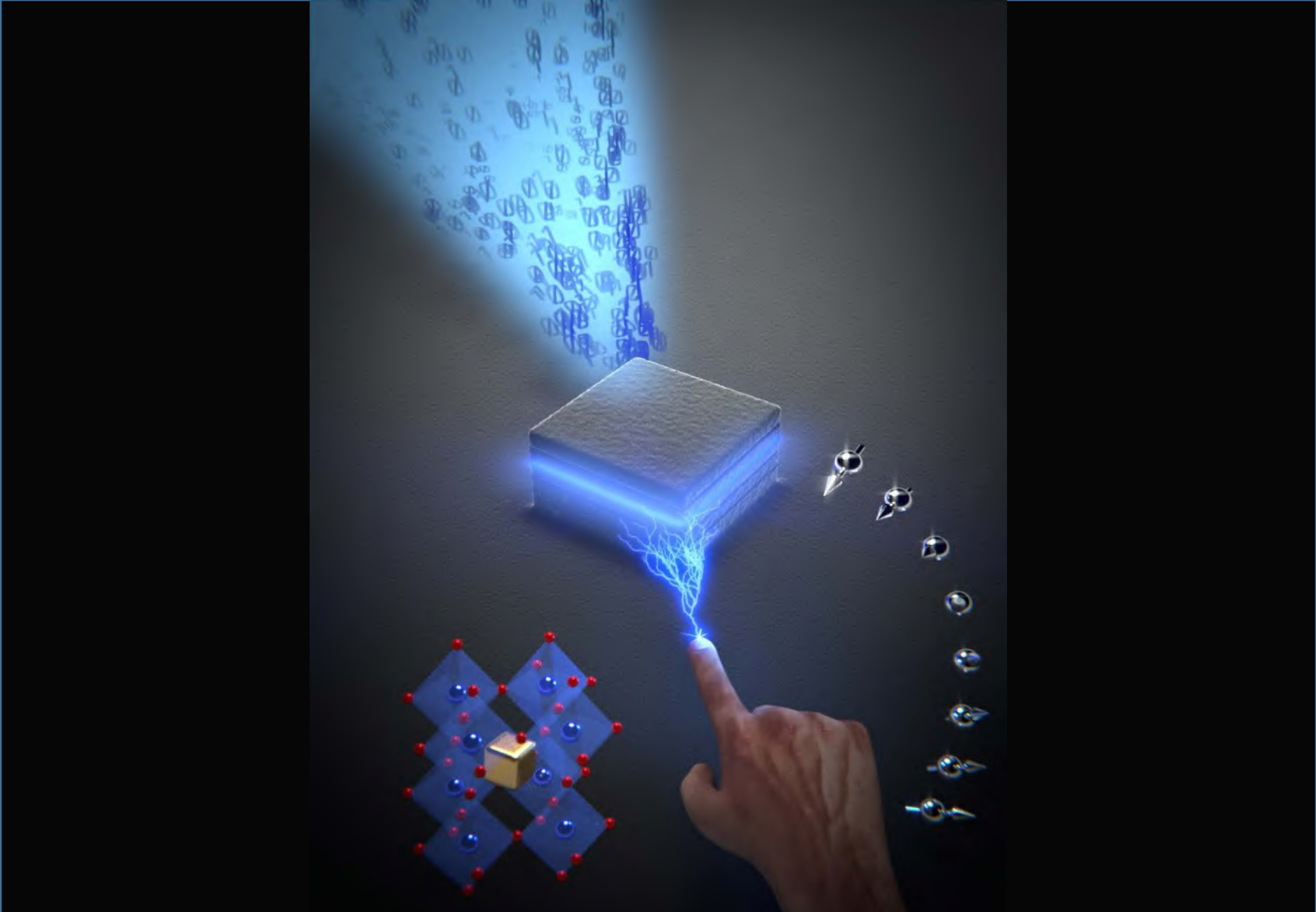
# 3d TRANSITION METAL OXIDES: correlated electrons

Los Alamos National Laboratory Chemistry Division

Periodic Table of the Elements

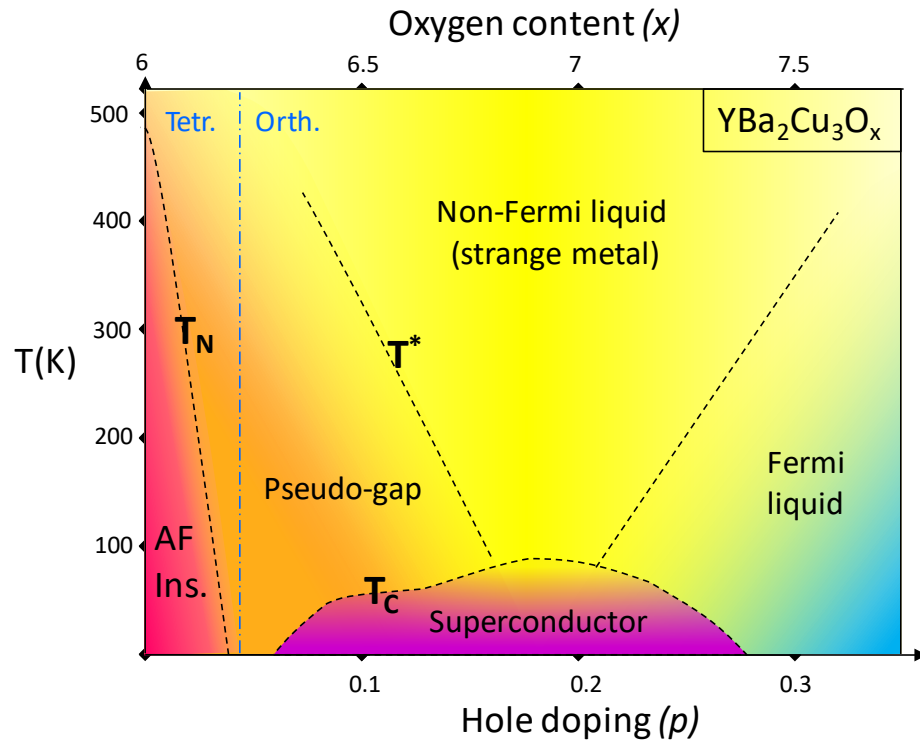
3d

1A 1 <b>H</b> hydrogen 1.008	2A 4 <b>Be</b> beryllium 9.012											3A 5 <b>B</b> boron 10.81	4A 6 <b>C</b> carbon 12.01	5A 7 <b>N</b> nitrogen 14.01	6A 8 <b>O</b> oxygen 16.00	7A 9 <b>F</b> fluorine 19.00	8A 2 <b>He</b> helium 4.003	
3 <b>Li</b> lithium 6.941	11 <b>Na</b> sodium 22.99	12 <b>Mg</b> magnesium 24.31	21 <b>Sc</b> scandium 44.96	22 <b>Ti</b> titanium 47.88	23 <b>V</b> vanadium 50.94	24 <b>Cr</b> chromium 52.00	25 <b>Mn</b> manganese 54.94	26 <b>Fe</b> iron 55.85	27 <b>Co</b> cobalt 58.93	28 <b>Ni</b> nickel 58.69	29 <b>Cu</b> copper 63.55	30 <b>Zn</b> zinc 65.39	31 <b>Ga</b> gallium 69.72	32 <b>Ge</b> germanium 72.58	33 <b>As</b> arsenic 74.92	34 <b>Se</b> selenium 78.96	35 <b>Br</b> bromine 79.90	36 <b>Kr</b> krypton 83.80
19 <b>K</b> potassium 39.10	37 <b>Rb</b> rubidium 85.47	38 <b>Sr</b> strontium 87.62	39 <b>Y</b> yttrium 88.91	40 <b>Zr</b> zirconium 91.22	41 <b>Nb</b> niobium 92.91	42 <b>Mo</b> molybdenum 95.94	43 <b>Tc</b> technetium (98)	44 <b>Ru</b> ruthenium 101.1	45 <b>Rh</b> rhodium 102.9	46 <b>Pd</b> palladium 106.4	47 <b>Ag</b> silver 107.9	48 <b>Cd</b> cadmium 112.4	49 <b>In</b> indium 114.8	50 <b>Sn</b> tin 118.7	51 <b>Sb</b> antimony 121.8	52 <b>Te</b> tellurium 127.6	53 <b>I</b> iodine 126.9	54 <b>Xe</b> xenon 131.3
55 <b>Cs</b> cesium 132.9	87 <b>Fr</b> francium (223)	56 <b>Ba</b> barium 137.3	57 <b>La*</b> lanthanum 138.9	72 <b>Hf</b> hafnium 178.5	73 <b>Ta</b> tantalum 180.9	74 <b>W</b> tungsten 183.9	75 <b>Re</b> rhenium 186.2	76 <b>Os</b> osmium 190.2	77 <b>Ir</b> iridium 190.2	78 <b>Pt</b> platinum 195.1	79 <b>Au</b> gold 197.0	80 <b>Hg</b> mercury 200.5	81 <b>Tl</b> thallium 204.4	82 <b>Pb</b> lead 207.2	83 <b>Bi</b> bismuth 208.9	84 <b>Po</b> polonium (209)	85 <b>At</b> astatine (210)	86 <b>Rn</b> radon (222)
		88 <b>Ra</b> radium (226)	89 <b>Ac~</b> actinium (227)	10 <b>R<sup>a</sup></b> rutherfordium (25)								111 <b>Rg</b> roentgenium (272)	112 <b>Uub</b> unbinilium (277)	114 <b>Uuq</b> ununquadium (296)	116 <b>Uuh</b> ununhexium (298)	118 <b>Uuo</b> ununoctium (?)		

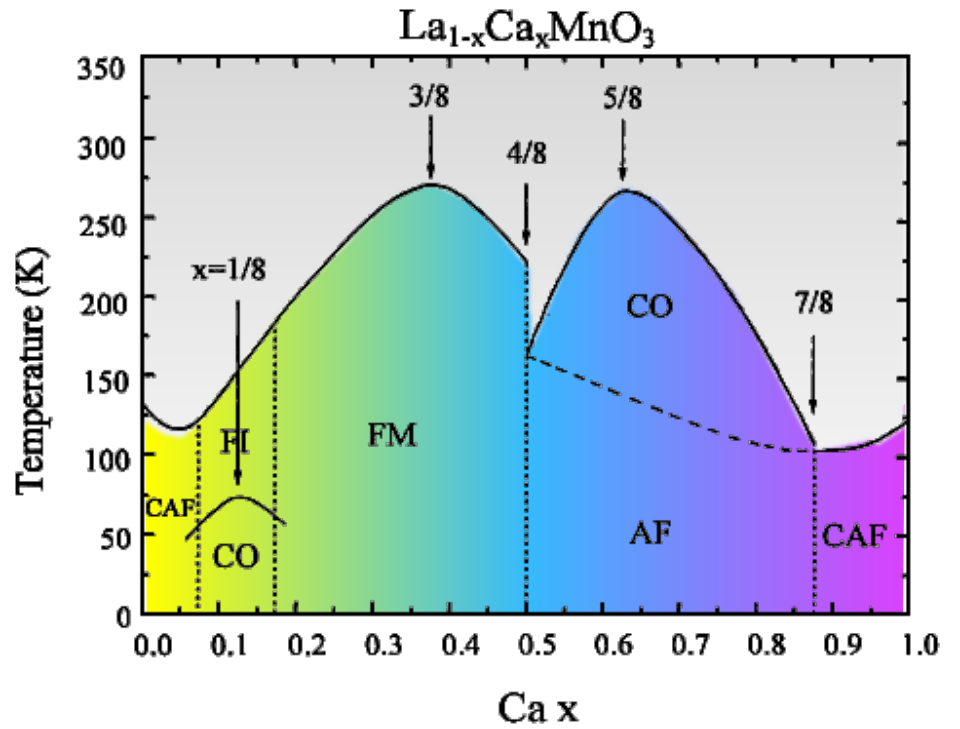


**The interface is the device**

## Different ground states. Complex phase diagrams

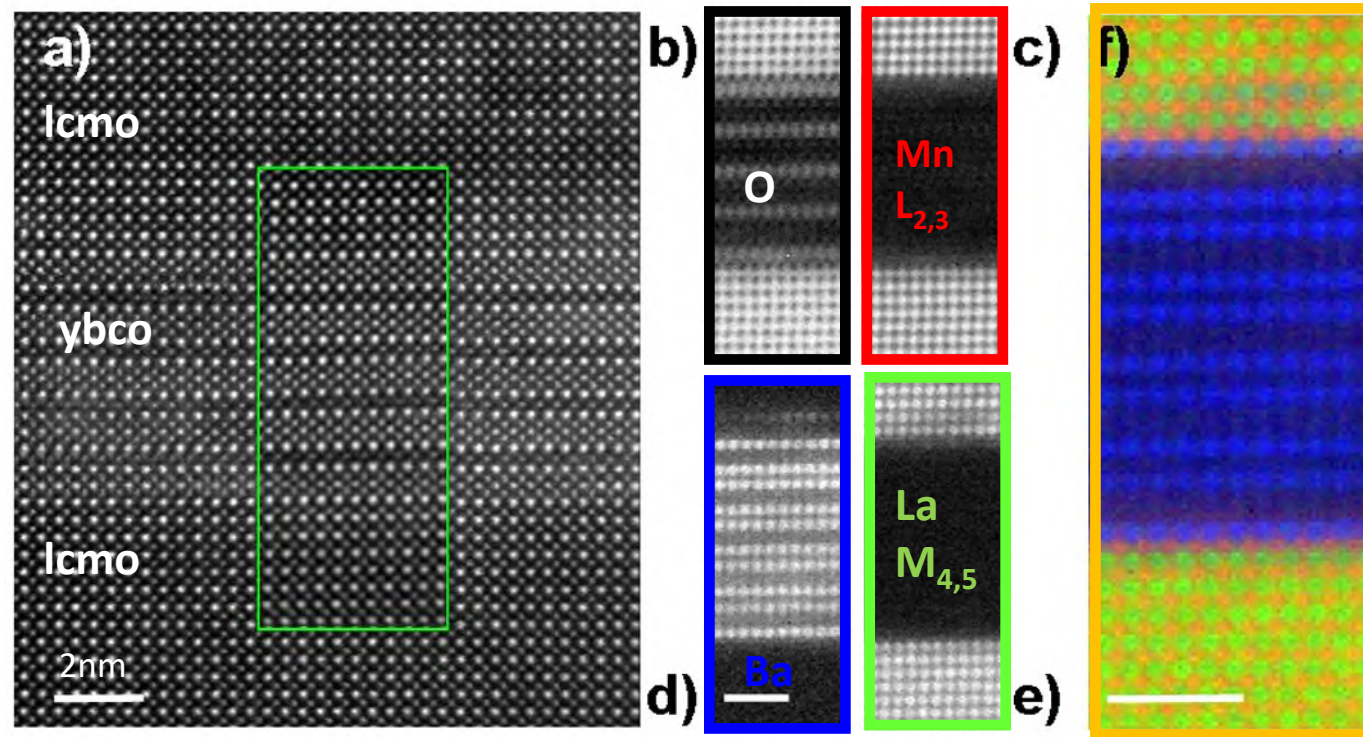


cuprates



manganites

# [La<sub>0.7</sub>Ca<sub>0.3</sub>MnO<sub>3</sub> / YBa<sub>2</sub>Cu<sub>3</sub>O<sub>7</sub>] Interface



Phys. Rev. Lett. **113**, 189902 (2014)

# Thanks to collaborators

• **D. Sanchez-Manzano, F. Cuellar, V. Rouco, G. Orfila, M. Rocci \***, **J. Garcia-Barriocanal#**, **F. Gallego, J. Tornos, A. Rivera, Z. Sefrioui, C. Leon**, (*GFMC-U. Complutense de Madrid*)



• **M. Cabero, J. Gonzalez-Calbet** (*CNME Luis Bru. U. Complutense de Madrid*)

• **F. Mompean, M. Garcia-Hernandez** (*Instituto de Ciencia de Materiales ICMM- CSIC*)



• **S. Mesoraca, X. Palermo, A. Balan, A. Sander, J. Villegas**,  
*Unité Mixte de Physique CNRS/Thales*,



• **Cheryl Feuillet-Palma, N. Bergeal, J. Lesueur**, *Laboratoire de Physique et d'Etude des Matériaux, CNRS, ESPCI Paris, PSL Research University*



• **A. Buzdin**. *Université Bordeaux, CNRS, LOMA, UMR 5798, F-33405 Talence, France*



• **L. Marcano, S. Valencia**, *Helmholtz-Zentrum Berlin für Materialien und Energie, Albert-Einstein-Strasse 15, D-12489, Berlin, Germany*



# In this talk.....

- We examine the **FM/SC** proximity effect in **cuprate/manganite** planar nanostructures.
- We demonstrate an **extremely long range (ONE MICRON)** Josephson effect across a HM ferromagnet

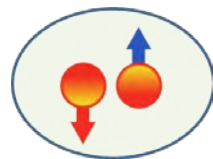
Orbital effect

$$H_o = \frac{1}{2m} (p - qA)^2$$

Ginzburg V L 1957 Ferromagnetic superconductors *Sov Phys.—JETP* **4** **153** (*Engl. transl.*)

Superconductivity in Gd

Exchange effect



$$H_s = \varepsilon(p) - J\sigma$$

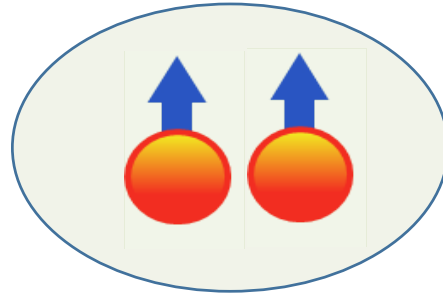
$$B_{eff} = \frac{J}{\mu}$$

Matthias B T, Suhl H and Corenzwitz C 1958 Spin exchange in superconductors  
*Phys. Rev. Lett.* **1** **92–4**

Effect of Gd impurities on La superconductivity

Clogston A M 1962 Upper limit for the critical field in hard superconductors  
*Phys. Rev. Lett.* **9** **266–7**

# Equal spin TRIPLETS



Aoki, D. & Jaques Flouquet. Ferromagnetism and Superconductivity in Uranium Compounds. *J. Appl. Phys.* **81**, 1–11 (2012).

## Boundary Effects in Superconductors

P. G. DE GENNES

*Faculté des Sciences, Orsay (S & O) France*

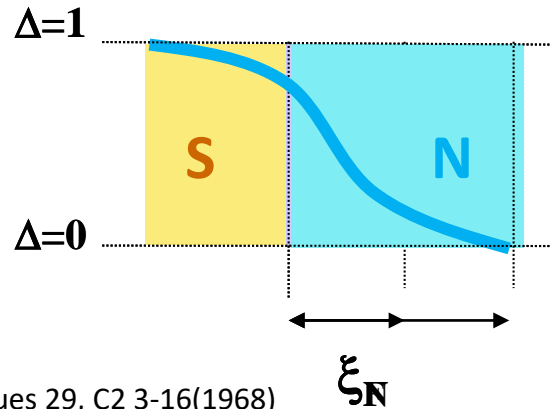
P. G. De Gennes Rev. Mod Phys, 36, 225 (1964)

JOURNAL DE PHYSIQUE

*Colloque C 2, supplément au n° 2-3, Tome 29, Février-Mars 1968, page C 2 - 3*

### THE PROXIMITY EFFECT BETWEEN SUPERCONDUCTING AND NORMAL THIN FILMS IN ZERO FIELD

JOHN CLARKE  
Cavendish Laboratory, Cambridge, England



$$\xi_N = \left( \frac{\hbar D}{2\pi k_B T} \right)^{1/2}$$

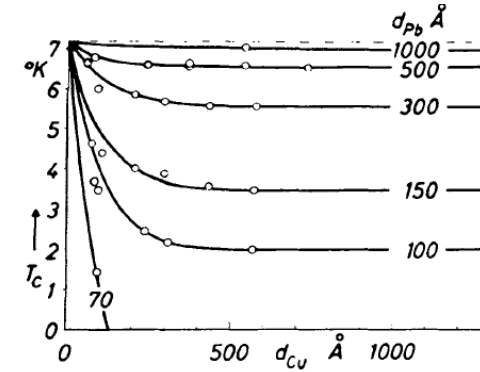


FIG. 2. — Transition temperature ( $T_c$ ) of Pb/Cu sandwiches as a function of Cu thickness ( $d_{Cu}$ ) for various thicknesses of Pb. (Reproduced from Hilsch et al. [11].)

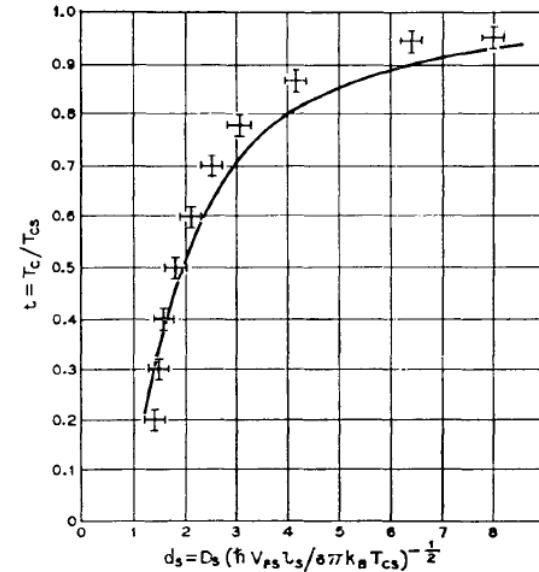
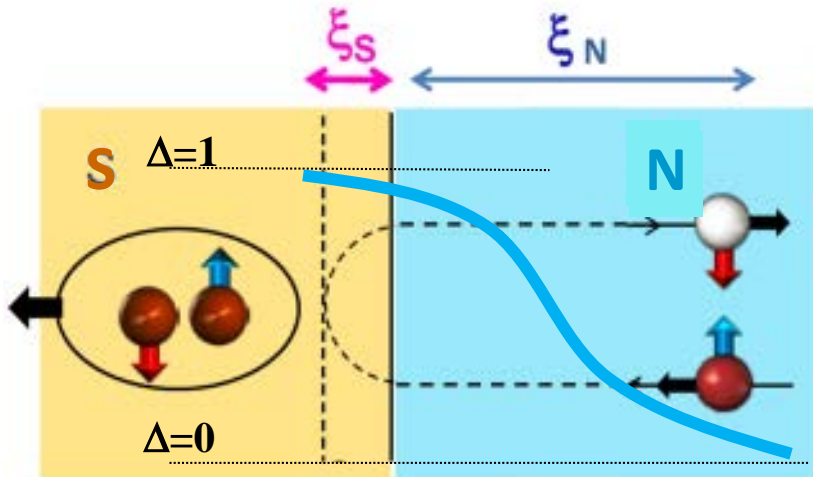


FIG. 4. — Reduced transition temperature ( $t$ ) of Pb/Cu sandwiches as a function of reduced lead thickness ( $d_s$ ) as predicted by the Werthamer theory (solid curve). Data points are from Hilsch's data [9, 11]. (Reproduced from Werthamer [69].)

N. R. Werthamer, Phys. Rev.  
132, 2440 (1963)

# ANDREEV REFLECTION AT N/S and F/S INTERFACE

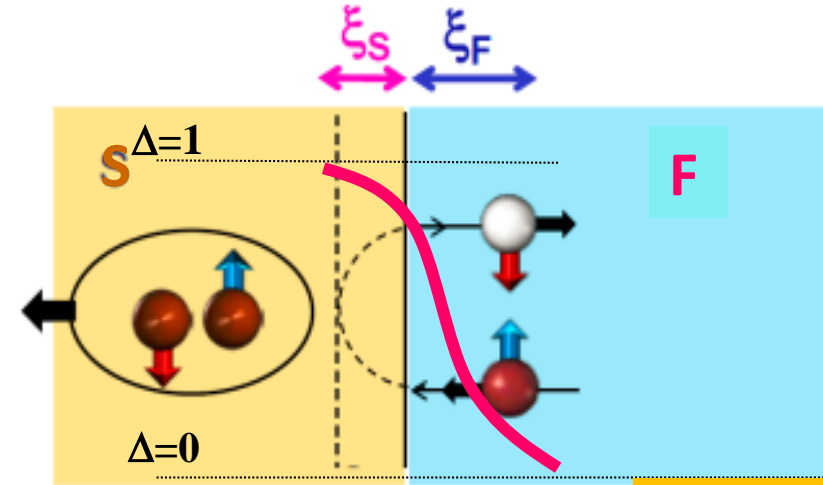


Sketch courtesy of J. Villegas

$$\xi_N = \left( \frac{\hbar D}{2\pi k_B T} \right)^{1/2}$$

Andreev A F 1964 *Sov. Phys.—JETP* **19** 1228–3

De Gennes P G and Saint-James D 1963 *Phys. Lett.* **4** 151–2

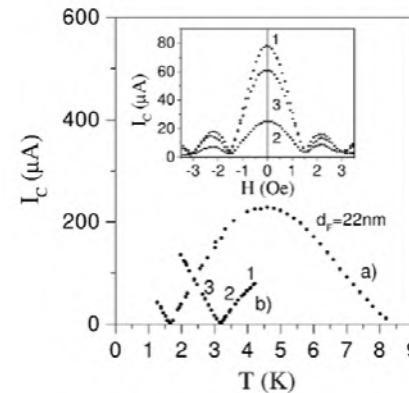


$$\xi_N = \left( \frac{\hbar D}{J} \right)^{1/2}$$

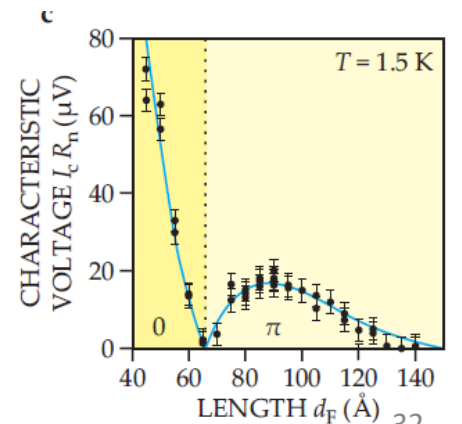
$$\langle \Psi | = \frac{1}{\sqrt{2}} [ \langle \uparrow \downarrow | e^{iQx} - \langle \downarrow \uparrow | e^{-iQx} ] =$$

$$= \frac{1}{\sqrt{2}} [ \langle \uparrow \downarrow | - \langle \downarrow \uparrow | ] \cos Qx + i \frac{1}{\sqrt{2}} [ \langle \uparrow \downarrow | + \langle \downarrow \uparrow | ] \sin Qx$$

Spin mixing



PRL 86, 2428 (2001)



PRL 89, 137002, (2002)

## Theoretical scenario I: ((helical) magnetic inhomogeneities

### Long-Range Proximity Effects in Superconductor-Ferromagnet Structures

F. S. Bergeret,<sup>1</sup> A. F. Volkov,<sup>1,2</sup> and K. B. Efetov<sup>1,3</sup>

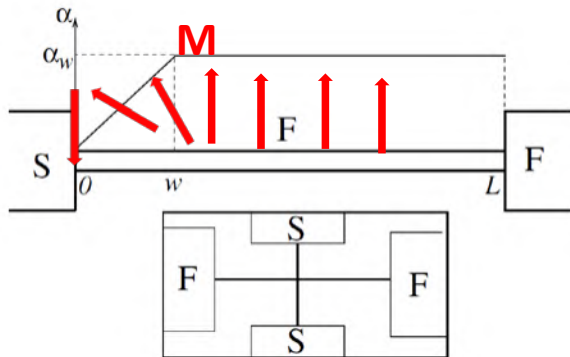
<sup>1</sup>Theoretische Physik III, Ruhr-Universität Bochum, D-44780 Bochum, Germany

<sup>2</sup>Institute of Radioengineering and Electronics of the Russian Academy of Sciences, 103907 Moscow, Russia

<sup>3</sup>L. D. Landau Institute for Theoretical Physics, 117940 Moscow, Russia

(Received 24 November 2000)

We analyze the proximity effect in a superconductor/ferromagnet (S/F) structure with a local inhomogeneity of the magnetization in the ferromagnet near the S/F interface. We demonstrate that not only the singlet but also the triplet component of the superconducting condensate is induced in the ferromagnet due to the proximity effect. The singlet component penetrates into the ferromagnet over a short length  $\xi_h = \sqrt{D/h}$  ( $h$  is the exchange field and  $D$  the diffusion coefficient), whereas the triplet component penetrates over a long length  $\sqrt{D/\epsilon}$  and leads to a significant increase of the ferromagnet conductance below the superconducting critical temperature  $T_c$ .



F. S. Bergeret et al PRL 86, 4096 (2001)

Odd frequency triplets

**Spin active=Spin mixing + spin rotation**

## Theoretical scenario II: Spin flip scattering

VOLUME 90, NUMBER 13

PHYSICAL REVIEW LETTERS

week ending  
4 APRIL 2003

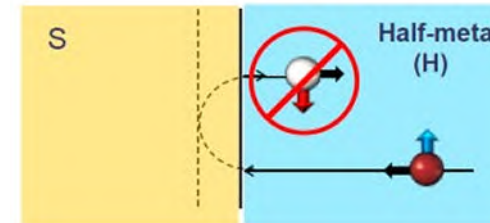
### Theory of Half-Metal/Superconductor Heterostructures

M. Eschrig,<sup>1</sup> J. Kopu,<sup>1</sup> J. C. Cuevas,<sup>1</sup> and Gerd Schön<sup>1,2</sup>

<sup>1</sup>Institut für Theoretische Festkörperphysik, Universität Karlsruhe, 76128 Karlsruhe, Germany

<sup>2</sup>Forschungszentrum Karlsruhe, Institut für Nanotechnologie, 76021 Karlsruhe, Germany  
(Received 17 June 2002; published 3 April 2003)

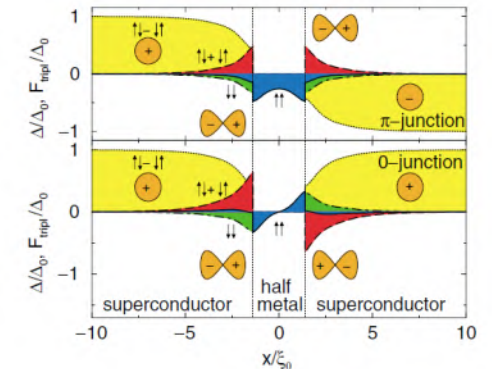
We investigate the Josephson coupling between two singlet superconductors separated by a half-metallic magnet. The mechanism behind the coupling is provided by the rotation of the quasiparticle spin in the superconductor during reflection events at the interface with the half metal. Spin rotation induces triplet correlations in the superconductor which, in the presence of surface spin-flip scattering, results in an indirect Josephson effect between the superconductors. We present a theory appropriate for studying this phenomenon and calculate physical properties for a superconductor/half-metal/superconductor heterostructure.



**Spin rotation**

Odd frequency triplets

**Magnetic inhomogeneity  
in momentum space**



p-wave triplets

M. Eschrig et al PRL 90, 137003 (2003)

See also Asano, Y., Tanaka, Y. & Golubov, A. A. *Phys. Rev. Lett.* **98**, 107002 (2007). Eschrig, M. & Löfwander, *Nat. Phys.* **4**, 138–143 (2008).

Bergeret, F. S. & Tokatly, I. V. *Phys. Rev. Lett.* **110**, 1–6 (2013).

# LONG RANGE FM PROXIMITY: Equal spin $S_z = \pm 1$ TRIPLET

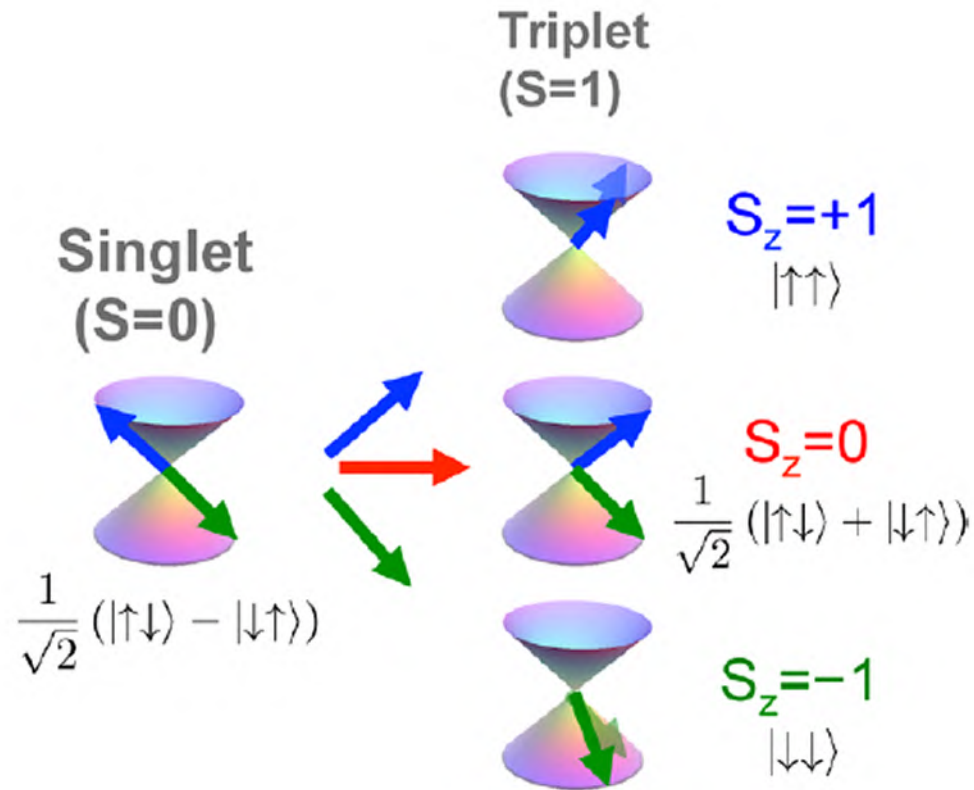
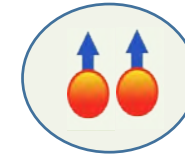


Figure adapted from M. Eschrig Rep. Prog. Phys. 78, 104501 (2015)

Spin rotation



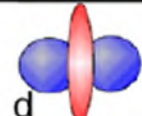
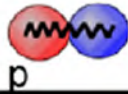
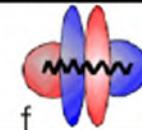
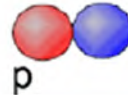
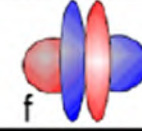
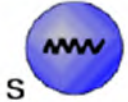
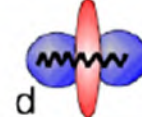
Buzdin, A. I. Proximity effects in superconductor-ferromagnet heterostructures. *Rev. Mod. Phys.* **77**, 935–976 (2005).

Bergeret, F. S., Volkov, A. F. & Efetov, K. B., *Rev. Mod. Phys.* **77**, 1321 (2005).

Linder, J. & Robinson, J. W. A. Superconducting spintronics. *Nature Physics* **11**, 307–315 (2015).

Eschrig, M. Spin-polarized supercurrents for spintronics: a review of current progress. *Rep. Prog. Phys.* **78**, 104501 (2015).

# SYMMETRY CLASSIFICATION OF PAIRING STATES

Spin	Frequency	Momentum	Overall	Type
Singlet (odd) $\uparrow\downarrow - \downarrow\uparrow$	Even	Even  	Odd	A
	Odd	Odd  	Odd	B
Triplet (even) $\uparrow\uparrow \downarrow\downarrow$ $\uparrow\downarrow + \downarrow\uparrow$	Even	Odd  	Odd	C
	Odd	Even  	Odd	D



M. Eschrig and T. Lofwander Nature Physics 4, 138 (2008)

M. Giroud, H. Courtois, K. Hasselbach, D. Mailly, and B. Pannetier *Phys. Rev. B* **58**, R11872(R)

## LETTERS

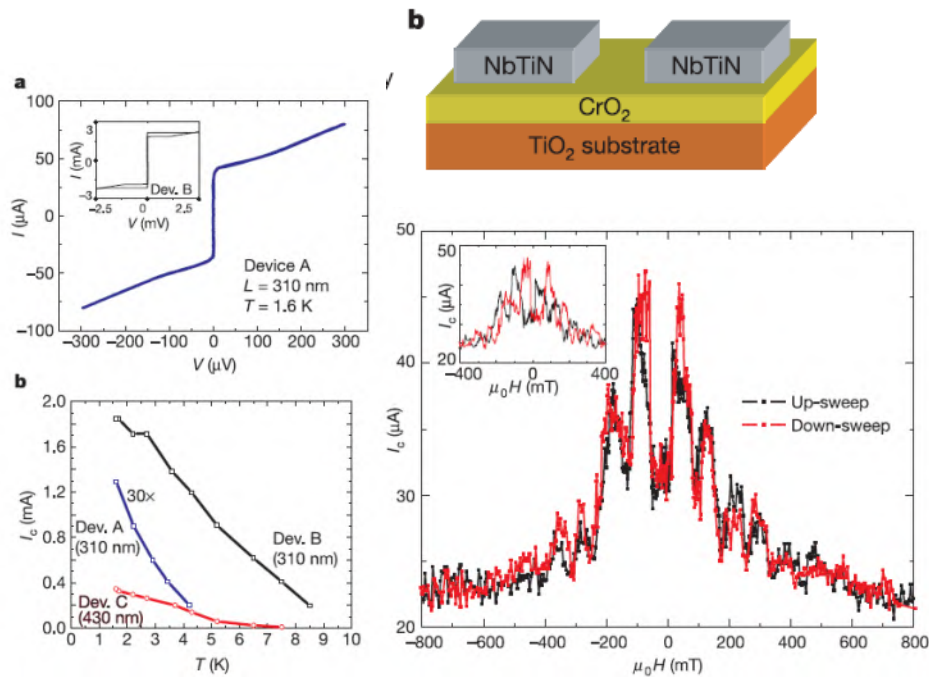
### A spin triplet supercurrent through the half-metallic ferromagnet CrO<sub>2</sub>

R. S. Keizer<sup>1</sup>, S. T. B. Goennenwein<sup>1†</sup>, T. M. Klapwijk<sup>1</sup>, G. Miao<sup>2,3</sup>, G. Xiao<sup>3</sup> & A. Gupta<sup>2</sup>

Nature 438, 836 (2006)

CrO<sub>2</sub>, HM FM T<sub>c</sub> = 390 K

NbTi contacts separated **300 nm!!**



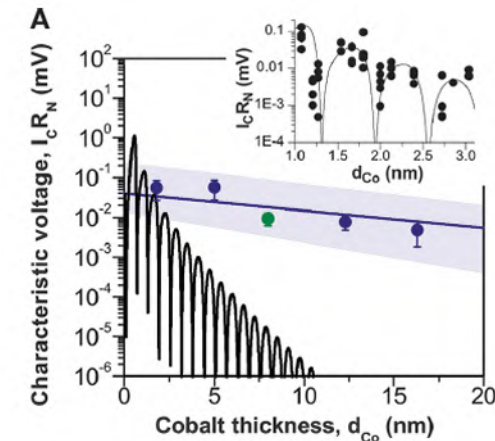
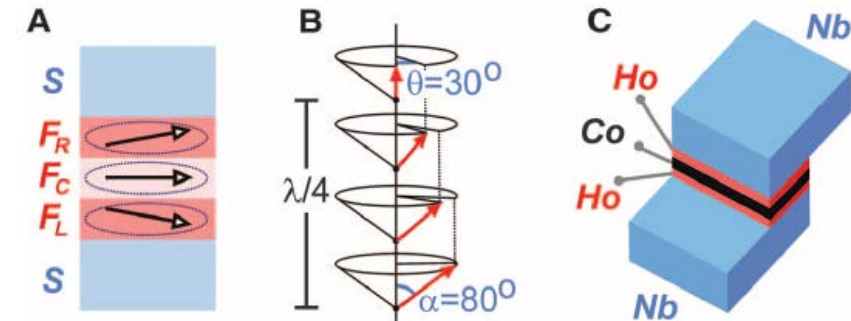
See also Anwar, M. S., Czeschka, F., Hesselberth, M., Porcu, M. & Aarts, *Phys. Rev. B* **82**, 100501 (2010).

### Controlled Injection of Spin-Triplet Supercurrents into a Strong Ferromagnet



J. W. A. Robinson,\* J. D. S. Witt, M. G. Blamire *Science* **329**, 59 (2010);

The superconductor-ferromagnet proximity effect describes the fast decay of a spin-singlet supercurrent originating from the superconductor upon entering the neighboring ferromagnet.



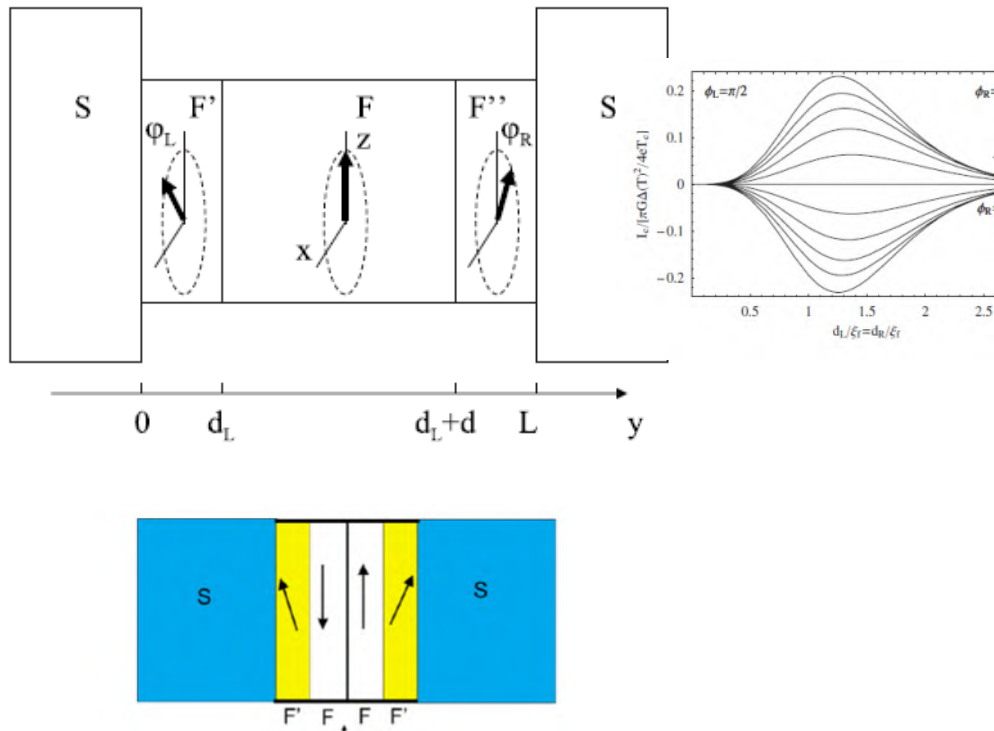
## Long range triplet Josephson effect through a ferromagnetic trilayer

M. Houzet<sup>1</sup> and A. I. Buzdin<sup>2</sup>

<sup>1</sup>DRFMC/SPSMS, CEA Grenoble, 17, rue des Martyrs, 38054 Grenoble Cedex 9, France

<sup>2</sup>Institut Universitaire de France and Université Bordeaux I, CPMOH, UMR 5798, 33405 Talence, France

(Received 16 July 2007; published 15 August 2007)



Sperstad, I. B., Linder, J. & Sudbø, A. *Phys. Rev. B* **78**, 104509 (2008).

Halterman, K., Valls, O. & Barsic, P. *Phys. Rev. B* **77**, 174511 (2008).

A. F. Volkov and K. B. Efetov, *Phys. Rev. B* **81**, 144522 (2010)

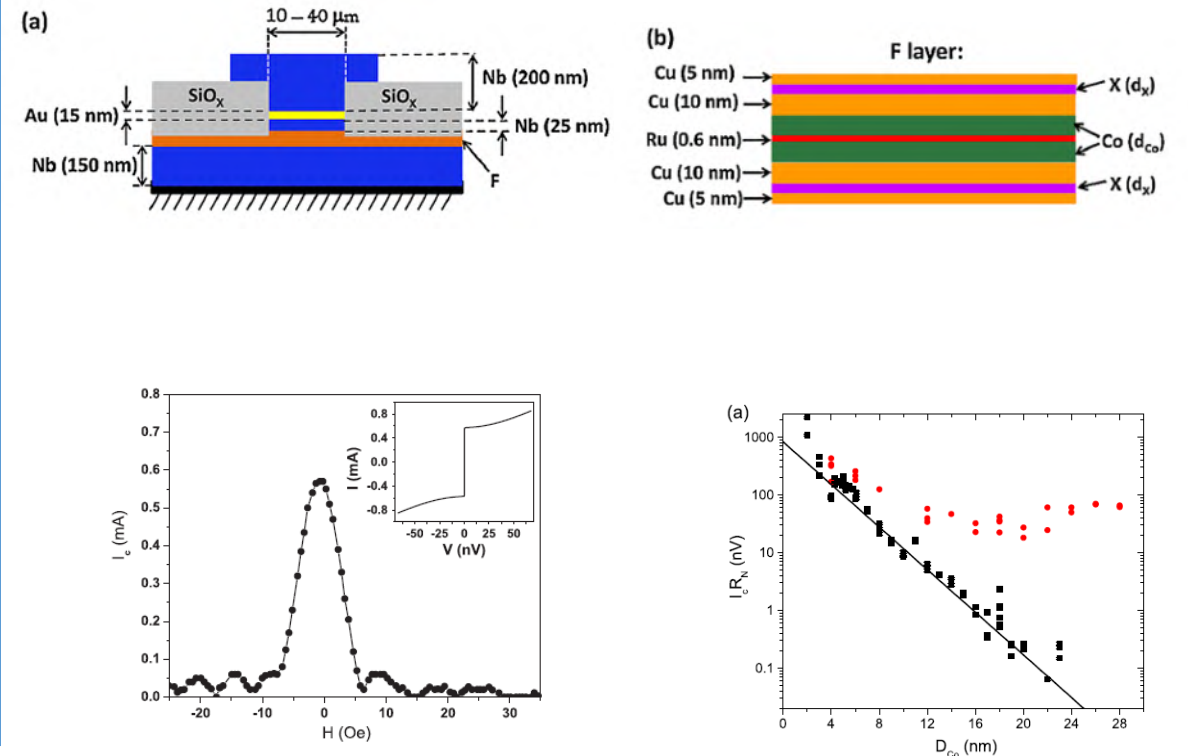
## Observation of Spin-Triplet Superconductivity in Co-Based Josephson Junctions

Trupti S. Khaire, Mazin A. Khasawneh, W. P. Pratt, Jr., and Norman O. Birge\*

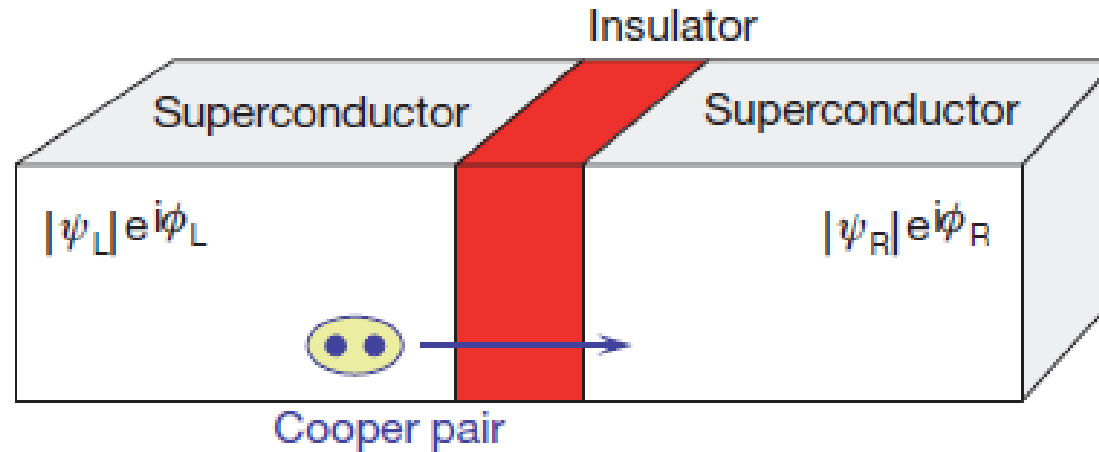
Department of Physics and Astronomy, Michigan State University, East Lansing, Michigan 48824-2320, USA

(Received 1 December 2009; published 29 March 2010)

We have measured a long-range supercurrent in Josephson junctions containing Co (a strong ferromagnetic material) when we insert thin layers of either PdNi or CuNi weakly ferromagnetic alloys between the Co and the two superconducting Nb electrodes. The critical current in such junctions hardly



# LONG RANGE TRIPLET JOSEPHSON EFFECT HAS REMAINED ELUSIVE



Phase-coherent quantum state

## Josephson equations in SC

by Leggett

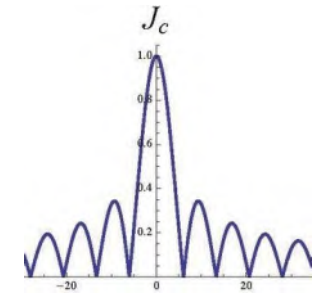
$$\left[ \begin{array}{l} I = I_c \sin \phi \quad ; \text{ Josephson current} \\ \rightarrow \text{ "charge current"} \\ \frac{d}{dt} \phi(t) = \frac{2eV(t)}{\hbar} = \frac{2\pi V}{\Phi_0}, \quad \Phi_0 = h/2e \quad (\text{quantized magnetic flux}) \end{array} \right.$$

✓ **dc Josephson effect;**  $\frac{d}{dt} \phi(t) \propto V(t) = 0$

→ **Relative phase is time-independent;**  $\frac{d}{dt} \phi(t) = 0$

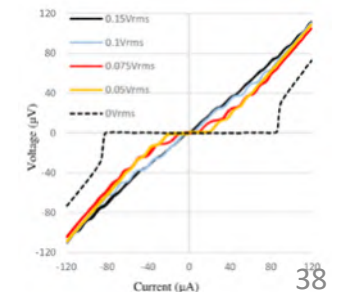
Space-domain interference

**Fraunhofer pattern**

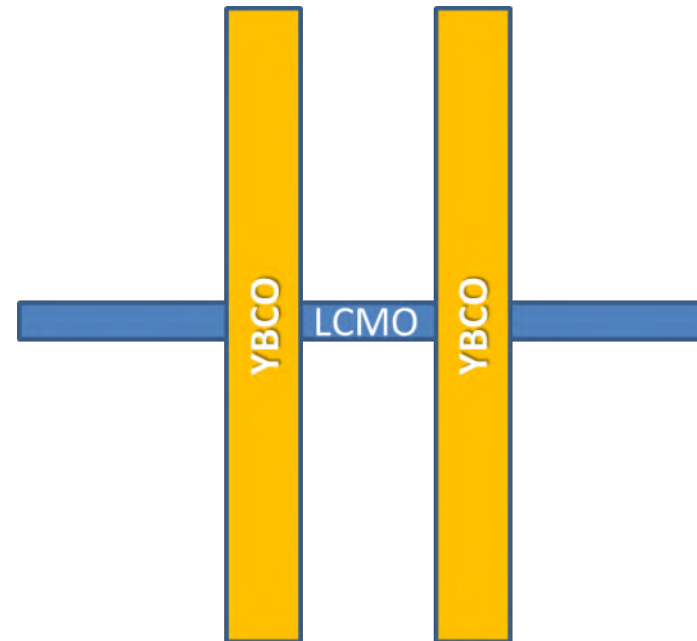


Time-domain interference

**Shapiro steps**



**microwires**  
**YBCO/LSMO**

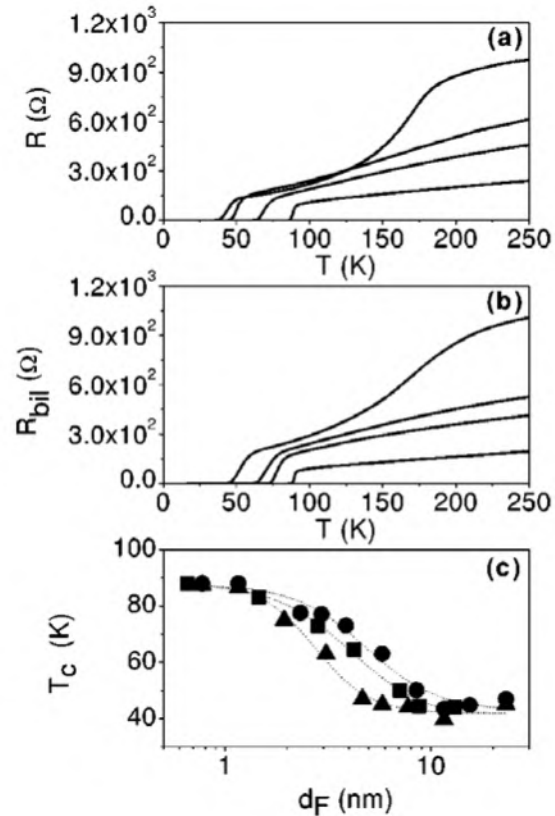


- **Well defined current geometry and magnetic state**

# TRIPLET PAIRING IN $\text{YBa}_2\text{Cu}_3\text{O}_7/\text{La}_{0.7}\text{Ca}_{0.3}\text{MnO}_3$ heterostructures

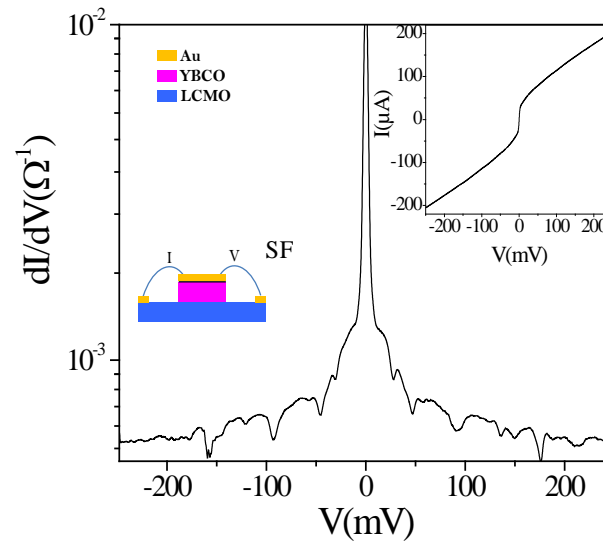
PHYSICAL REVIEW B 69, 224502 (2004)

Coupling of superconductors through a half-metallic ferromagnet: Evidence for a long-range proximity effect



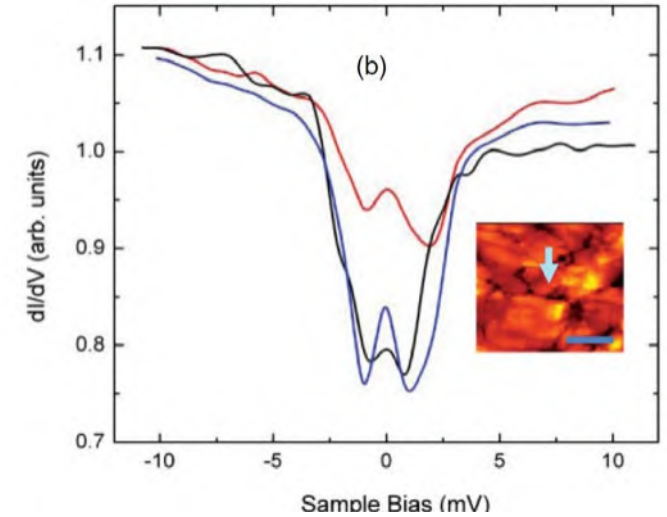
V. Peña et al Phys. Rev. B 69, 224502 (2004)

Equal-spin Andreev reflection and long-range coherent transport in high-temperature superconductor/half-metallic ferromagnet junctions



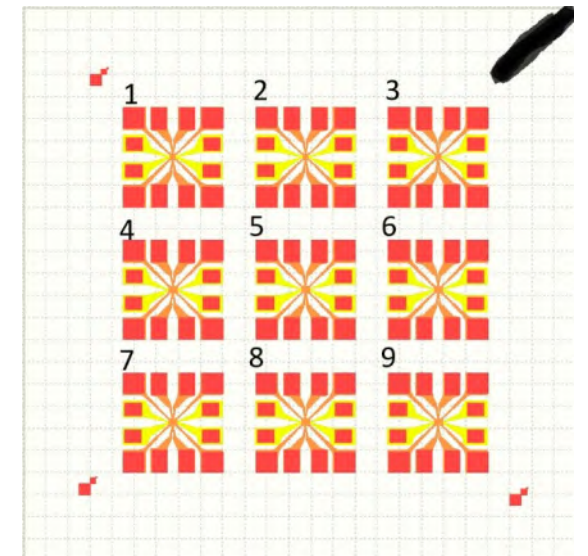
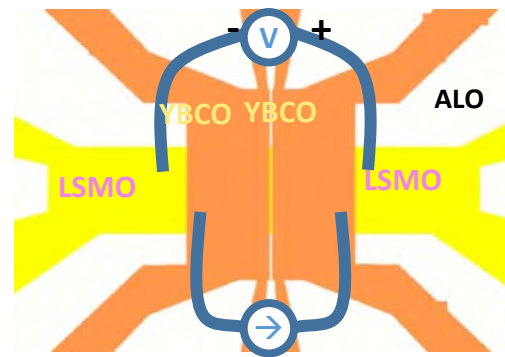
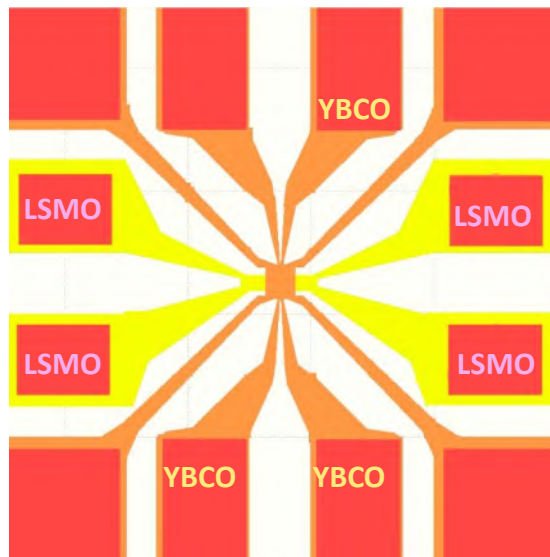
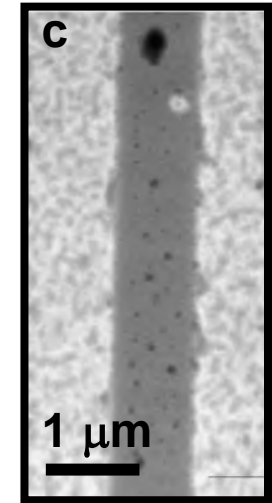
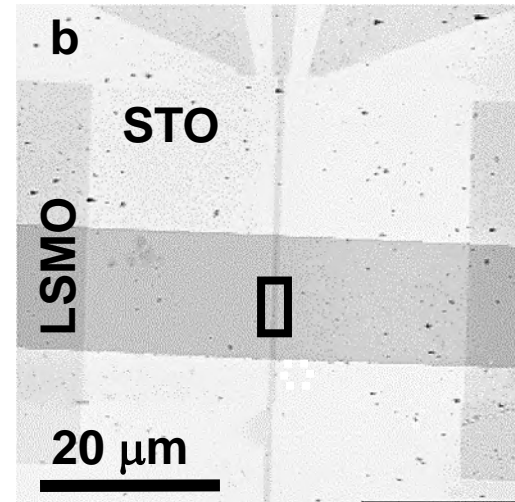
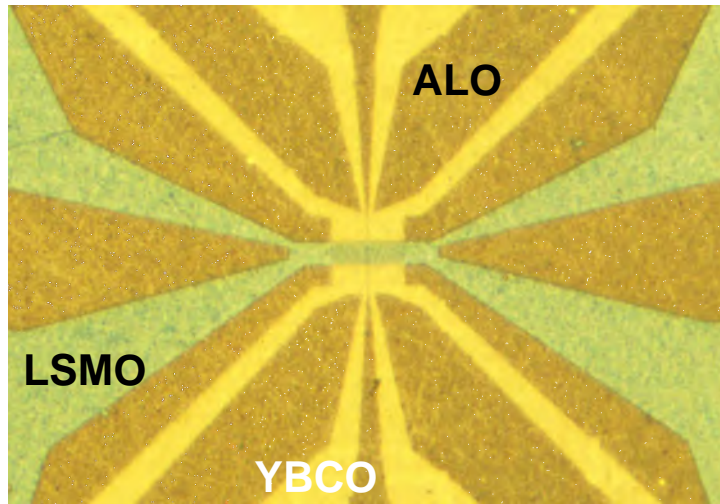
C. Visani et al. Nature Physics, 8, 539 (2012)

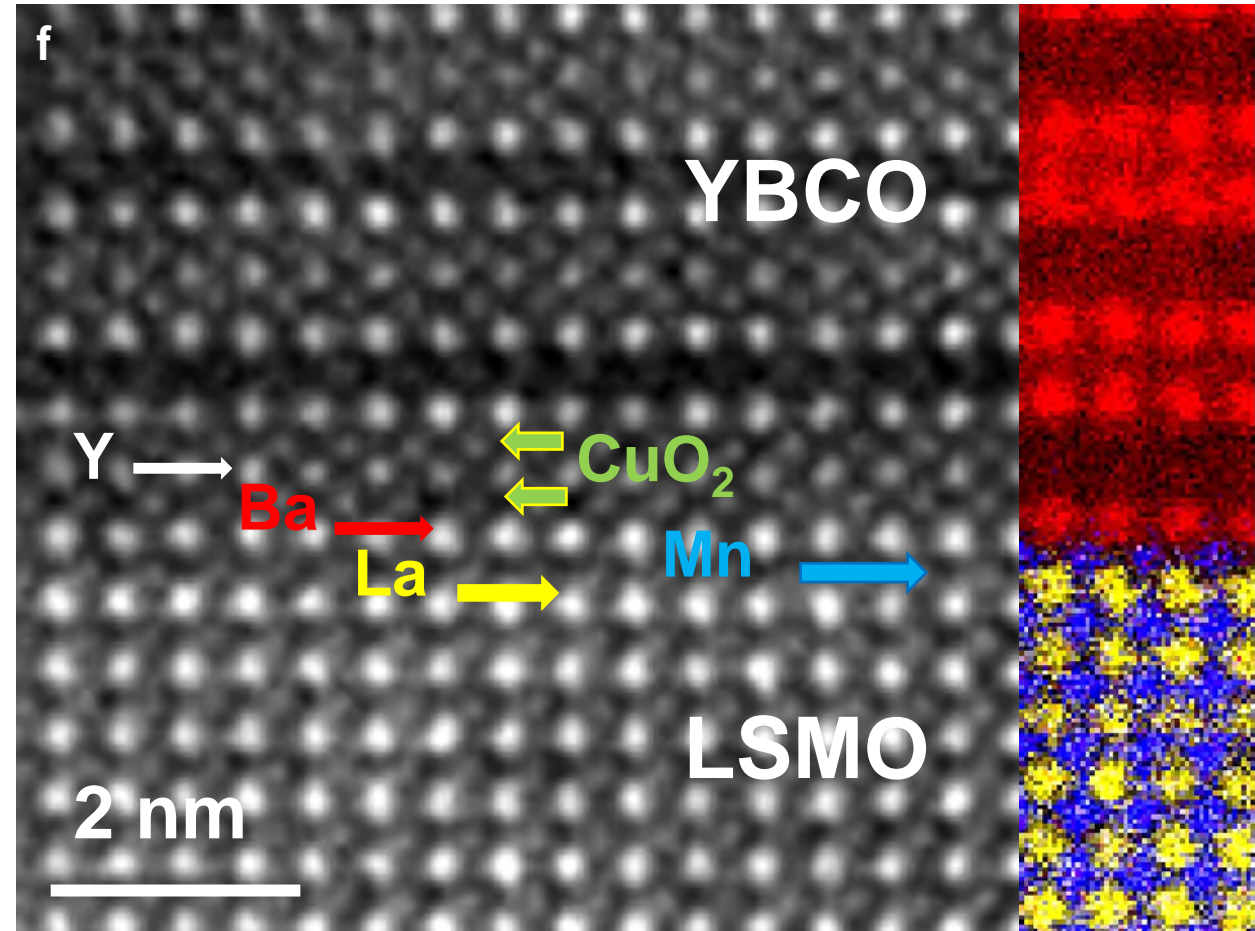
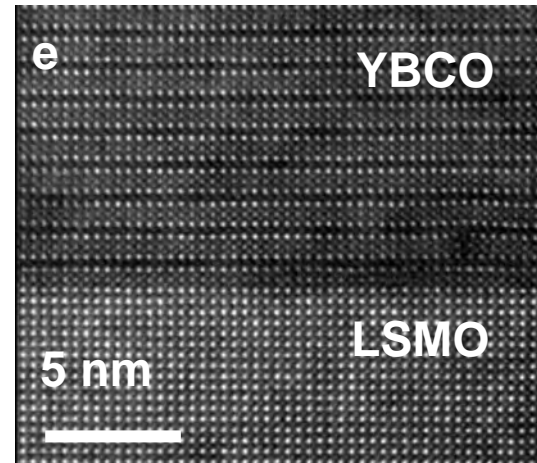
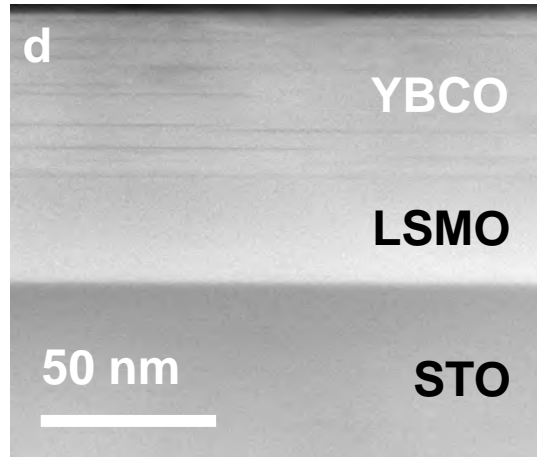
Evidence for anisotropic triplet superconductor order parameter in half-metallic ferromagnetic  $\text{La}_{0.7}\text{Ca}_{0.3}\text{Mn}_3\text{O}$  proximity coupled to superconducting  $\text{Pr}_{1.85}\text{Ce}_{0.15}\text{CuO}_4$



Kalcheim, Millo et al. et al. Phys. Rev. B Egilmez, Robinson and Blamire Phys. Rev. B , 85, 104504 (2012)

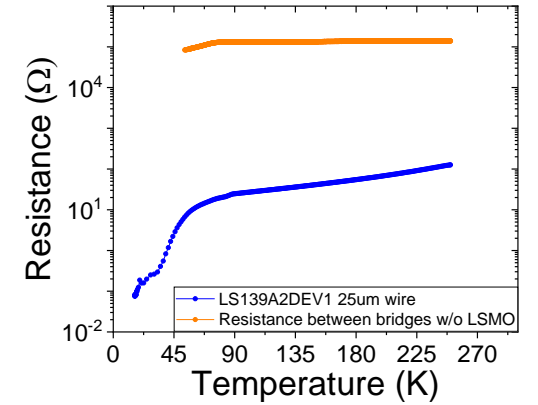
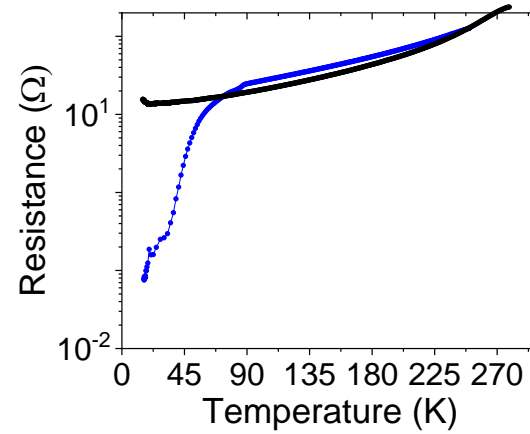
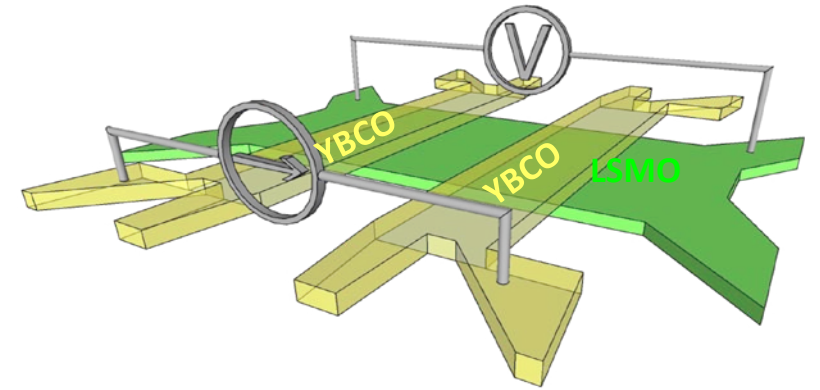
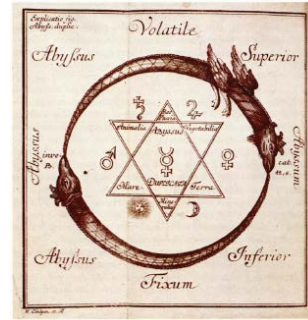
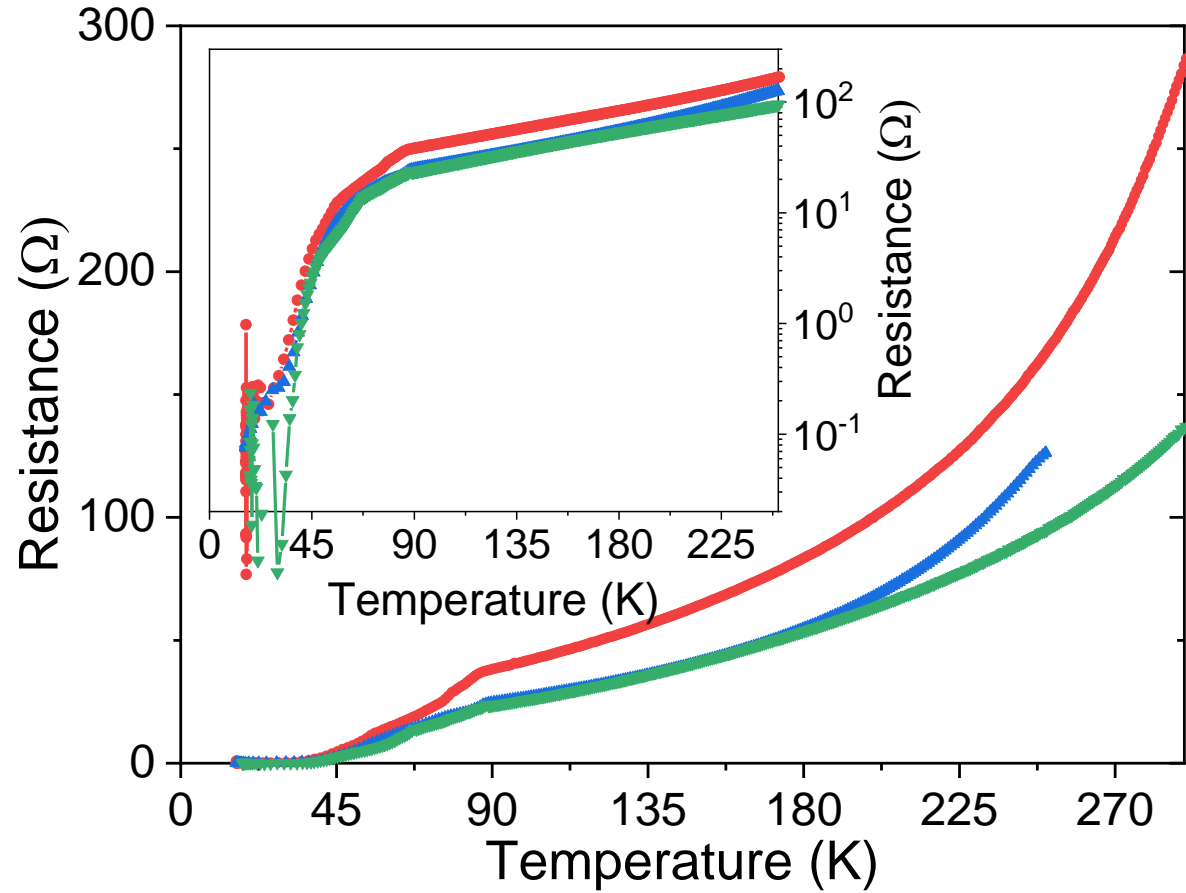
# DEVICE FABRICATION (III). Actual device's structure



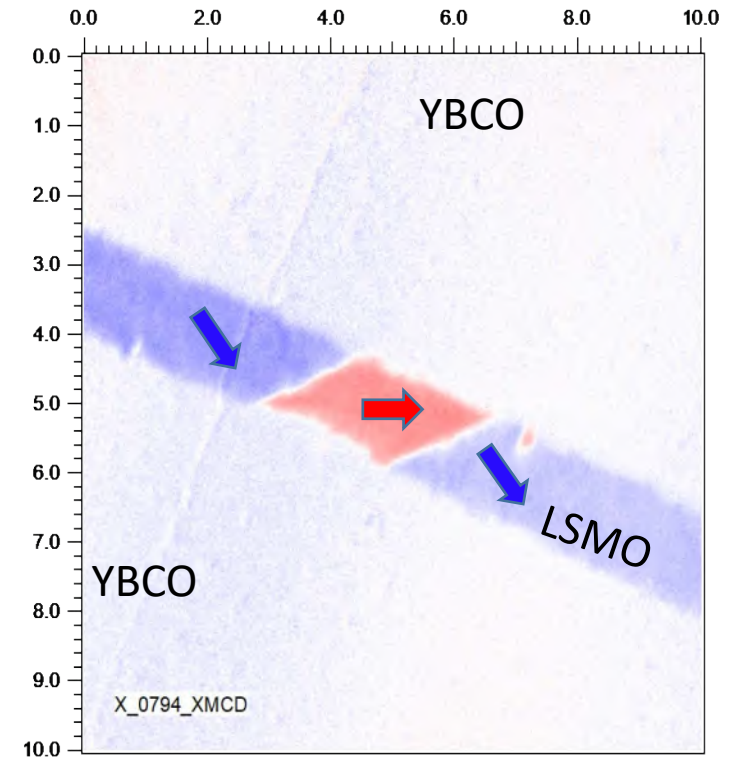
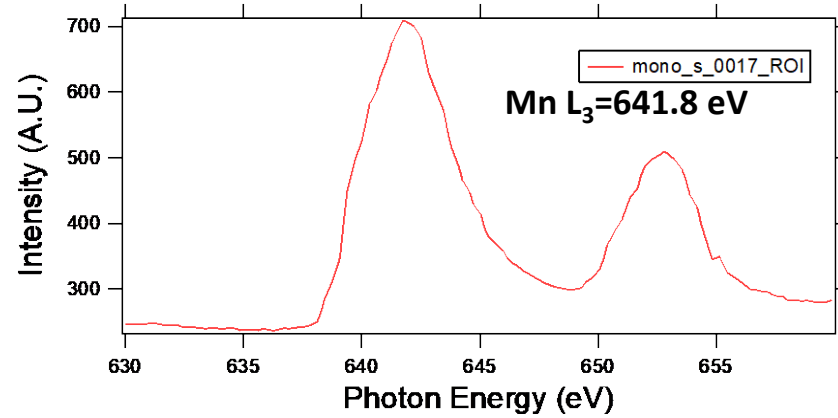
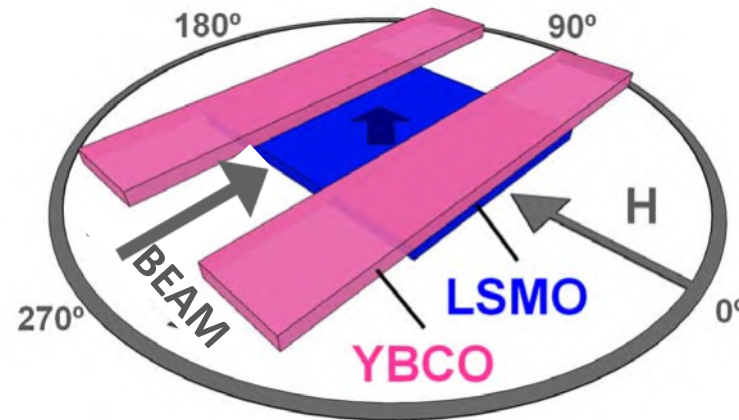
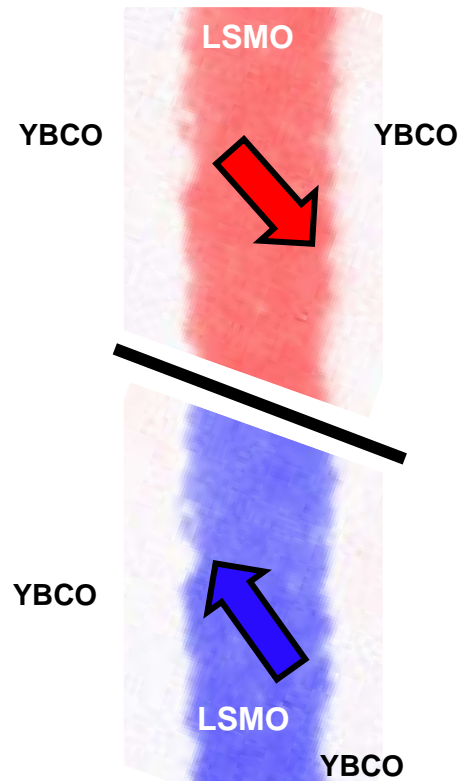


Microscopy by M. Cabero & J. M. González-Calbet

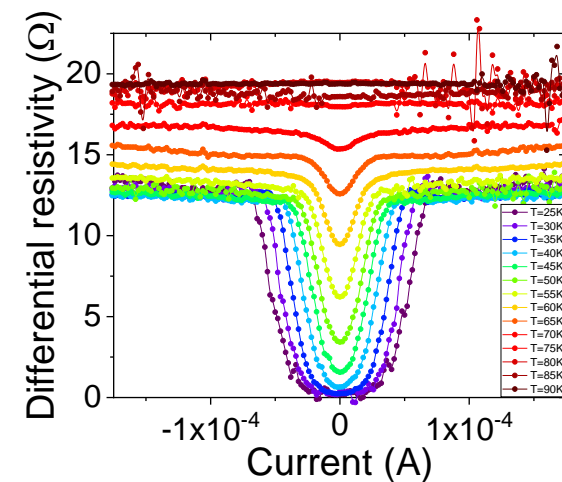
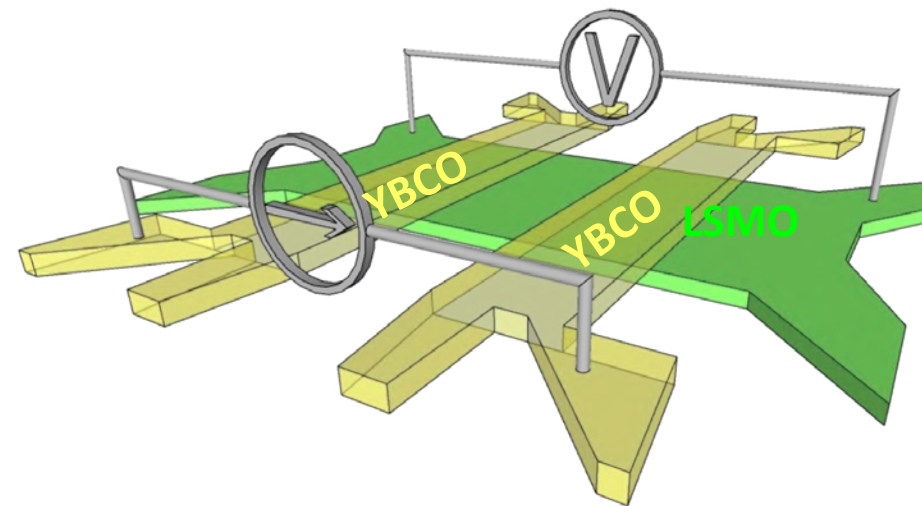
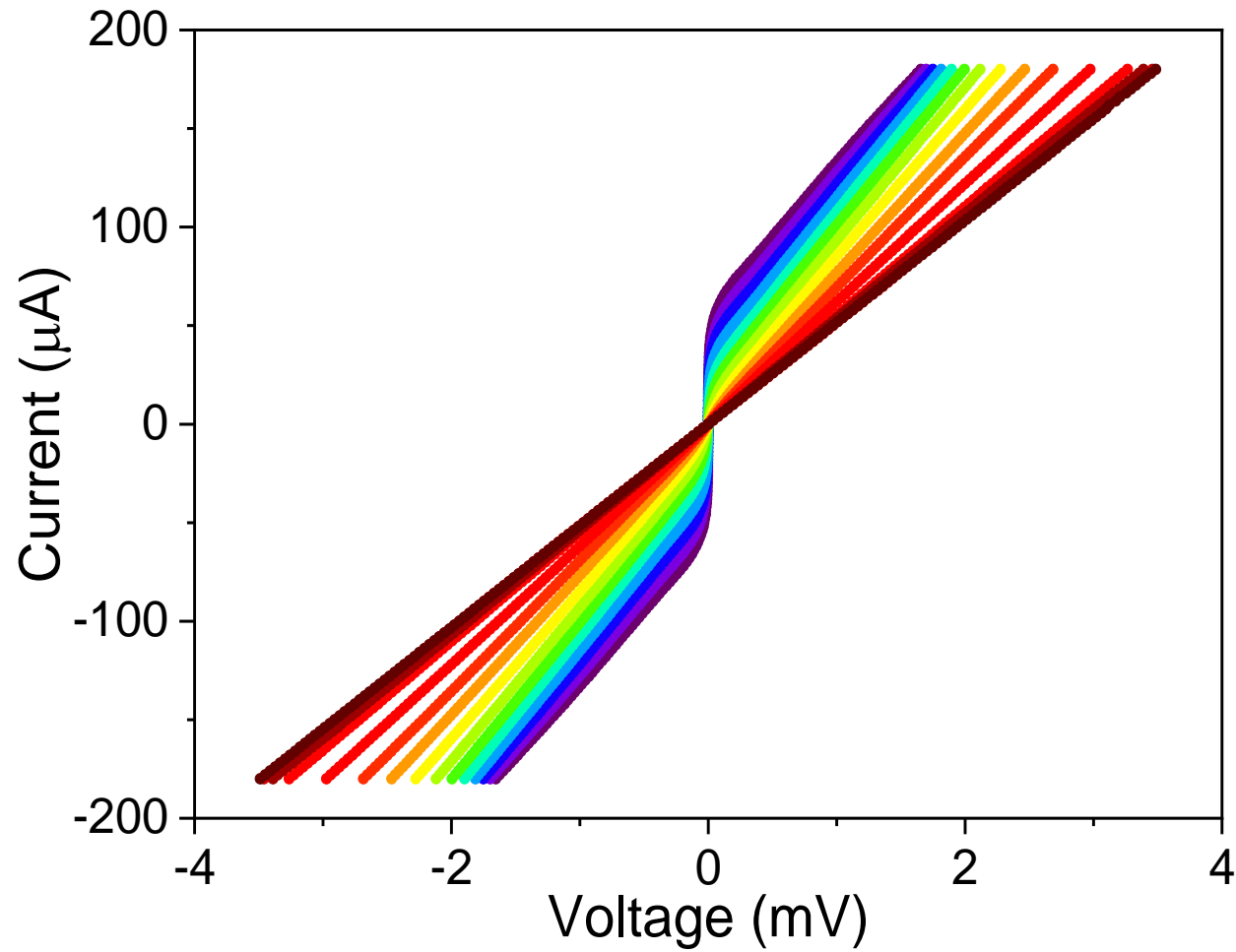
# SUPERCONDUCTING (zero resistance) STATE IN THE LSMO



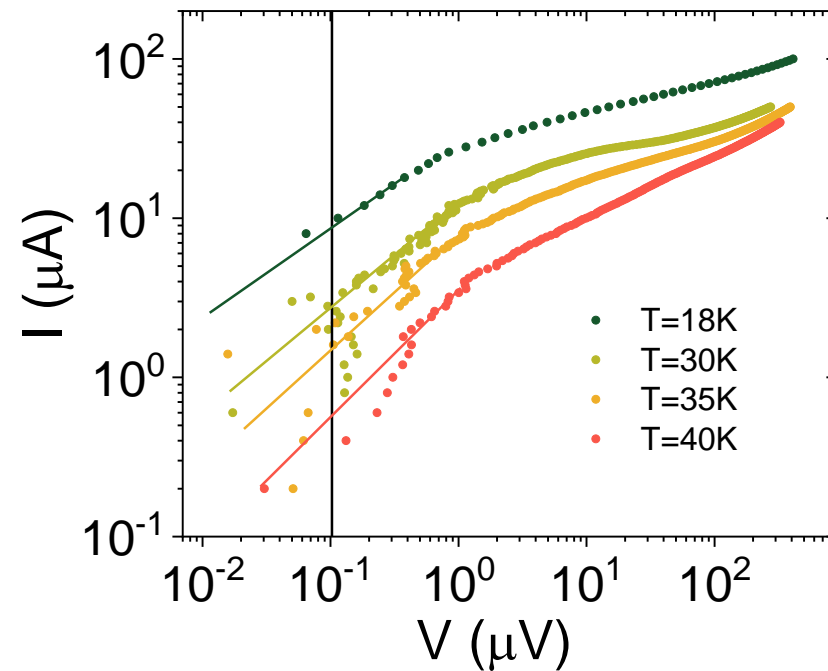
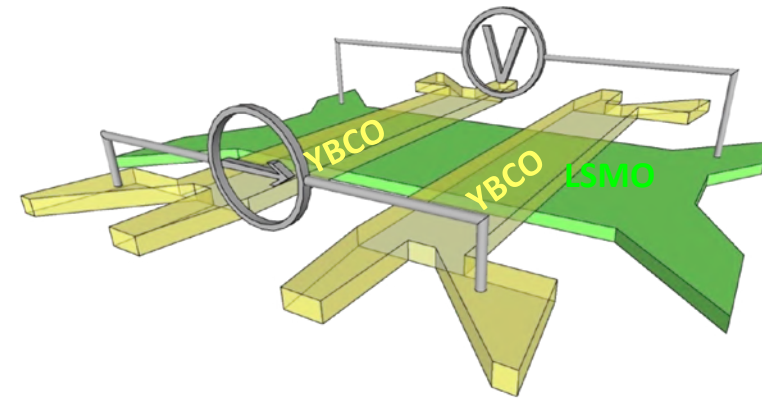
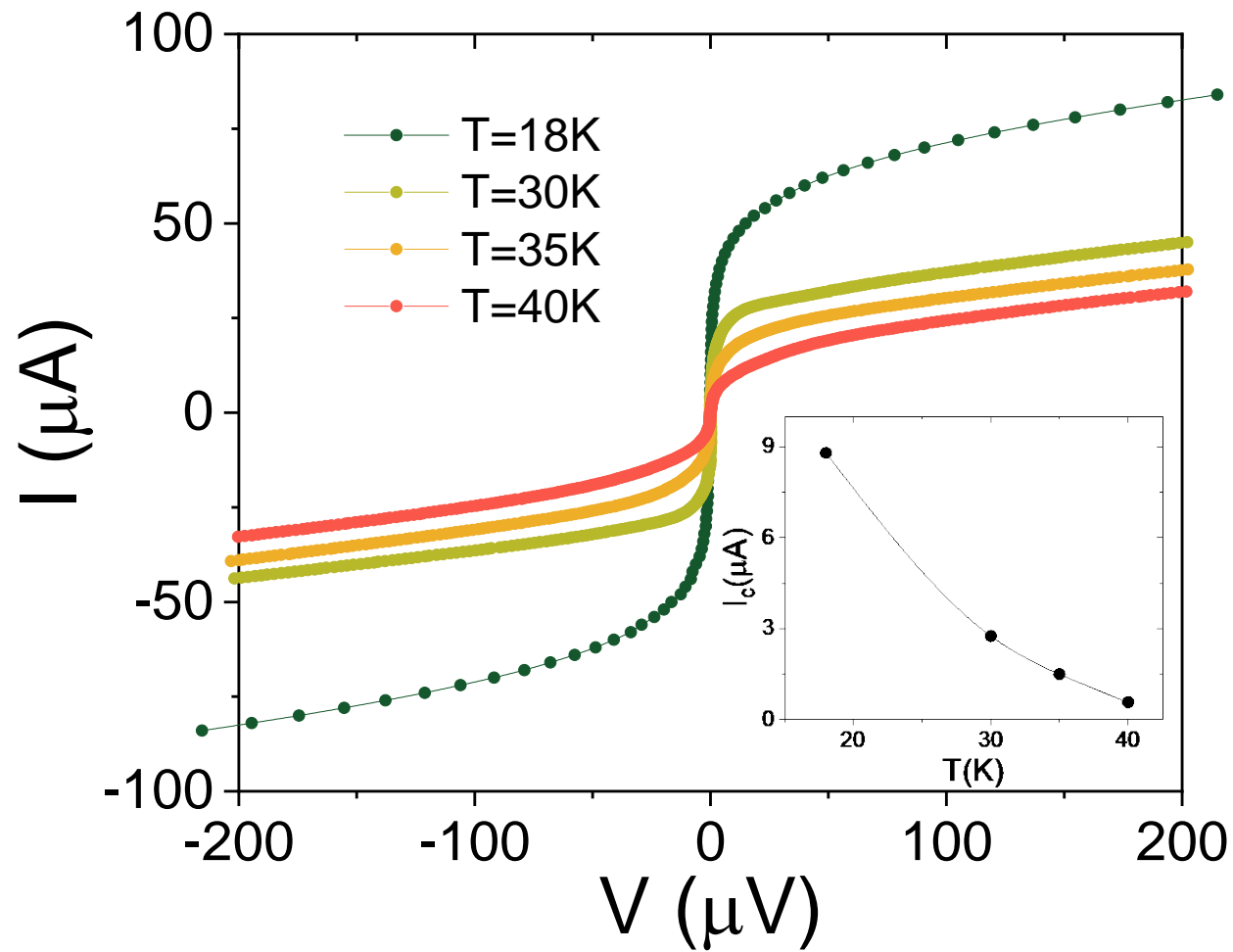
# MAGNETIC STRUCTURE. X-ray absorption (PEEM)



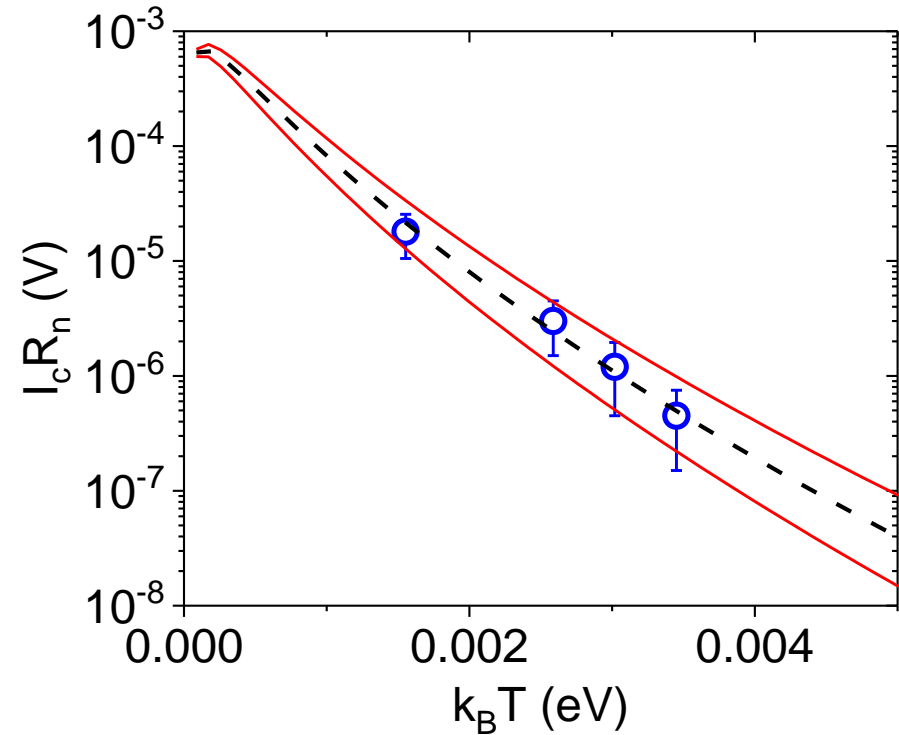
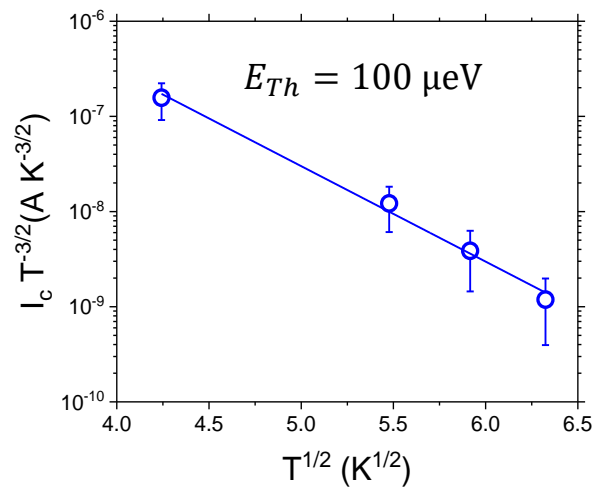
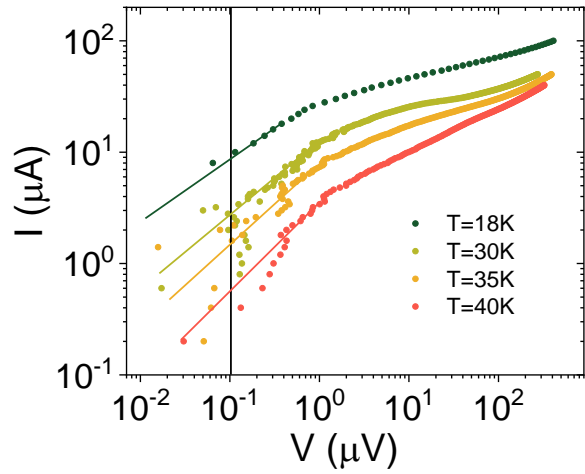
# CRITICAL CURRENT in the LSMO wire



# CRITICAL CURRENT in the LSMO wire



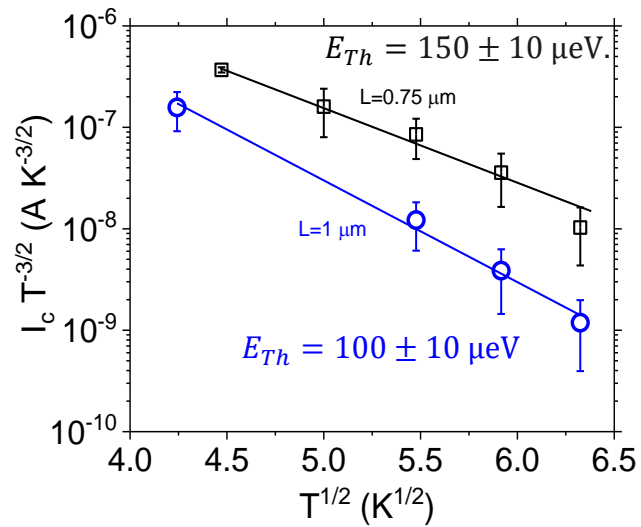
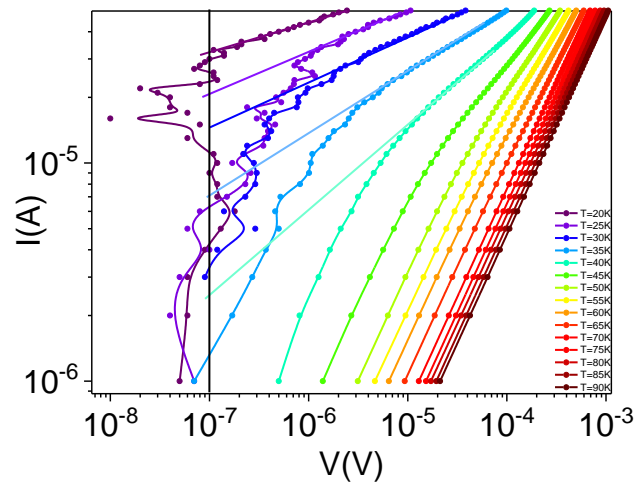
# CRITICAL CURRENT in the LSMO wire: Temperature dependence



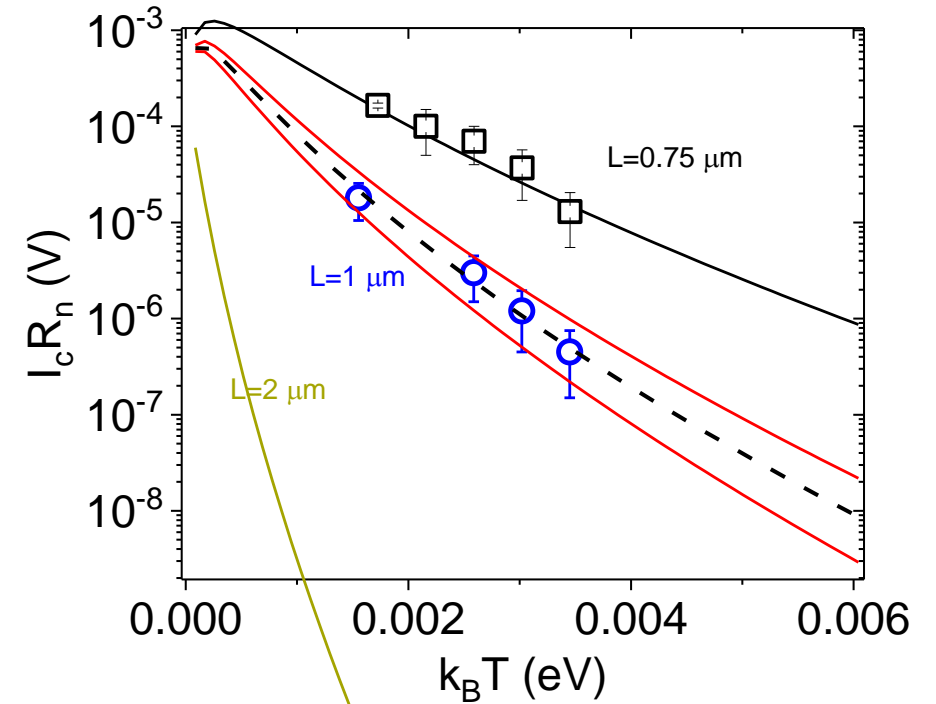
$$eI_c R_n = \frac{32}{3 + 2\sqrt{2}} E_{Th} \left[ \frac{2\pi k_B T}{E_{Th}} \right]^{3/2} e^{-[2\pi k_B T / E_{Th}]^{1/2}}$$

Dubos, P. *et al.* Josephson critical current in a long mesoscopic S-N-S junction. *Phys. Rev. B* **63**, 1–5 (2001)

# CRITICAL CURRENT in the LSMO wire: length dependence



$$E_{Th} = \frac{\hbar D}{L^2}$$



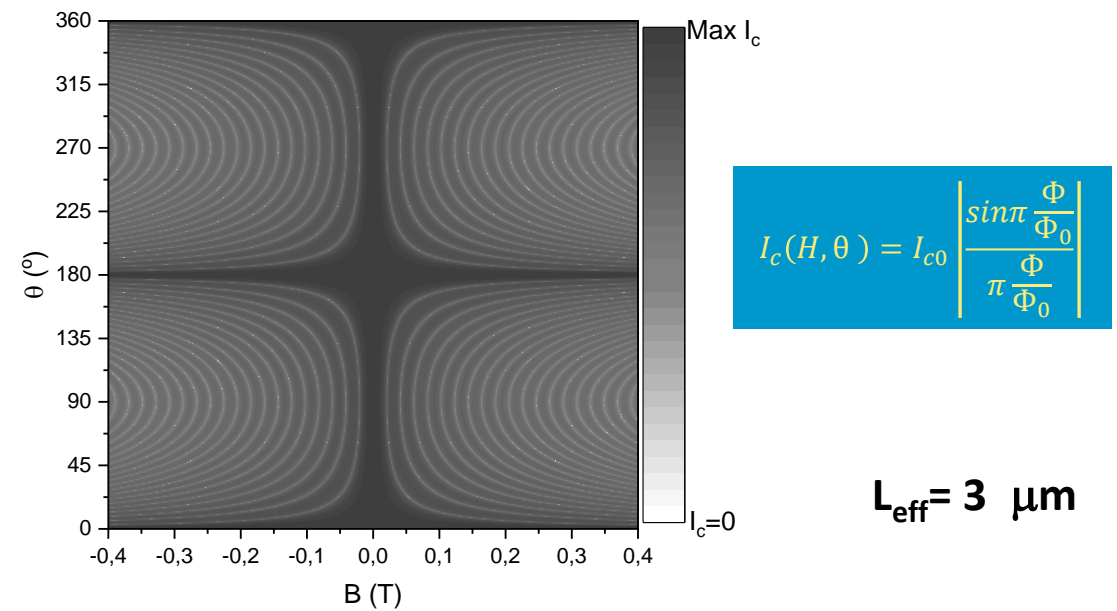
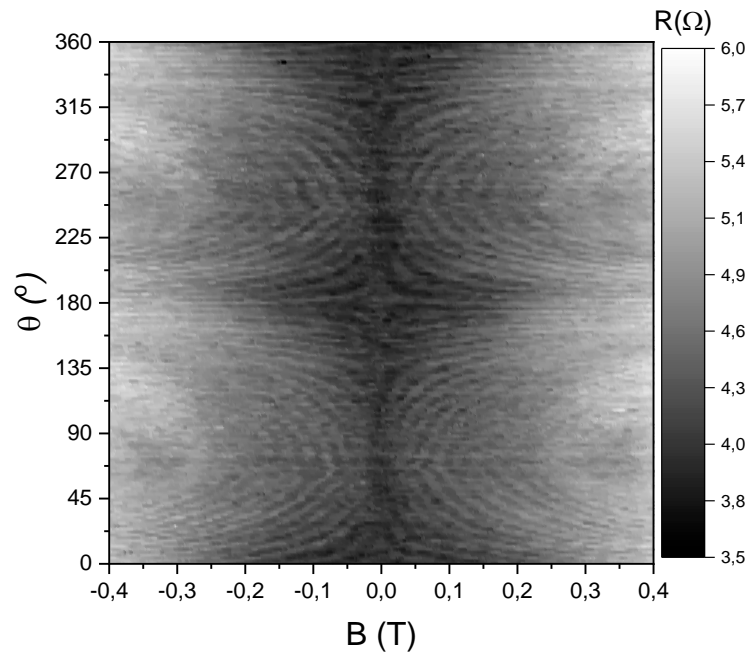
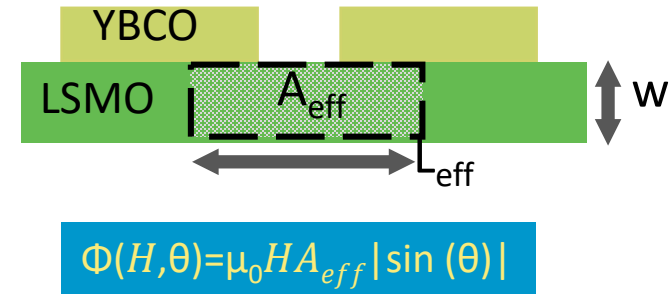
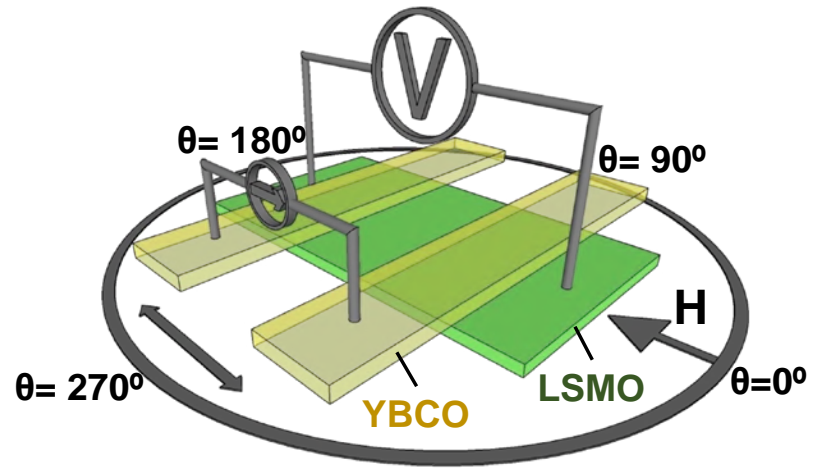
$$eI_c R_n = \frac{32}{3 + 2\sqrt{2}} E_{Th} \left[ \frac{2\pi k_B T}{E_{Th}} \right]^{3/2} e^{-[2\pi k_B T / E_{Th}]^{1/2}}$$

Dubos, P. *et al.* Josephson critical current in a long mesoscopic S-N-S junction. *Phys. Rev. B* **63**, 1–5 (2001)

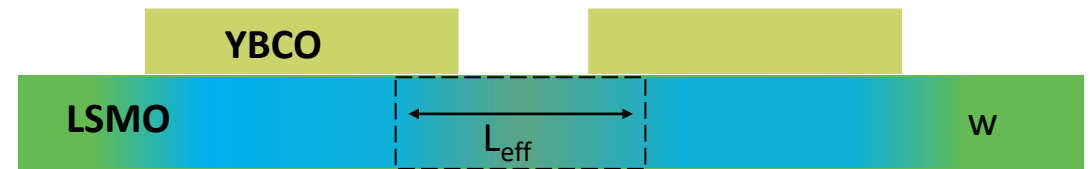
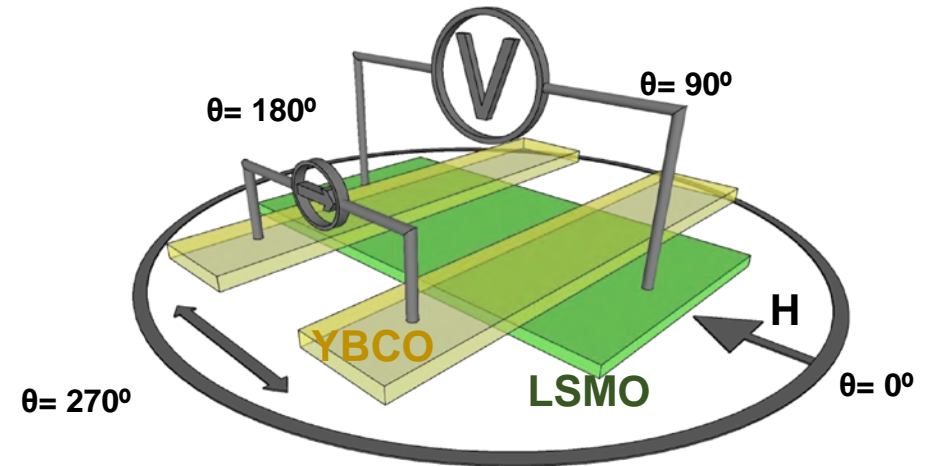
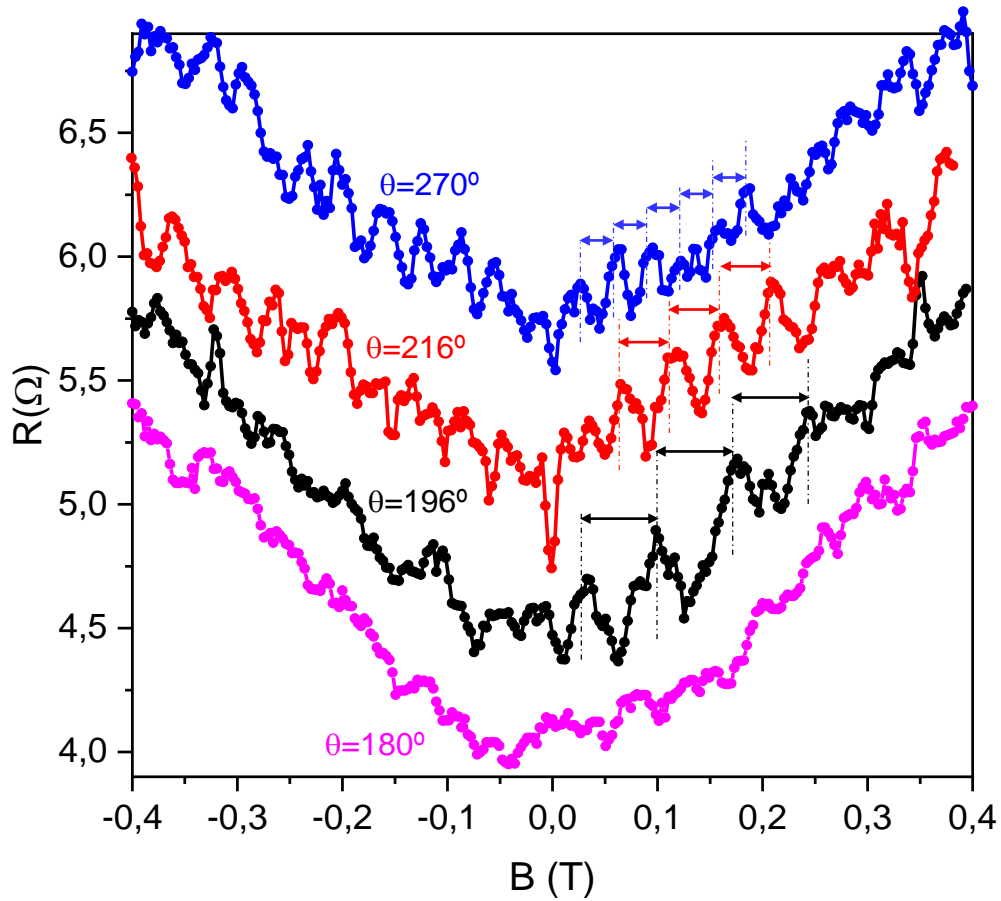
Anwar, M. S., Veldhorst, M., Brinkman, A. & Aarts, J. *Appl. Phys. Lett.* **100**, 052602 (2012).

$$I_c(H, \theta) = I_{c0} \left| \frac{\sin \pi \frac{\Phi}{\Phi_0}}{\pi \frac{\Phi}{\Phi_0}} \right|$$

# CURRENT INTERFERENCE: FRAUNHOFER PATTERN



# CURRENT INTERFERENCE: FRAUNHOFER PATTERN



$$I_c(H, \theta) = I_{c0} \left| \frac{\sin \pi \frac{\Phi}{\Phi_0}}{\pi \frac{\Phi}{\Phi_0}} \right|$$

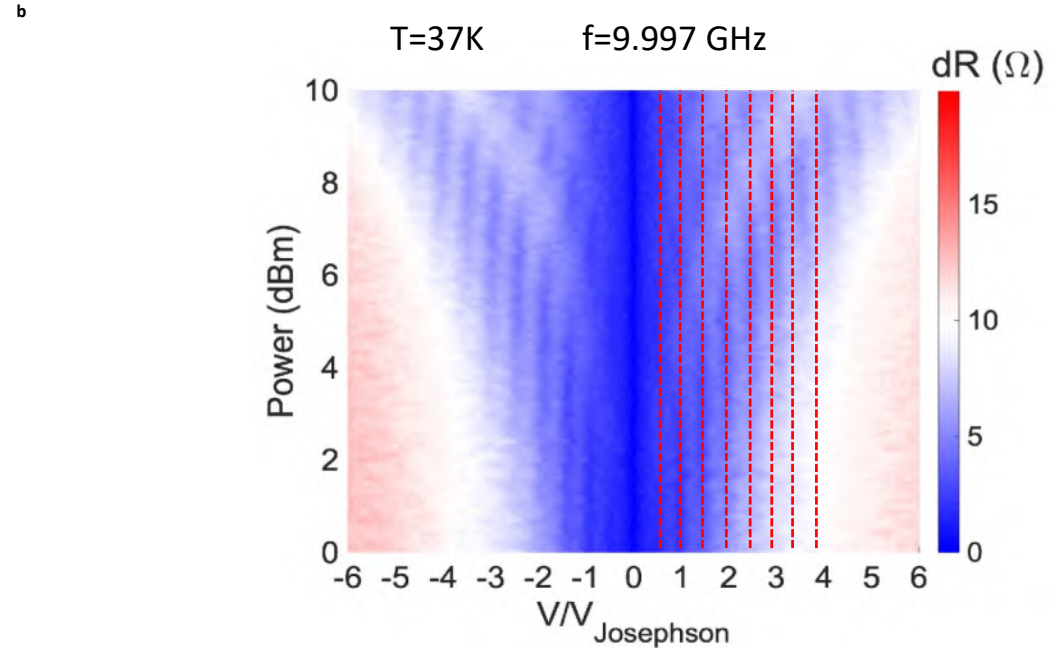
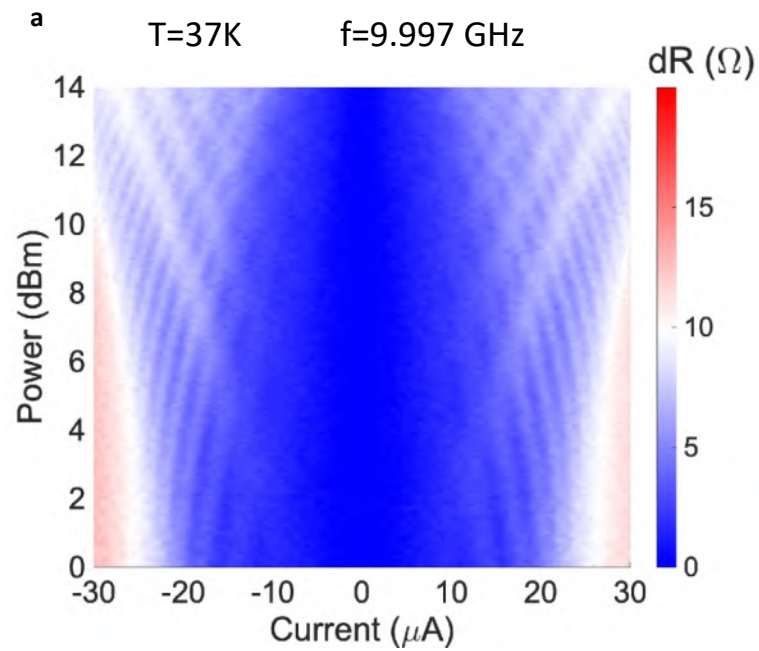
$$\Phi(H, \theta) = \mu_0 H A_{eff} |\sin(\theta)|$$

$$\frac{d\varphi}{dt} = 2\pi \frac{V}{\Phi_0}$$

$$\frac{V}{\Phi_0} = n f_{MW} \rightarrow \frac{V}{f_{MW} \Phi_0} = n$$

 $V_J$

# PHASE LOCKING: (fractional) SHAPIRO STEPS



$$V_{\text{Josephson}} = \Phi_0 f$$

$$j_s = j_{c1} \sin(\phi),$$

**S/F/S**

$$j_s(\phi) = j_{c1} \sin(\phi) + j_{c2} \sin(2\phi)$$

A. A. Golubov, M. Y. Kupriyanov, and E. Il'ichev, Rev. Mod. Phys. **76**, 411 (2004).

S. Kashiwaya, and Y. Tanaka, Rep. Prog. Phys. **63**, 1641 (2000).

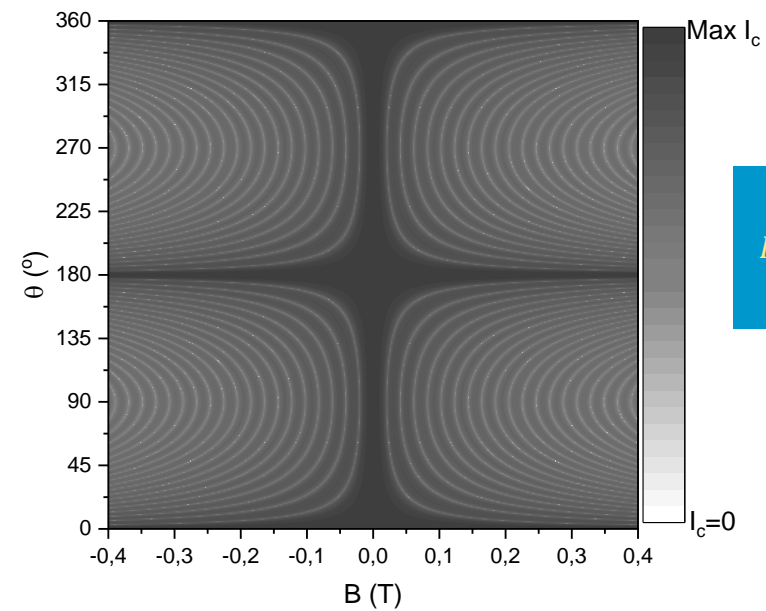
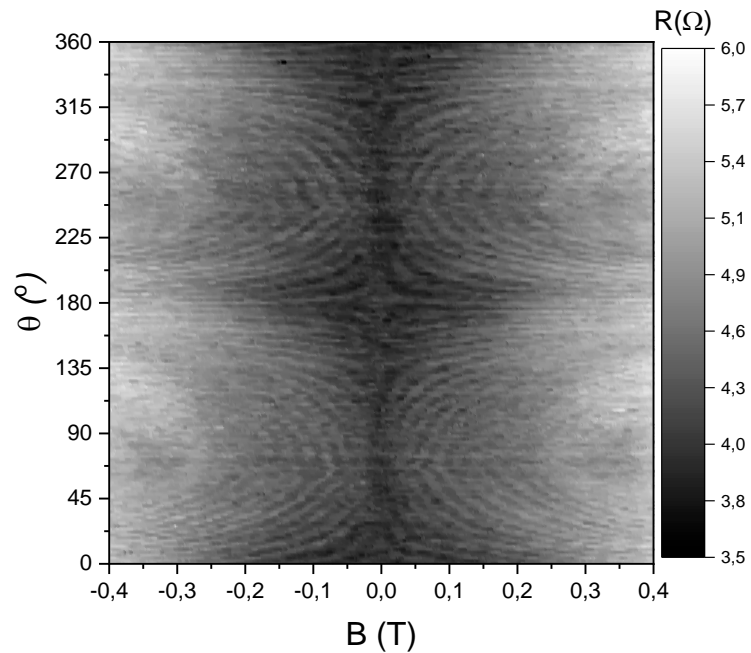
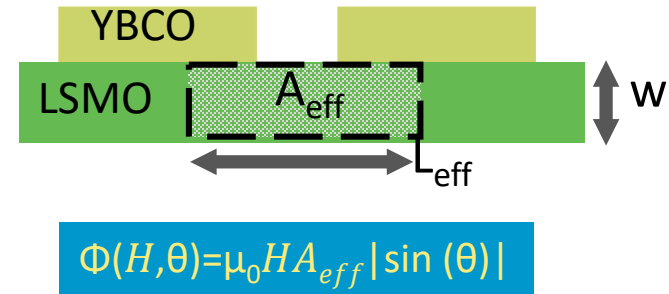
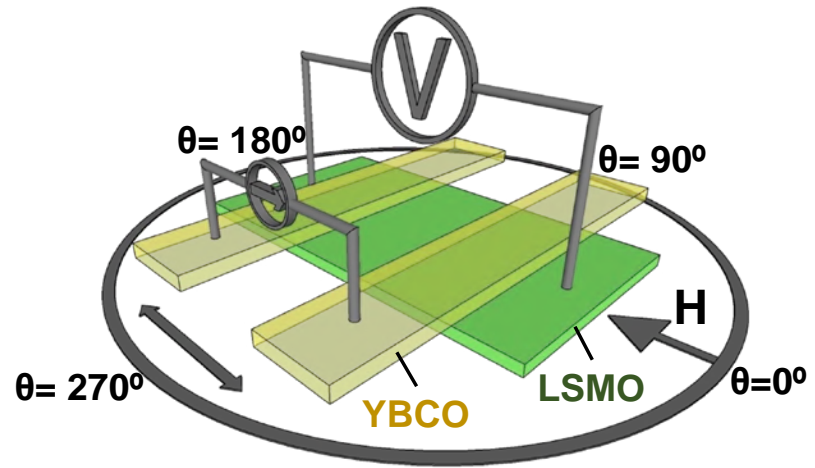
E. Goldobin *et al.*, Phys. Rev. B **76**, 224523 (2007).

Asano, Y., Sawa, Y., Tanaka, Y. & Golubov, A. A. Phys. Rev. B **76**, 224525 (2007).

➔ Junctions with dominant second harmonic term in the CPR

➔ (Triplet) junctions with spin flip scattering at interfaces  
CPR anomalous

# CURRENT INTERFERENCE: FRAUNHOFER PATTERN



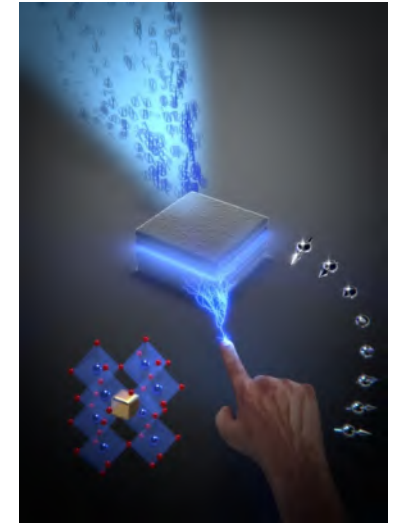
$$I_c(H, \theta) = I_{c0} \left| \frac{\sin \pi \frac{\Phi}{\Phi_0}}{\pi \frac{\Phi}{\Phi_0}} \right|$$

$L_{eff} = 1.5 \mu m$

- **Triplet unconventional Josephson effect** d-wave SC/HM
- Non-harmonic CPR (twice-shorter period Fraunhofer oscillations half-period super-harmonic Shapiro steps).
- Calls for theory on the d-wave/HM triplet proximity effect
- **$\varphi_0$ -junction**
- Outlook.

**-magnetic information is stored in the phase, allowing for a completely new spintronic quantum logic.**

**-non-dissipative phase batteries (theoretically proposed) important to reduce decoherence in quantum circuits**



# Part 2..... spin orbit int.: Topology Robustness



$$\mathcal{H}_{SO} = \frac{\xi}{\hbar} \hat{\sigma} (\nabla \phi \times \mathbf{p})$$

5d TRANSITION METAL OXIDES: strong spin orbit

Los Alamos National Laboratory Chemistry Division

Periodic Table of the Elements

**5d**

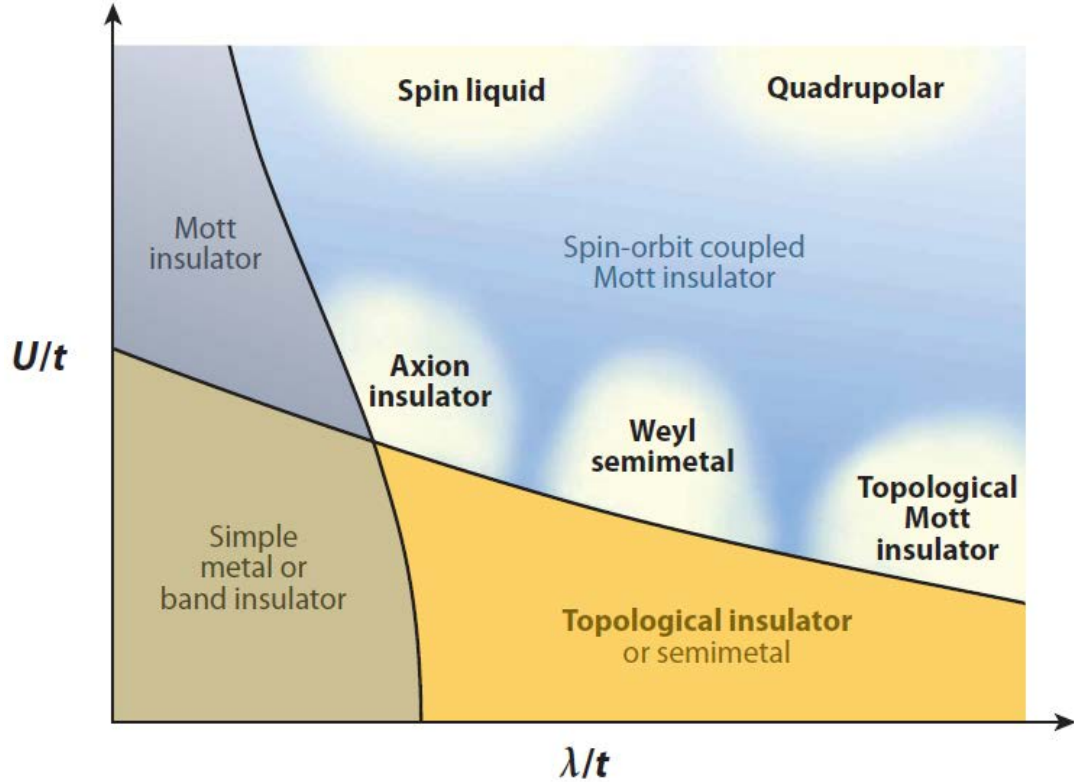
1A 1 <b>H</b> hydrogen 1.008	2A 4 <b>Be</b> beryllium 9.012	3A 13 <b>Al</b> aluminum 26.98	4A 14 <b>Si</b> silicon 28.09	5A 15 <b>P</b> phosphorus 30.97	6A 16 <b>S</b> sulfur 32.07	7A 17 <b>Cl</b> chlorine 35.45	8A 18 <b>Ar</b> argon 39.95										
19 <b>K</b> potassium 39.10	20 <b>Ca</b> calcium 40.08	21 <b>Sc</b> scandium 44.96	22 <b>Ti</b> titanium 47.88	23 <b>V</b> vanadium 50.94	24 <b>Cr</b> chromium 52.00	25 <b>Mn</b> manganese 54.94	26 <b>Fe</b> iron 55.85	27 <b>Co</b> cobalt 58.93	28 <b>Ni</b> nickel 58.69	29 <b>Cu</b> copper 63.55	30 <b>Zn</b> zinc 65.39	31 <b>Ga</b> gallium 69.72	32 <b>Ge</b> germanium 72.58	33 <b>As</b> arsenic 74.92	34 <b>Se</b> selenium 78.96	35 <b>Br</b> bromine 79.90	36 <b>Kr</b> krypton 83.80
37 <b>Rb</b> rubidium 85.47	38 <b>Sr</b> strontium 87.62	39 <b>Y</b> yttrium 88.91	40 <b>Zr</b> zirconium 91.22	41 <b>Nb</b> niobium 92.91	42 <b>Mo</b> molybdenum 95.94	43 <b>Tc</b> technetium (98)	44 <b>Ru</b> ruthenium 101.1	45 <b>Rh</b> rhodium 102.9	46 <b>Pd</b> palladium 106.4	47 <b>Ag</b> silver 107.9	48 <b>Cd</b> cadmium 112.4	49 <b>In</b> indium 114.8	50 <b>Sn</b> tin 118.7	51 <b>Sb</b> antimony 121.8	52 <b>Te</b> tellurium 127.6	53 <b>I</b> iodine 126.9	54 <b>Xe</b> xenon 131.3
55 <b>Cs</b> cesium 132.9	56 <b>Ba</b> barium 137.3	57 <b>La*</b> lanthanum 138.9	72 <b>Hf</b> hafnium 178.5	73 <b>Ta</b> tantalum 180.9	74 <b>W</b> tungsten 183.8	75 <b>Re</b> rhenium 186.2	76 <b>Os</b> osmium 190.2	77 <b>Ir</b> iridium 192.2	78 <b>Pt</b> platinum 195.1	79 <b>Au</b> gold 197.0	80 <b>Hg</b> mercury 200.6	81 <b>Tl</b> thallium 204.4	82 <b>Pb</b> lead 207.2	83 <b>Bi</b> bismuth 208.9	84 <b>Po</b> polonium (209)	85 <b>At</b> astatine (210)	86 <b>Rn</b> radon (222)
87 <b>Fr</b> francium (223)	88 <b>Ra</b> radium (226)	89 <b>Ac~</b> actinium (227)	104 <b>Rf</b> rutherfordium (261)	105 <b>Db</b> dubnium (262)	106 <b>Sg</b> seaborgium (263)	107 <b>Bh</b> bohrium (264)	108 <b>Hs</b> hassium (265)	109 <b>Mt</b> meitnerium (266)	110 <b>Ds</b> darmstadtium (271)	111 <b>Uuu</b> ununoctium (272)	112 <b>Uub</b> unbihassium (277)	113 <b>Uuq</b> unquincium (296)	114 <b>Uuh</b> unhexium (298)	115 <b>Uuq</b> unpentium (298)	116 <b>Uuh</b> unhexium (298)	117 <b>Uuq</b> unquincium (298)	118 <b>Uuo</b> unbinilium (?)

# Electric field control of symmetry breaking in SrIrO<sub>3</sub> ultrathin layers

F. Gallego<sup>1,2</sup>, A. Peralta<sup>1</sup>, J. Tornos<sup>1</sup>, **J. I. Beltran<sup>1</sup>**, Javier Garcia-Barriocanal<sup>3</sup>, Guichuan Yu<sup>3,4</sup>, Geoffrey Rojas<sup>3</sup>, C. Munuera<sup>2,5</sup>, M. Cabero<sup>6,7</sup>, D. Sanchez-Manzano<sup>1</sup>, F. Cuellar<sup>1</sup>, G. Sanchez-Santolino<sup>1,2</sup>, Z. Sefrioui<sup>1,5</sup>, A. Rivera-Calzada<sup>1,5</sup>, F. J. Mompean<sup>2,5</sup>, M. Garcia-Hernandez<sup>2,5</sup>, C. Leon<sup>1,5</sup>, **M. C. Muñoz<sup>8</sup>** and J. Santamaria<sup>1,5</sup>

F. Gallego et al. Communications Materials 4 (1), 36 (2023)

# 5d oxides



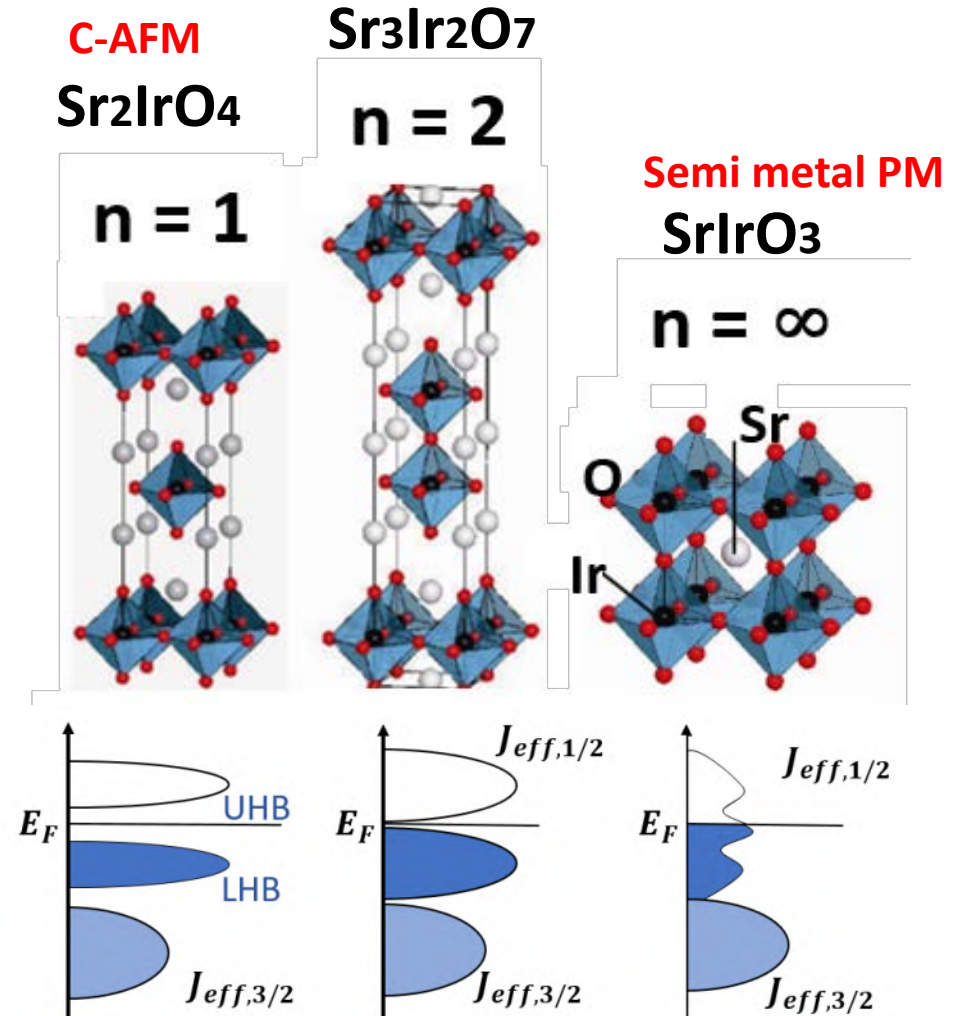
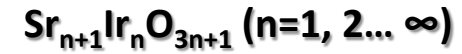
Witczak-Krempa et. al, *Annu. Rev. Condens. Matter Phys.* 5, 57–82 (2014).

B. J. Kim et. al, *Phys. Rev. Lett.*, 101, 076402 (2008)

S. J. Moon et al. *Phys. Rev. Lett.* 101, 226402 (2008)

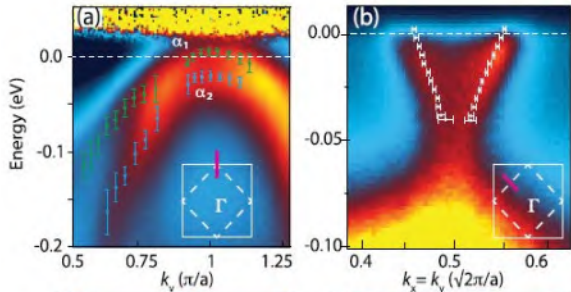
Y. Okada et al. *Nat.Mater.*12,707 (2013)

## Ruddlesden-Popper series:



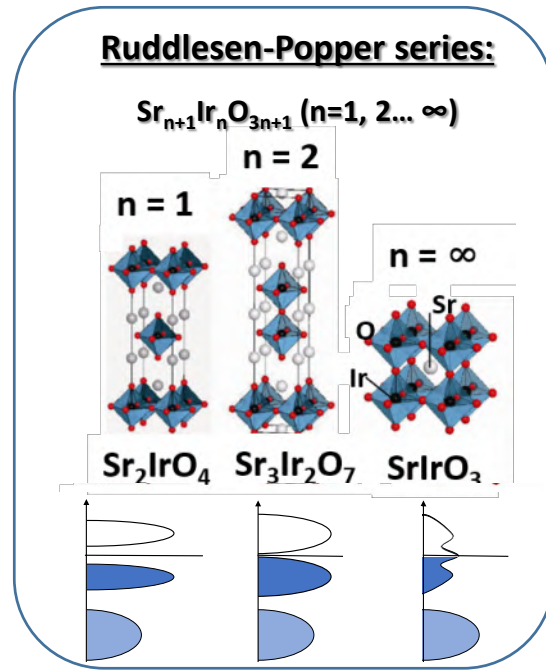
# SrIrO<sub>3</sub>

Narrow band semimetal

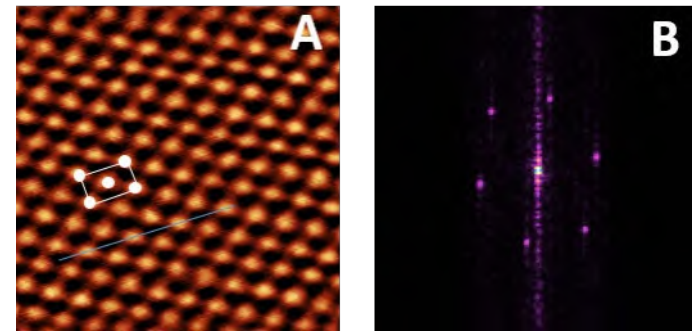
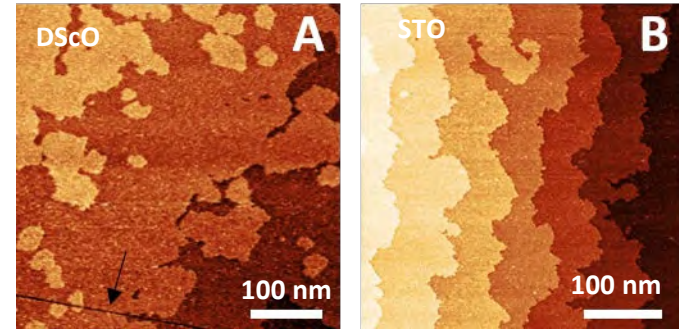


Y. F. Nie et al. Phys. Rev. Lett. 114, 016401 (2015)

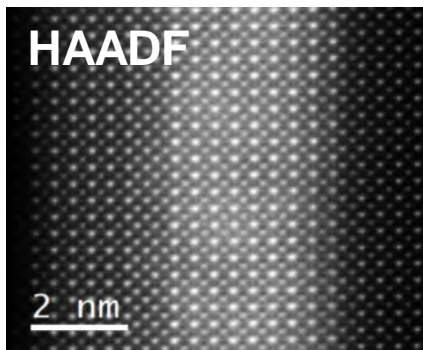
**Spin-orbit coupling**  
+  
**Strong Correlations**



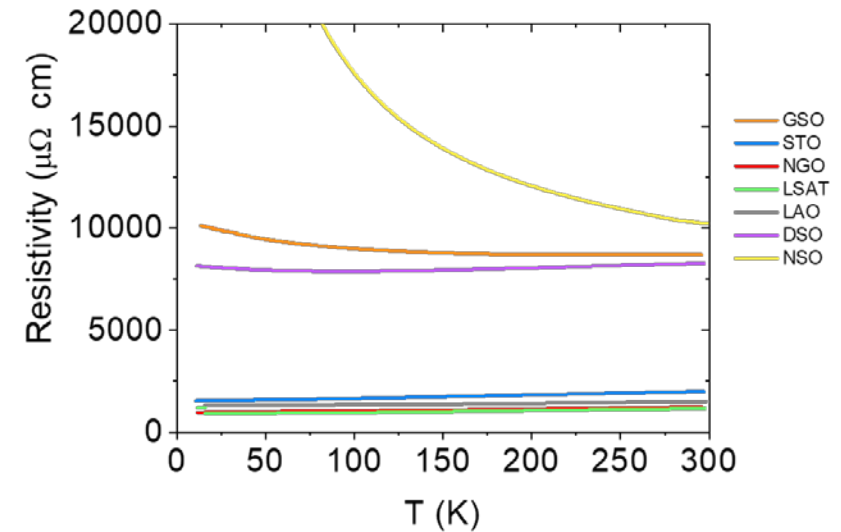
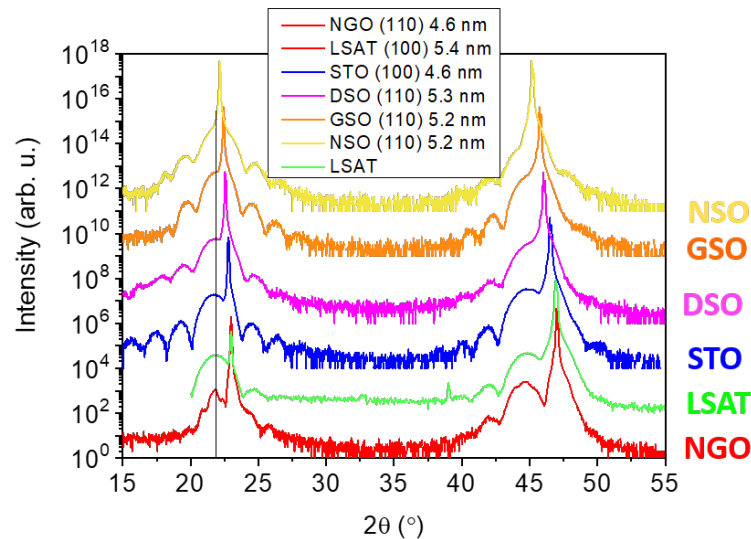
STM @ Char. Fac. U. Minnesota



Epitaxial ultra-thin layers

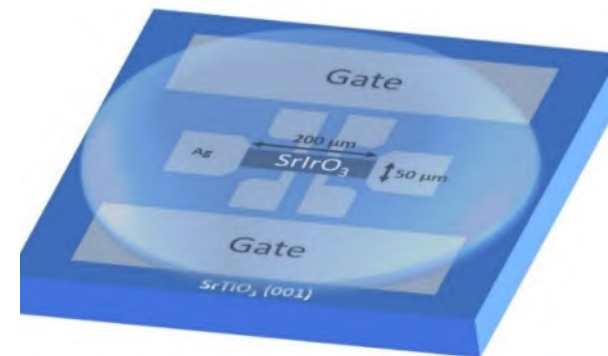
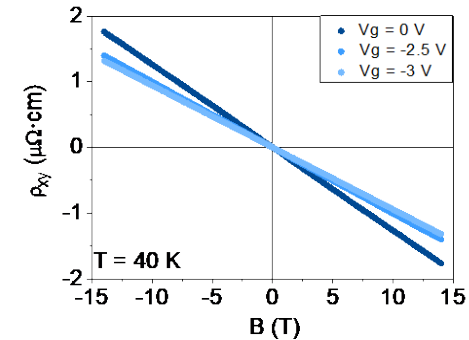
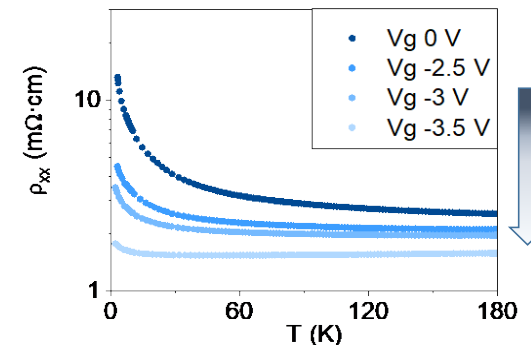
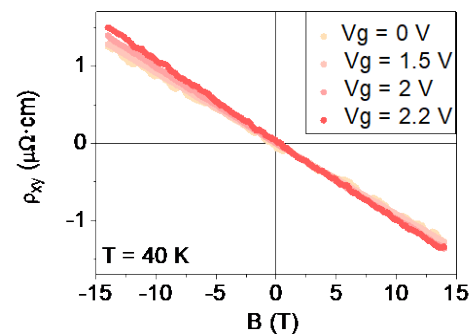
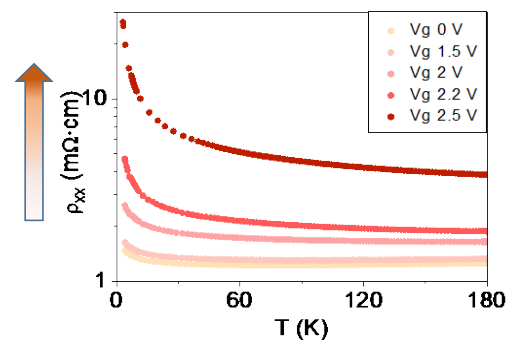
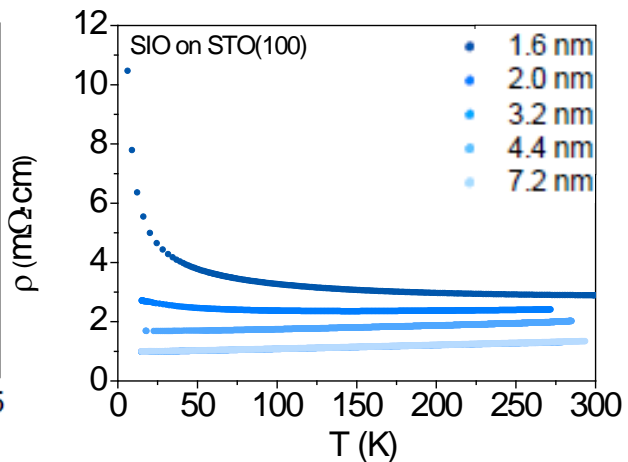
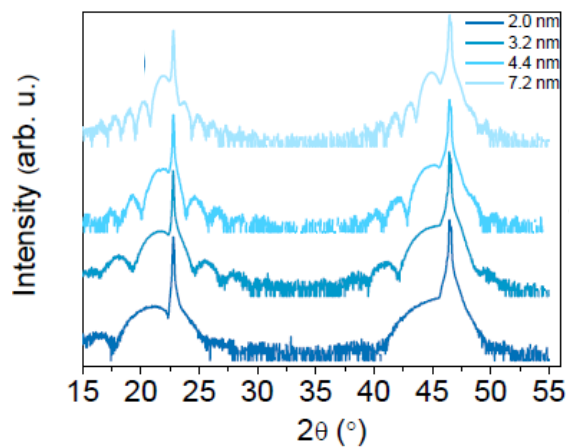


La<sub>0.7</sub>Sr<sub>0.3</sub>MnO<sub>3</sub> ■ SrIrO<sub>3</sub> ■ SrTiO<sub>3</sub>



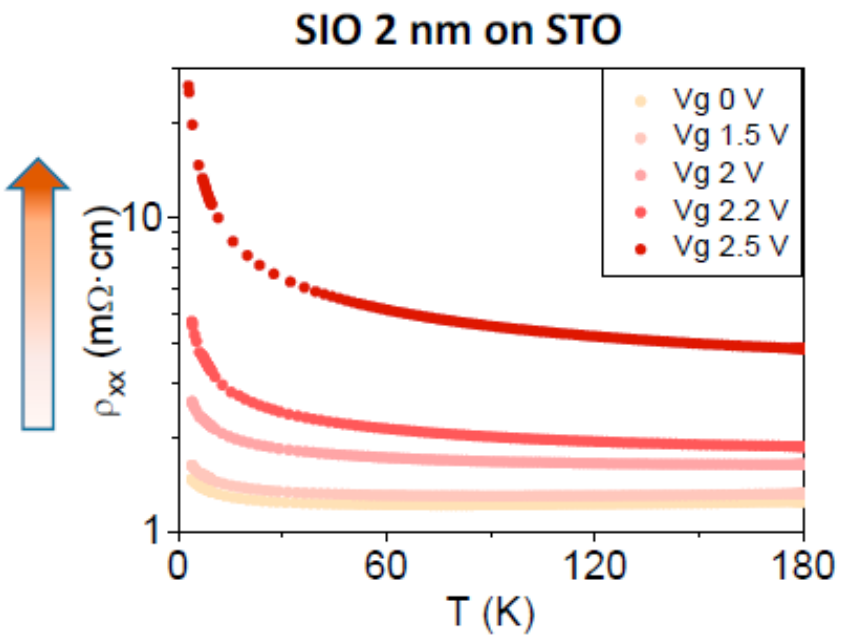
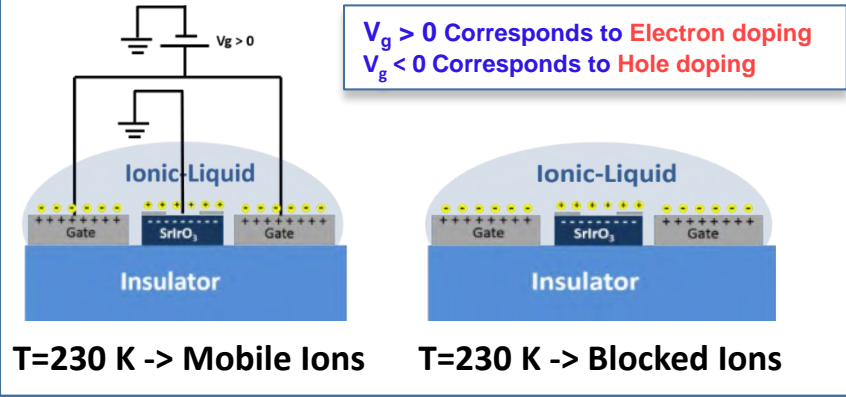
**Structure and transport of SrIrO<sub>3</sub> ultrathin films. Epitaxial strain**

### SrIrO<sub>3</sub> grown on STO

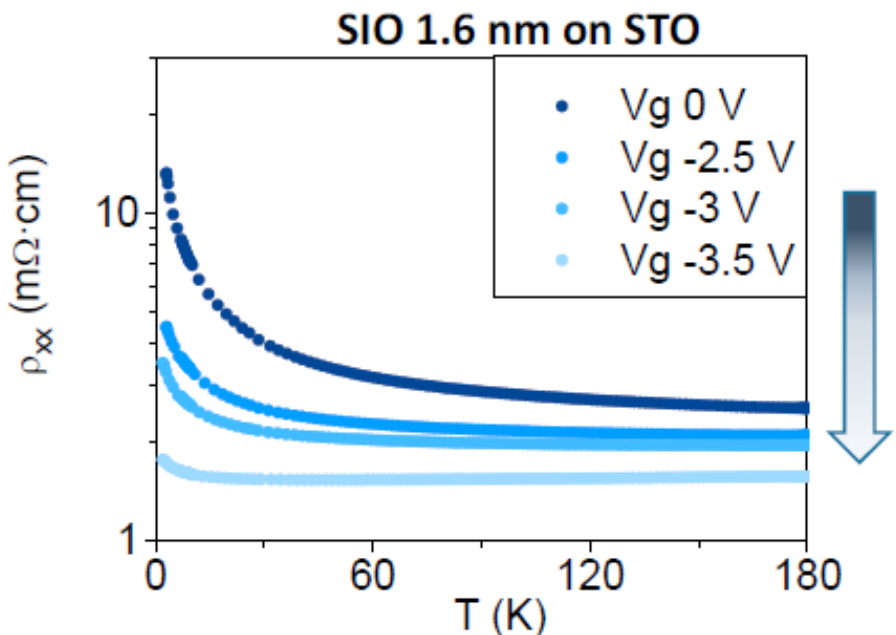


# Resistivity measurements

Unexpected electric field effect **beyond** electrostatic doping



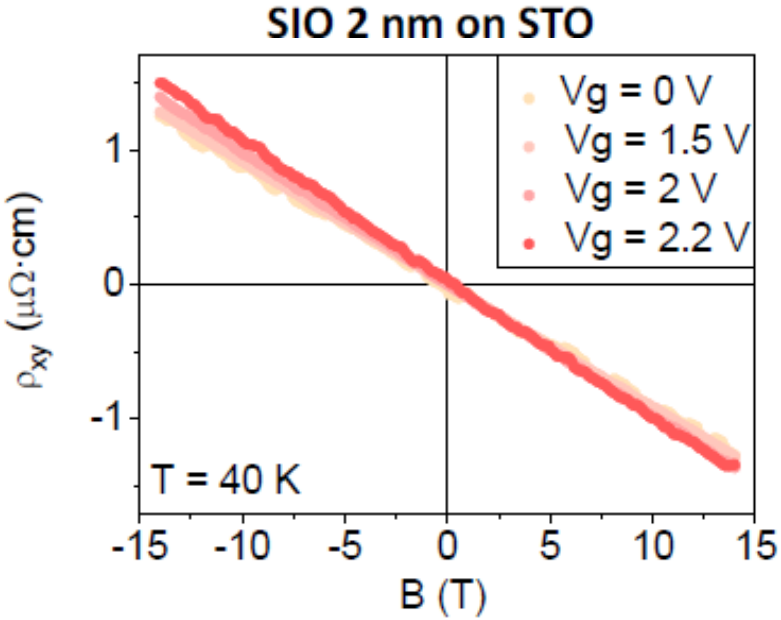
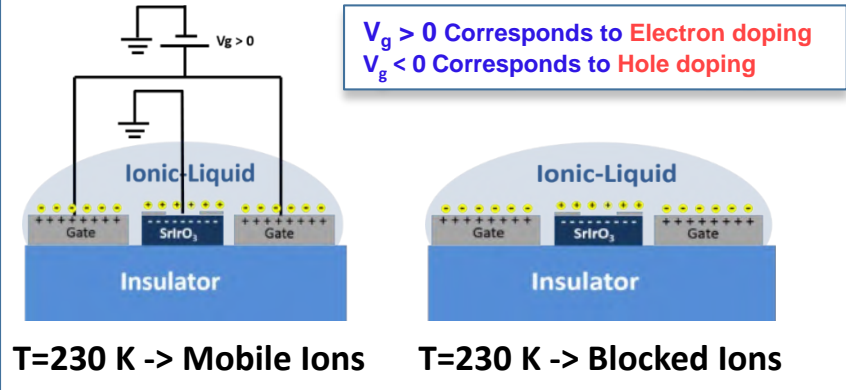
Expected electron doping ➔ Insulating state



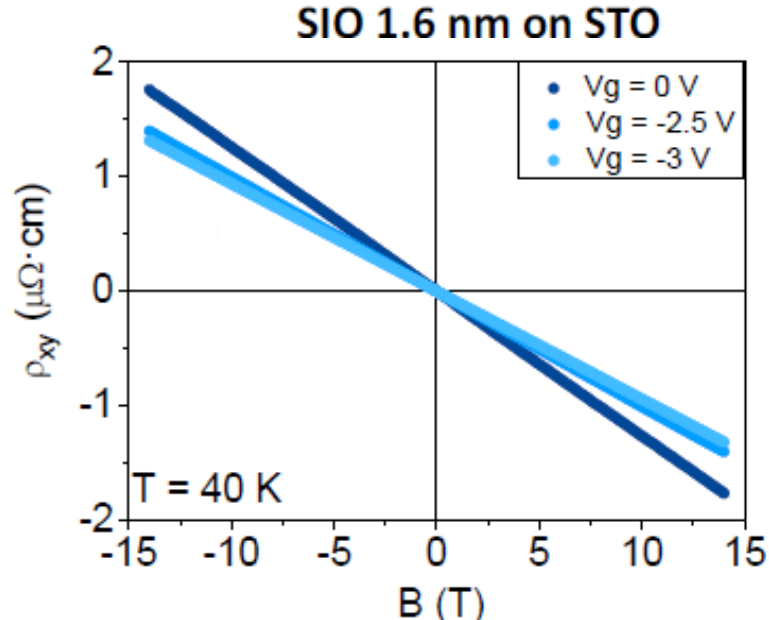
Expected hole doping ➔ Metallic state

# Hall effect measurements

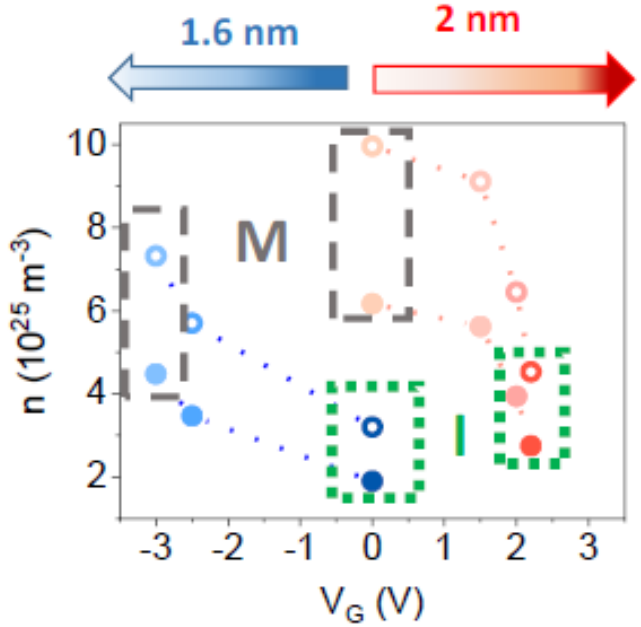
Unexpected electric field effect **beyond** electrostatic doping



Expected electron doping  
 ↓  
 Reduce electron densities



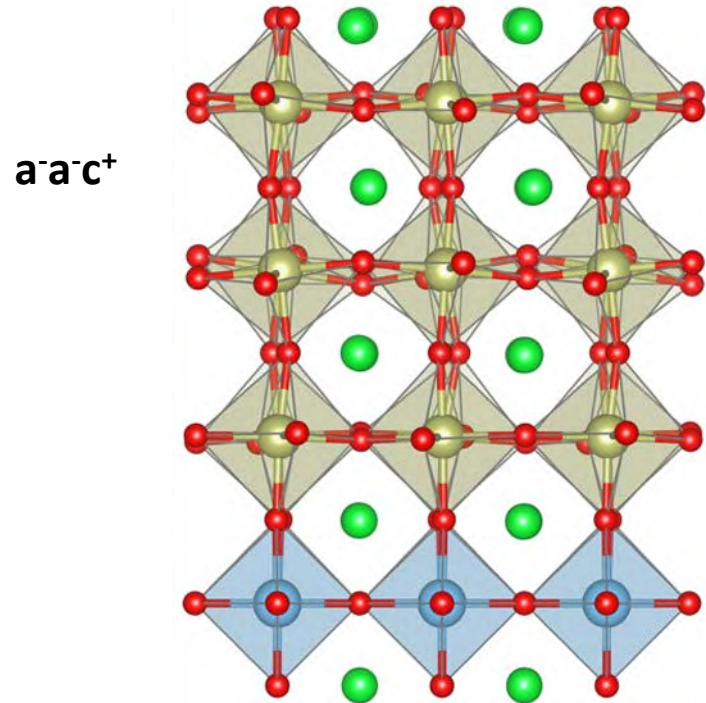
Expected hole doping  
 ↓  
 Increase electron densities



As the result of the reduced carrier density, screening effects on the charge density are less important

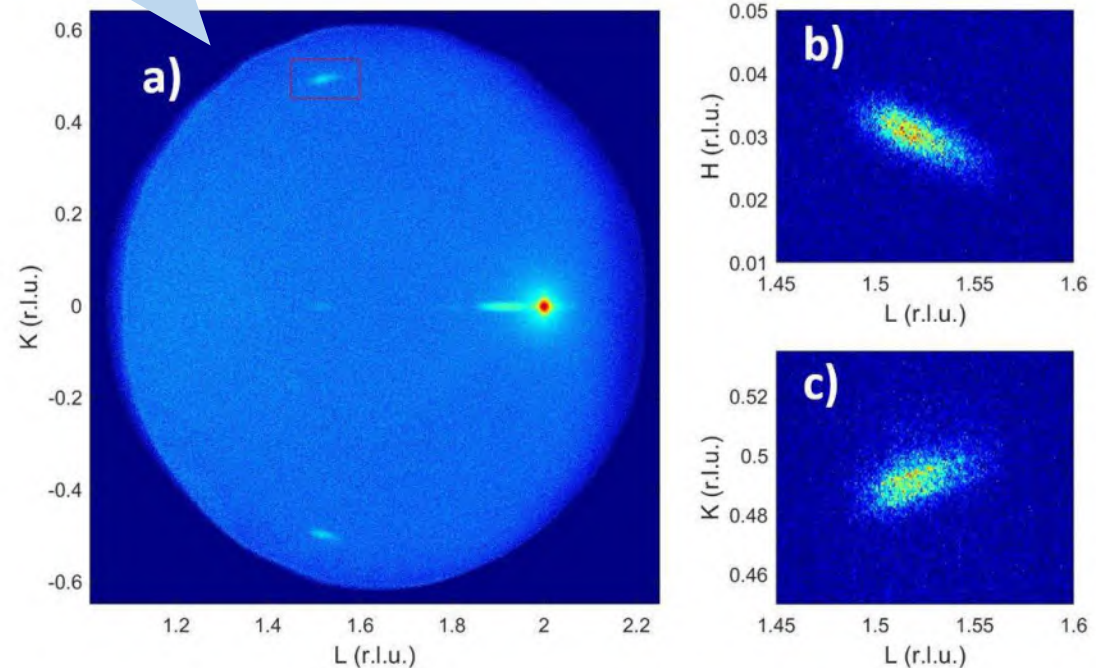
# DFT calculations

Juan Beltrán M.C. Muñoz @IMM-CSIC



Octahedral rotations

## X-ray reciprocal space maps



Asymmetric (001)  $SiO_m/STO$  slabs with two free SrO surfaces

The external electric field is added via a sawtoothlike potential, and conventional dipole corrections are used

For  $m \leq 2$  the films are insulators and a MIT occurs for  $m = 3$

In plane rotations  $a^0a^0c^-$  below 1 nm

Bulk  $\rightarrow a^-a^-c^+$  octahedral rotations

# DFT calculations

The external electric field is added via a sawtoothlike potential, and conventional dipole corrections are used

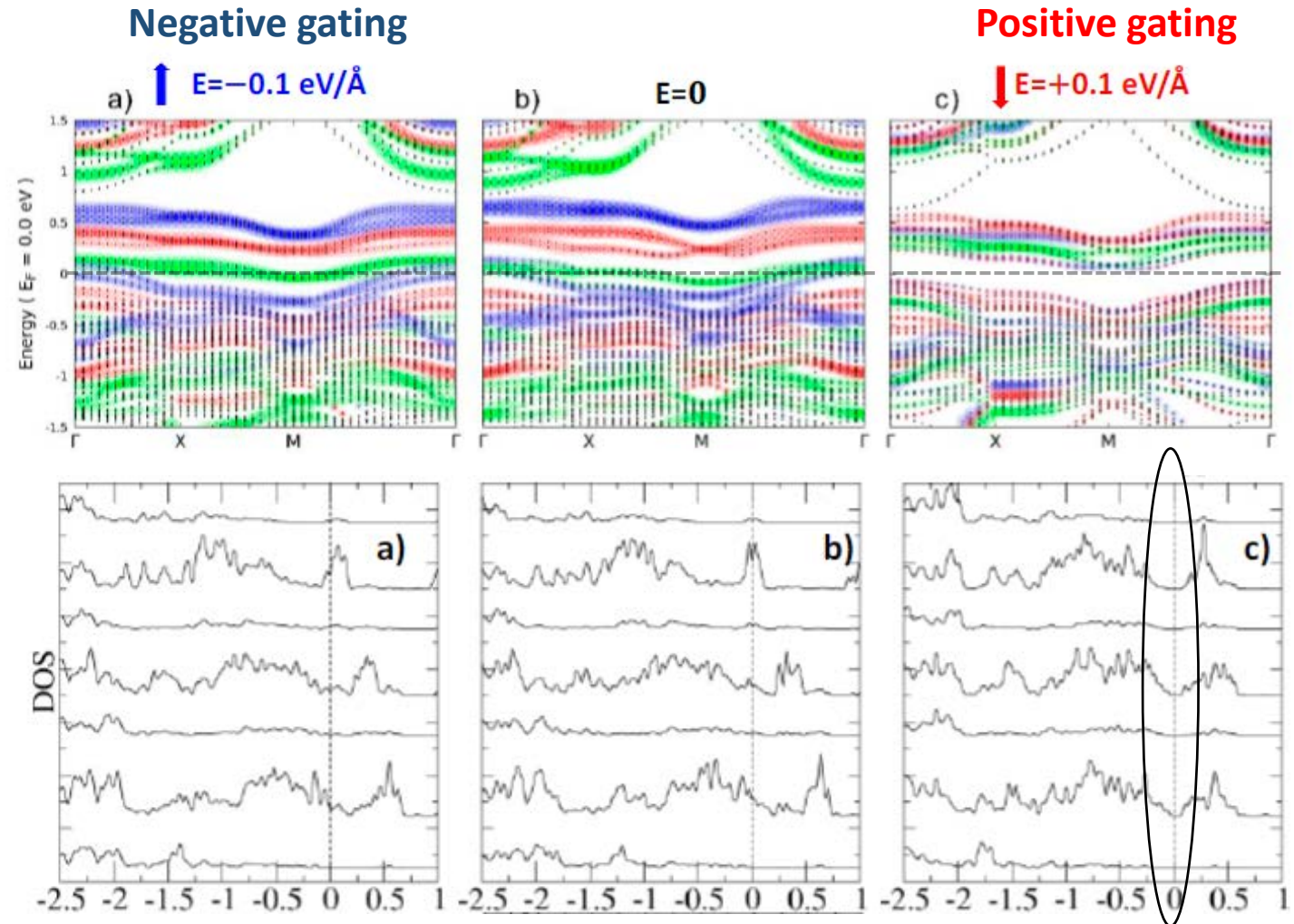
Meyer, B. & Vanderbilt *Phys. Rev. B* (2001)

Negative electric field increase film asymmetry

Positive electric field reduce film asymmetry

Compensation of the intrinsic asymmetry field of the film grown on STO

**GAP opening**



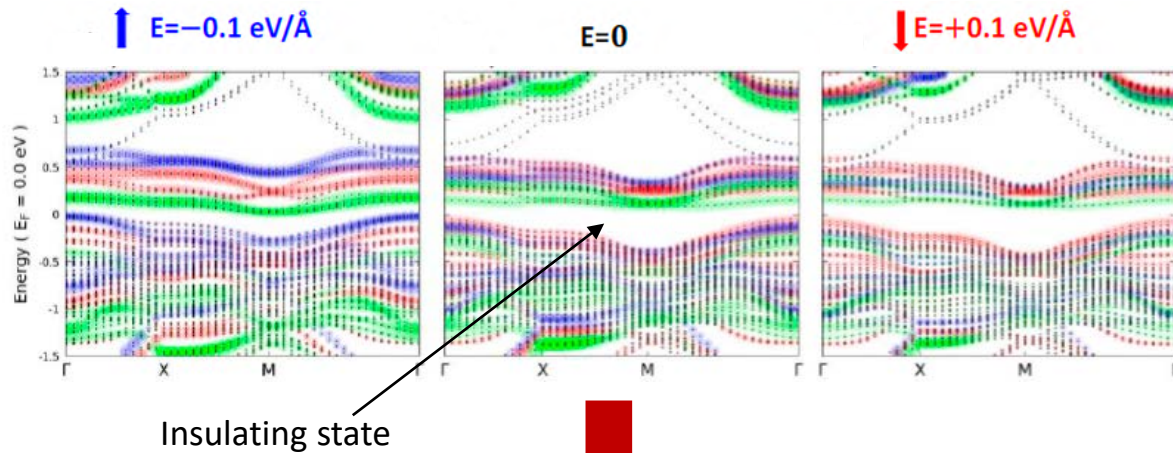
F. Gallego et al. *Communications Materials* 4 (1), 36 (2023)

**GAP**

*SrIrO3 ultrathin films on STO. Electric Field effect to tune the MIT*

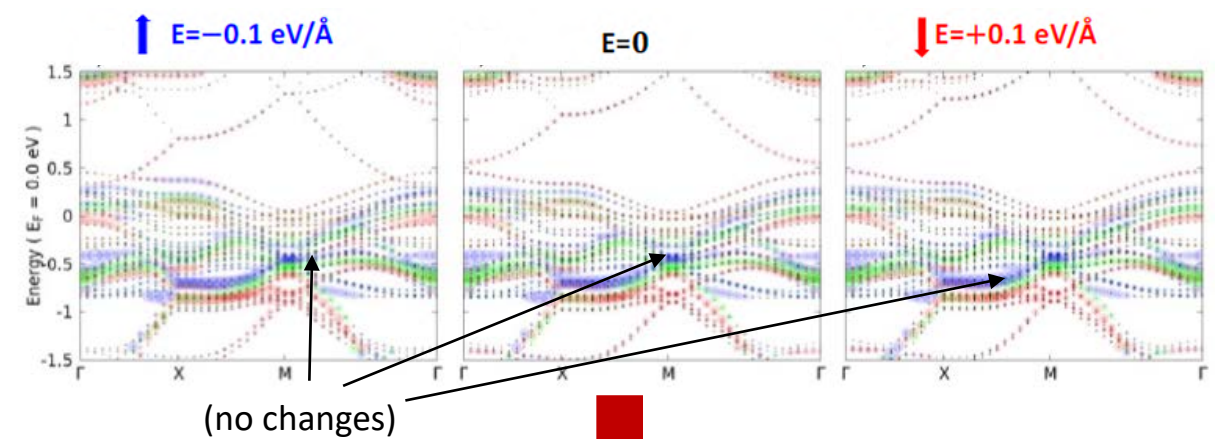
# DFT calculations

DFT simulations without STO layers



Symmetry breaking introduced by STO is similar to a negative electric field

DFT simulations not including spin-orbit interaction



Spin orbit interaction required for the coupling between the electronic structure and the electric field

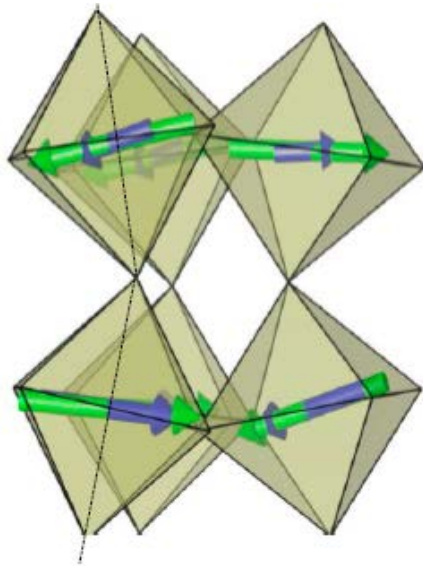
**Fundamental interplay:**  
**symmetry breaking + spin orbit coupling + electric field**

# Anomalous Hall effect

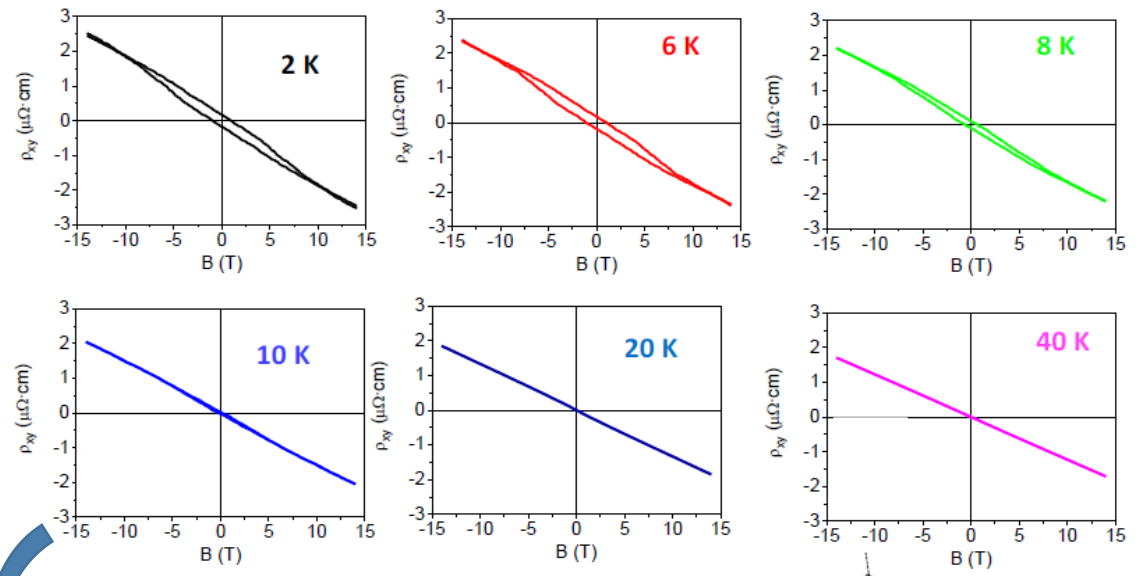
Insulator phase under positive field presents canted orbital ( $0.26 \mu_B$ ) and spin ( $0.17 \mu_B$ ) moments yielding out of plane components of  $0.04 \mu_B$  and  $0.02 \mu_B$  respectively.



Canting of the magnetic moments associated with the rotation and tilting of the  $\text{IrO}_6$  octahedra

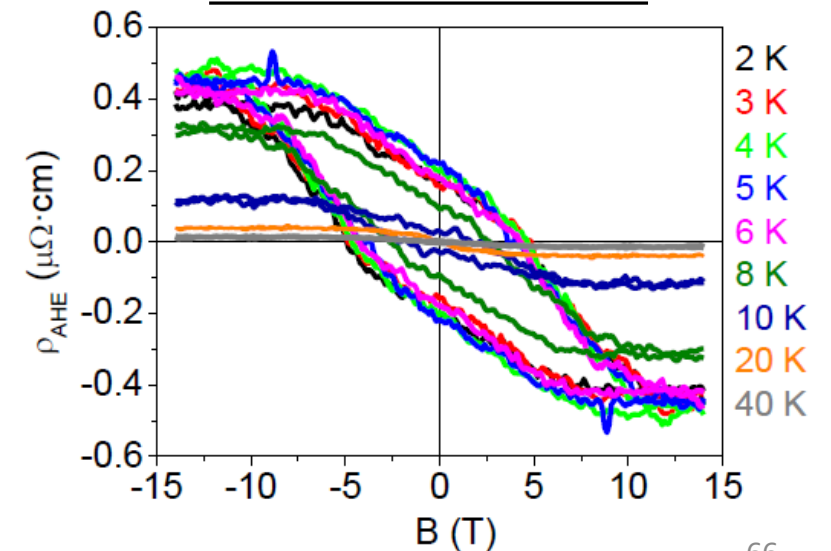


SrTiO<sub>3</sub> 2 nm on STO Hall effect



Subtraction of the linear component

Anomalous Hall effect



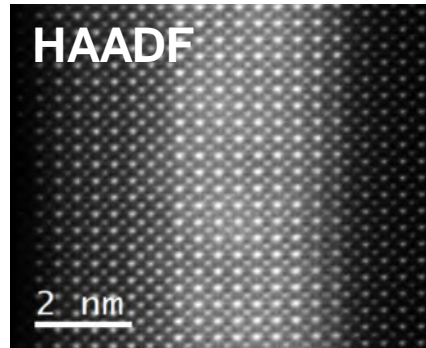
# Conclusions

- **We have shown a new perspective of ionic liquid gating producing effects on the electronic structure beyond doping**
- **Large electric fields couple strongly to the electronic structure producing deep modifications in SrIrO<sub>3</sub> ultrathin films.**
- **Electric field controlled symmetry breaking provides an effective knob to modulate the effective strength of the correlations yielding the MIT transition.**

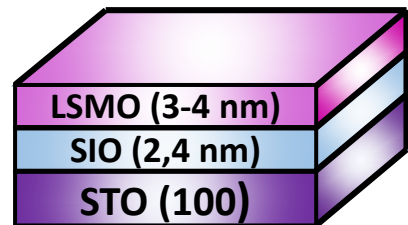
# Large topological Hall effect and spin textures in $\text{La}_{0.7}\text{Sr}_{0.3}\text{MnO}_3$ / $\text{SrIrO}_3$ bilayers

A. Peralta-Somoza , S. López , J.J. Riquelme, J. Tornos , Víctor Zamora, I. Barbero, D. Sánchez-Manzano, F. A. Cuellar, Sergio Valencia, C. Munuera, F. Mompeán, M. GarcíaHernández, C. León and Jacobo Santamaría

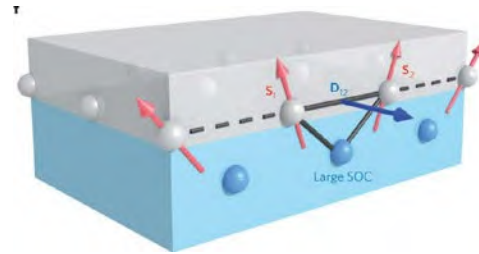
## Epitaxial ultra-thin layers



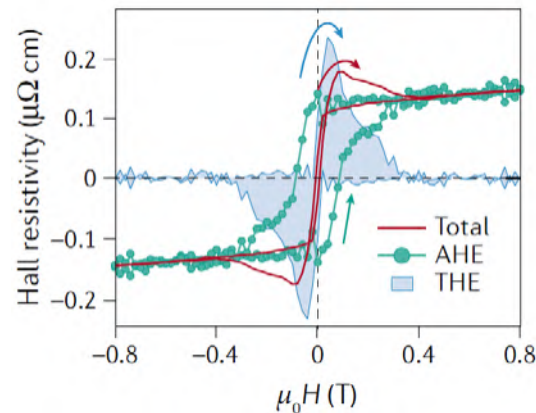
Experiment proposed to generate spin textures



## Spin textures



Fert, A. et al. Skyrmions on the track. *Nature Nanotech* **8**, 152–156 (2013).



J. Matsuno et al., *Sci. Adv.* **2**, (2016).

### Dzyaloshinskii-Moriya Interaction (DMI)

- ✓ Strong Spin-Orbit Coupling
- ✓ Breaking of inversion Symmetry

$$H_{DM} = \vec{D}_{ij} \cdot (S_i \times S_j)$$



# Magnetic textures

Interfaces 5d/3d

Spin-orbit coupling + Symmetry breaking



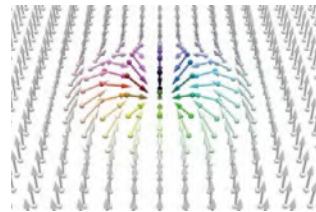
$$E_{DM} = \sum_{i,j} \mathbf{D}_{ij} \cdot (\mathbf{S}_i \times \mathbf{S}_j)$$



$$E_H = \sum_{i,j} J_{ij} \mathbf{S}_i \cdot \mathbf{S}_j$$

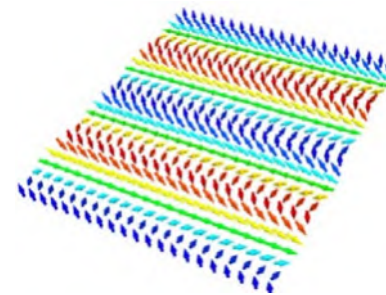
- I. Dzyaloshinsky, «A thermodynamic theory of “weak” ferromagnetism of antiferromagnetics», *J. Phys. Chem. Sol* 4, 241 (1958)
- T. Moriya, «Anisotropic Superexchange Interaction and Weak Ferromagnetism», *Phys. Rev.*, 120, 91 (1960)
- A. Fert y P. M. Levy, «Role of anisotropic exchange interactions in determining the properties of spin-glasses», *PRL*, 44, 1538 (1980).

## Skyrmions



Trier, F., Noël, P., Kim, J.V. *et al.* *Nat Rev Mater* 7, 258–274 (2022).

## Spirals



Wang, S. *et al.* *J Low Temp Phys* 197, 321–336 (2019)

M. Bode *et al.*, «Chiral magnetic order at surfaces driven by inversion asymmetry», *Nature*, 447, 190 (2007)

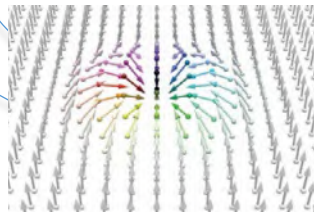
# Magnetic textures

Interfaces 5d/3d

Spin-orbit coupling + Symmetry breaking

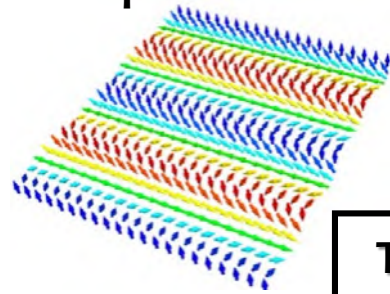


Skyrmions



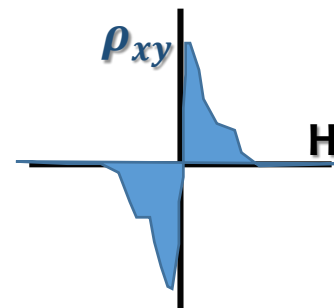
Trier, F., Noël, P., Kim, J.V. et al. *Nat Rev Mater* **7**, 258–274 (2022).

Spirals



Wang, S. et al. *J Low Temp Phys* **197**, 321–336 (2019)

Topological Hall Effect (THE)



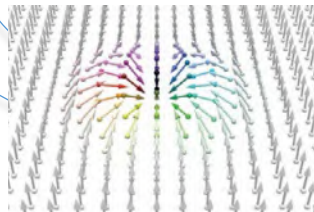
# Magnetic textures

Interfaces 5d/3d

Spin-orbit coupling + Symmetry breaking

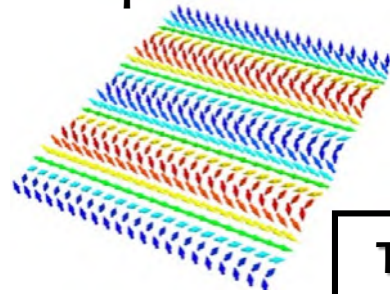


**Skyrmions**



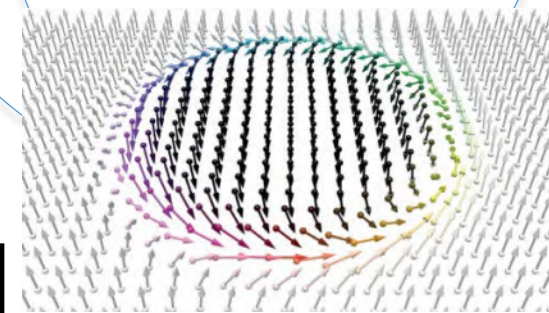
Trier, F., Noël, P., Kim, J.V. *et al.* *Nat Rev Mater* **7**, 258–274 (2022).

**Spirals**



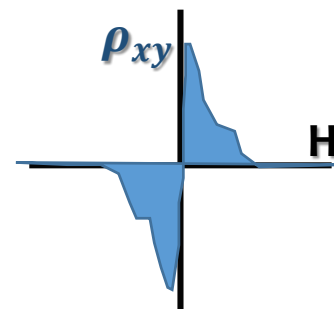
Wang, S. *et al.* *J Low Temp Phys* **197**, 321–336 (2019)

**Bubbles**



Trier, F., Noël, P., Kim, J.V. *et al.* *Nat Rev Mater* **7**, 258–274 (2022).

**Topological Hall Effect (THE)**



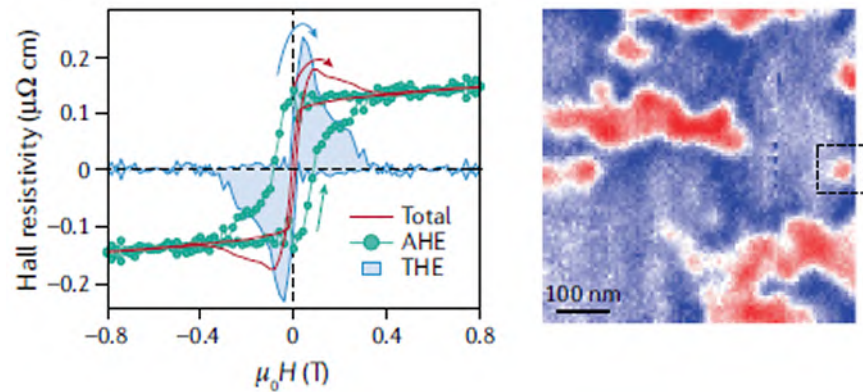
A. Fert, N. Reyren, y V. Cros, «Magnetic skyrmions: advances in physics and potential applications», *Nature Reviews Materials*, **2**, 7 (2017)

N. Nagaosa y Y. Tokura, «Topological properties and dynamics of magnetic skyrmions», *Nature nanotechnology*, **8**, 12 (2013)

A.P. Malozemoff y J. C. Slonczewski, «Magnetic Domain Walls in Bubble Materials (Academic)», *New York*, 1979.  
W. Jiang *et al.*, «Blowing magnetic skyrmion bubbles», *Science* **349**, 6245 (2015).

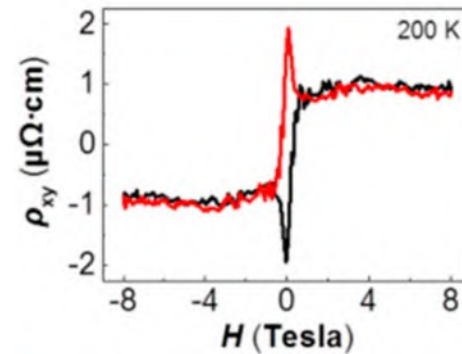
# Magnetic textures in correlated oxides

SrRuO<sub>3</sub> (5 u.c.) / SrIrO<sub>3</sub> (2 u.c.)



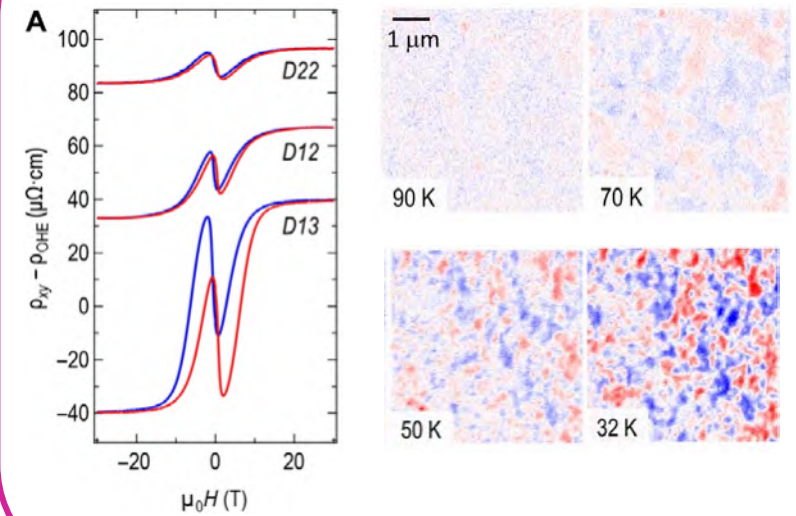
Matsuno, J. et al. *Sci. Adv.* **2** (2016)

La<sub>0.7</sub>Sr<sub>0.3</sub>MnO<sub>3</sub> (8 u.c.) / SrIrO<sub>3</sub> (2 u.c.)



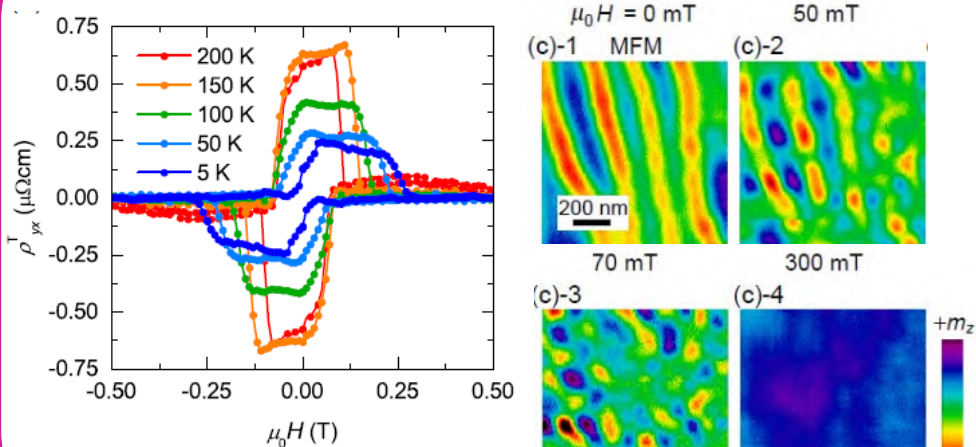
Yao Li et al. *ACS Appl. Mater. Interfaces* (2019), 11, 23

$[(\text{LaMnO}_3)_n/(\text{SrIrO}_3)_n]_m$



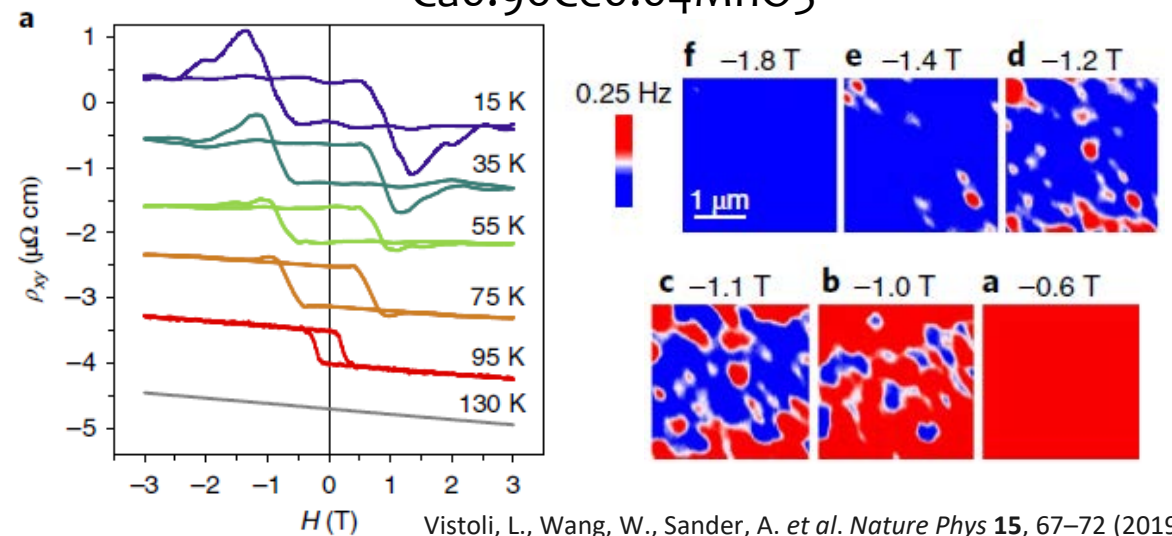
Skoropata E et al. *Sci Adv.* (2020)

La<sub>0.7</sub>Sr<sub>0.3</sub>Mn<sub>1-y</sub>Ru<sub>y</sub>O<sub>3</sub>



M. Nakamura et al. *J. Phys. Soc. Jpn.* **87**, 074704 (2018)

Ca<sub>0.96</sub>Ce<sub>0.04</sub>MnO<sub>3</sub>

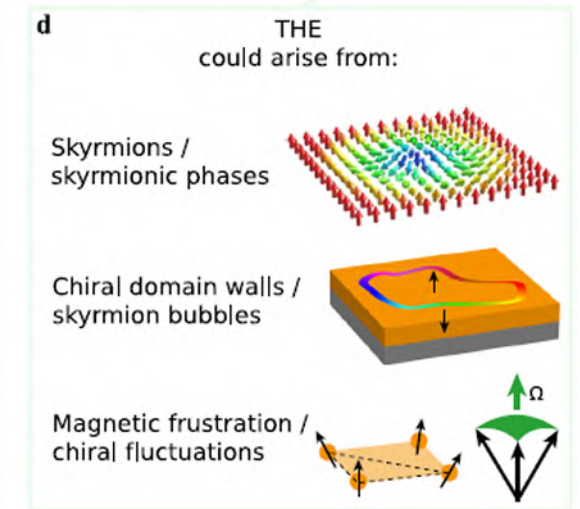
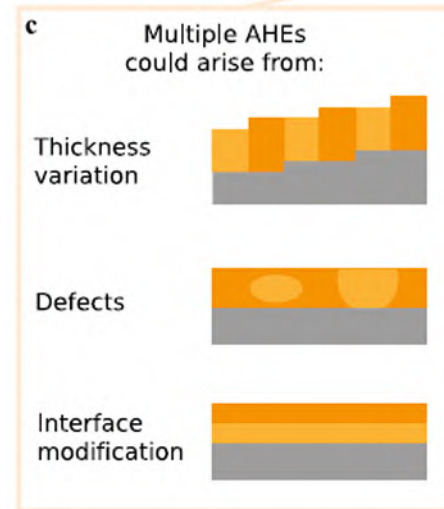
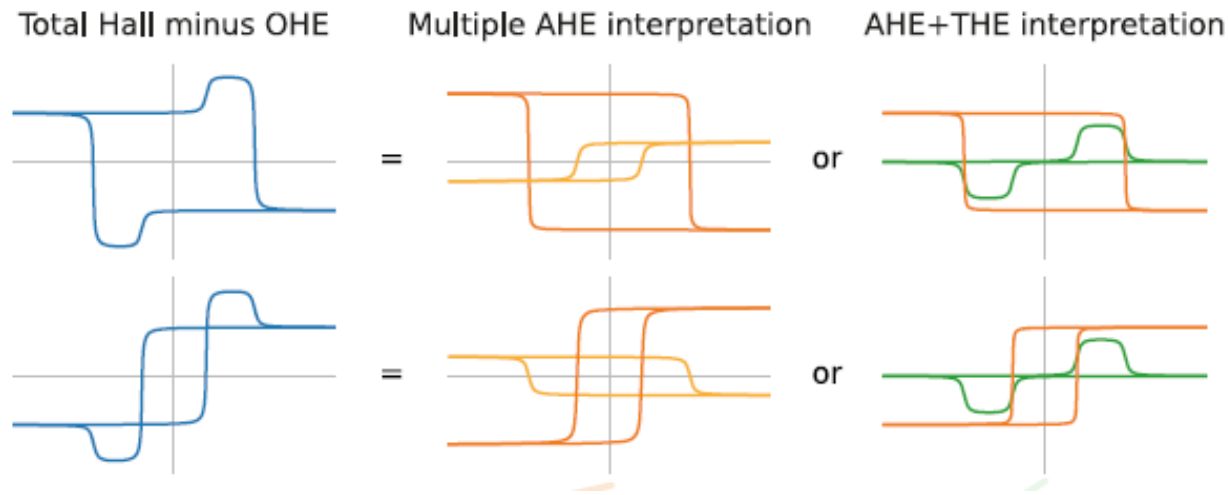


Vistoli, L., Wang, W., Sander, A. et al. *Nature Phys* **15**, 67–72 (2019)

# The debate

(1) Discrepancies between the skyrmion densities obtained from THE and MFM observations.

(2) Inhomogeneities may yield inhomogeneous multicomponent anomalous Hall effect which can be mistaken with THE. (TC van Thiel *et al* 2020 *J. Phys. Mater.*) (Groenendijk, D. J. *et al.* *Phys. Rev. Res.* 2, (2020))



Kimbell, G., Kim, C., Wu, W. *et al.* *Commun Mater* 3, 19 (2022)

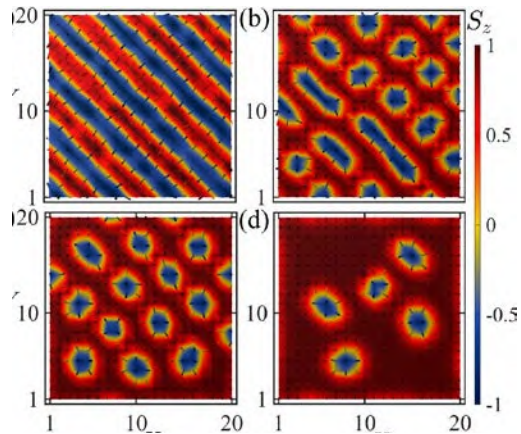
# Experiment

Hall Effect + MFM & PEEM

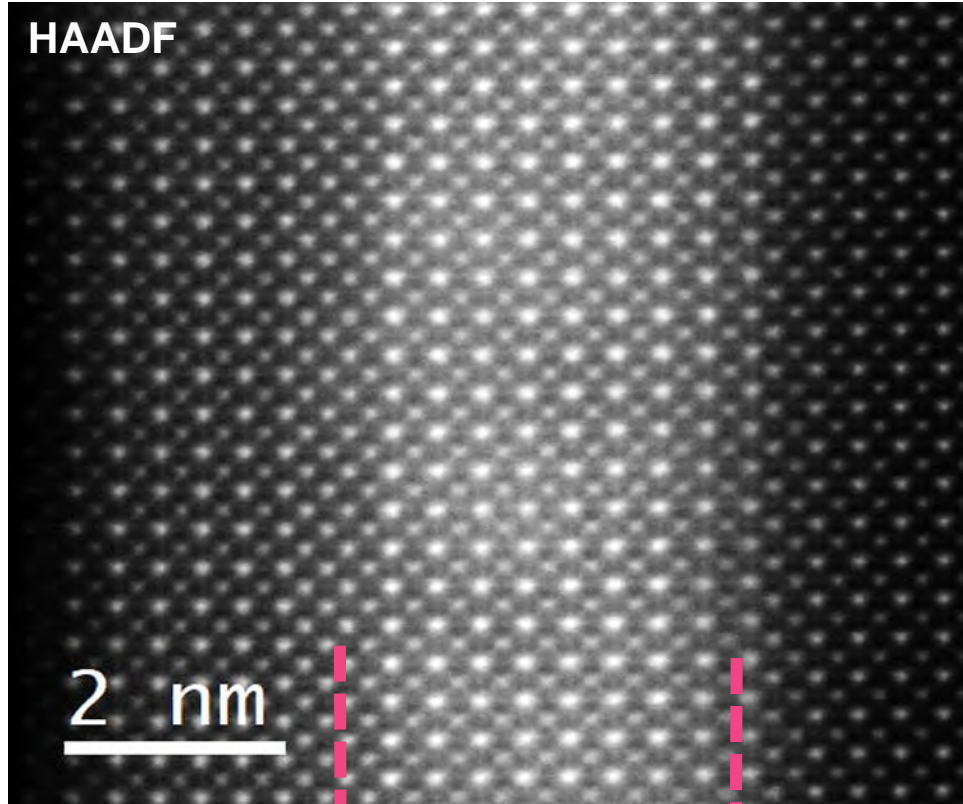
LSMO (3.5 nm)

SrO (2.4 nm)

STO (100)

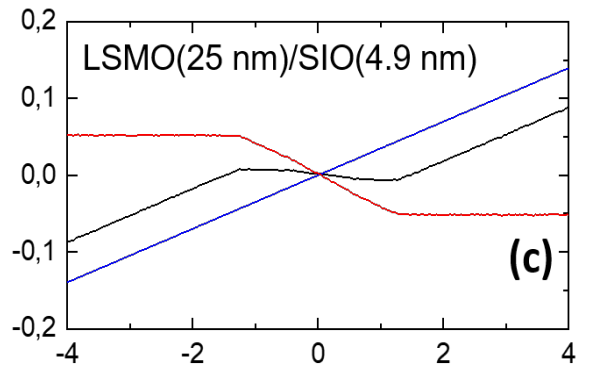
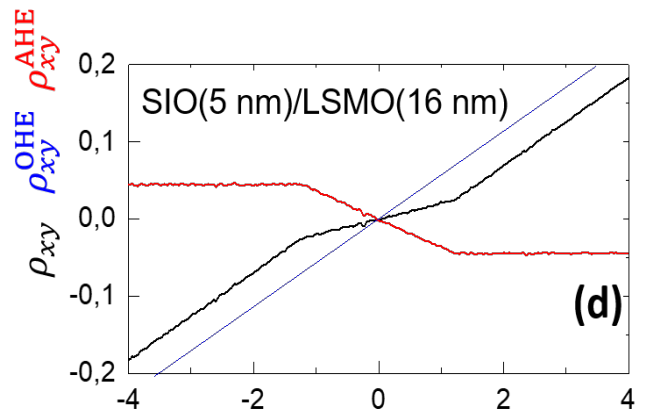
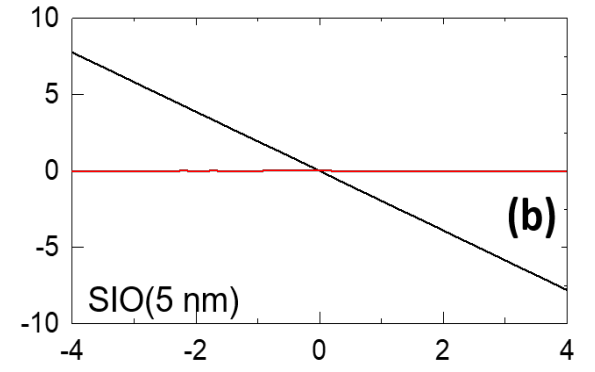
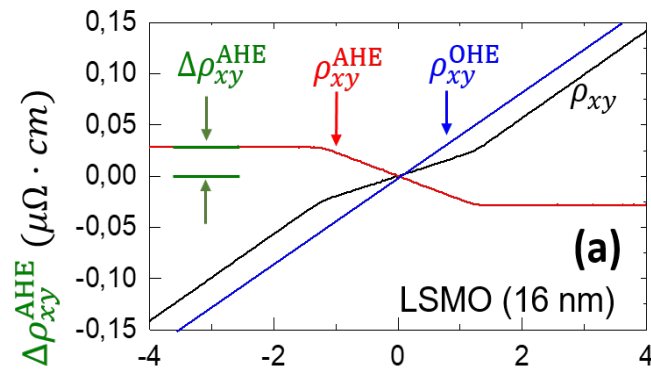
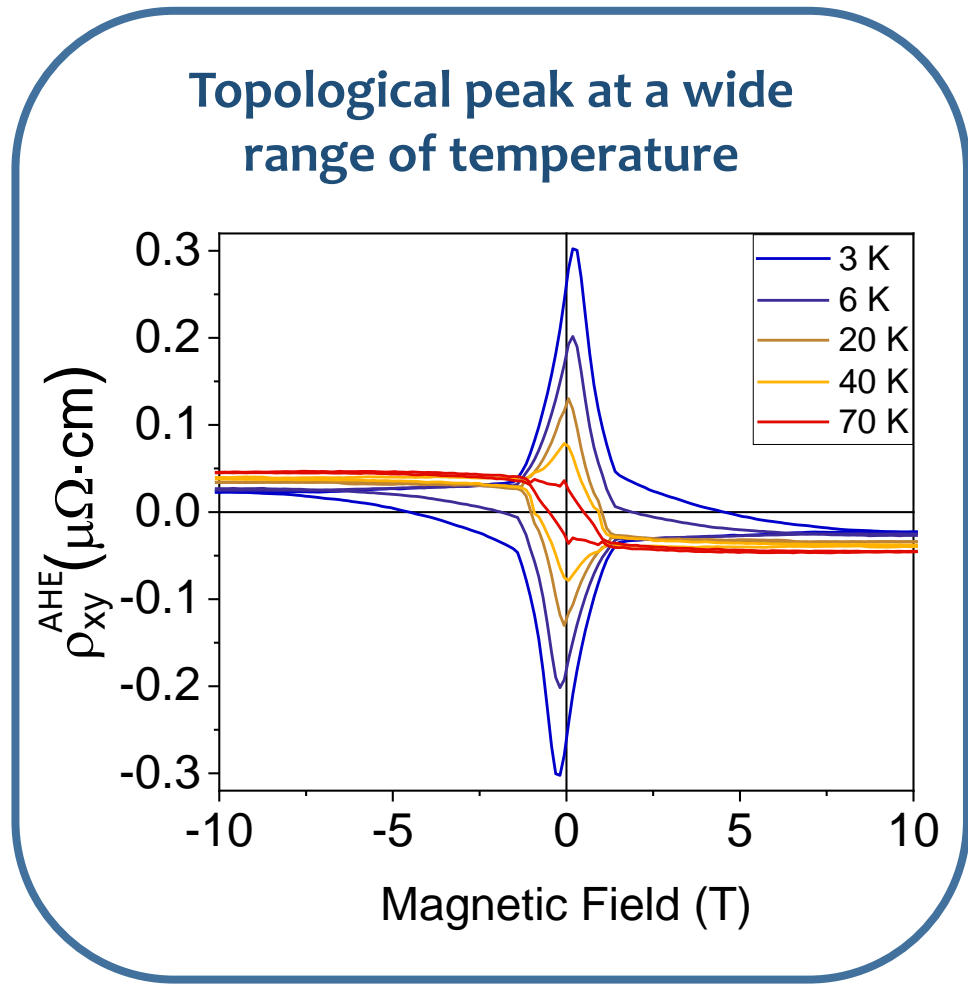


Mohanta, Dagotto, and Okamoto  
Physical Review B **100**, 064429 (2019)



$\text{La}_{0.7}\text{Sr}_{0.3}\text{MnO}_3$  |  $\text{SrIrO}_3$  |  $\text{SrTiO}_3$

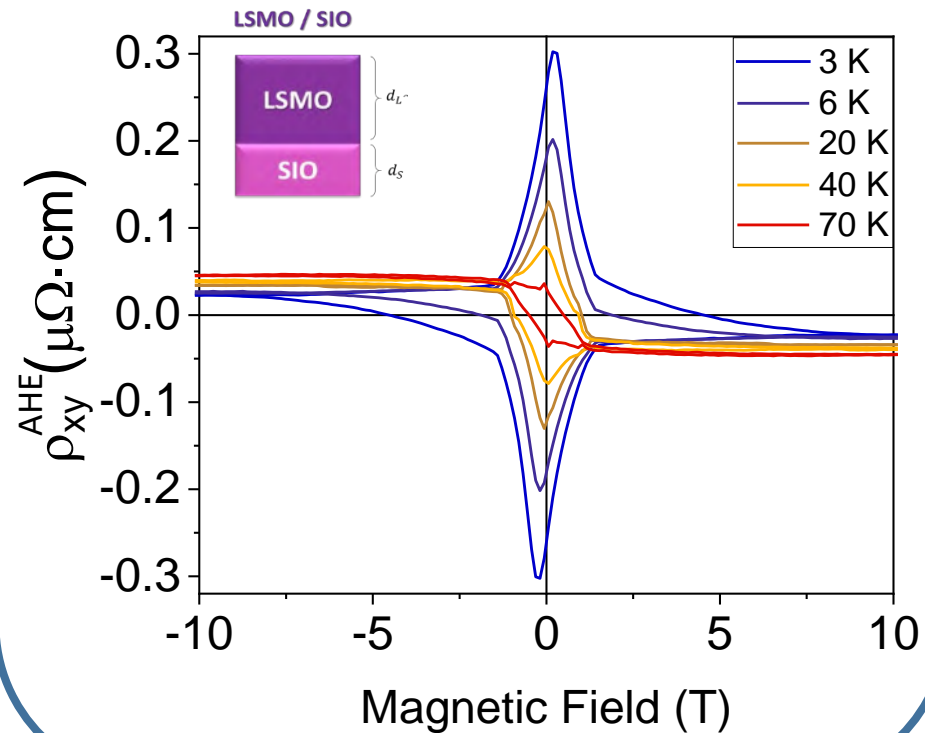
# THE and MFM/PEEM images



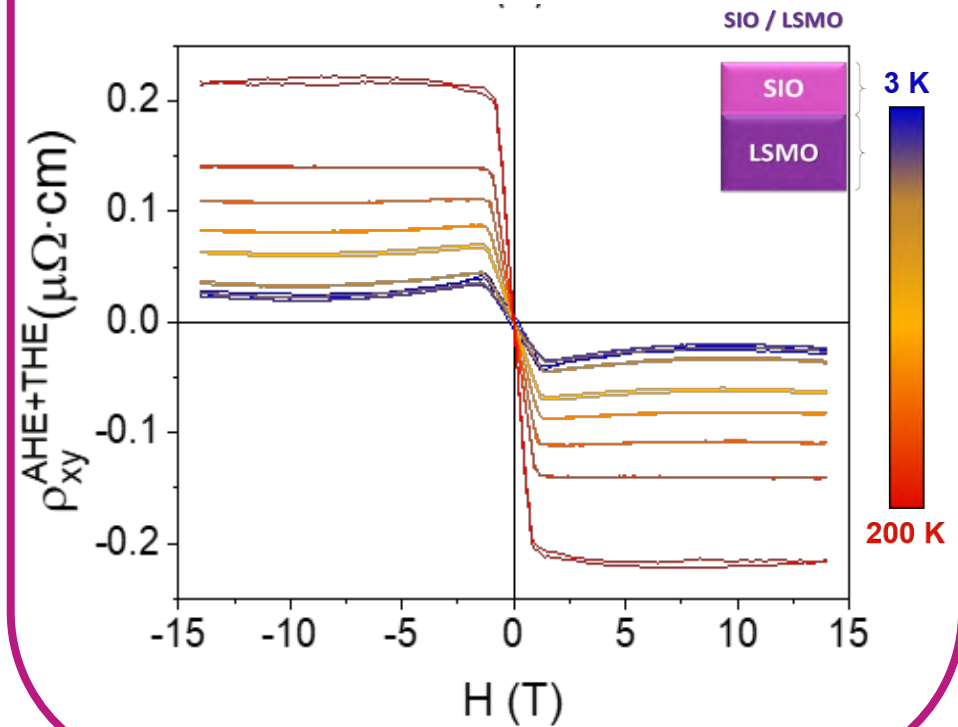
Nature Communications 12 (1), 3283 (2021)

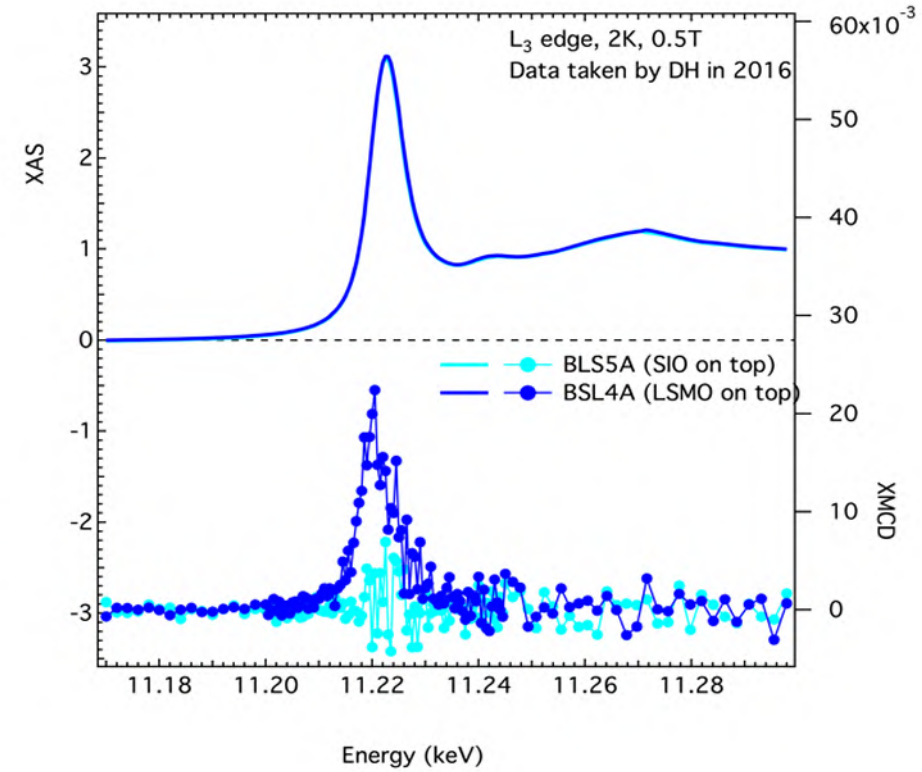
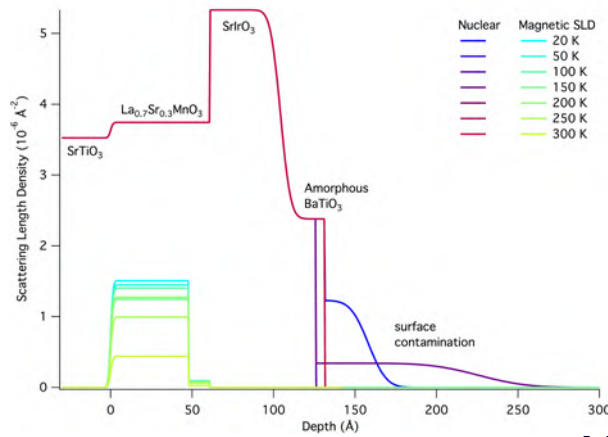
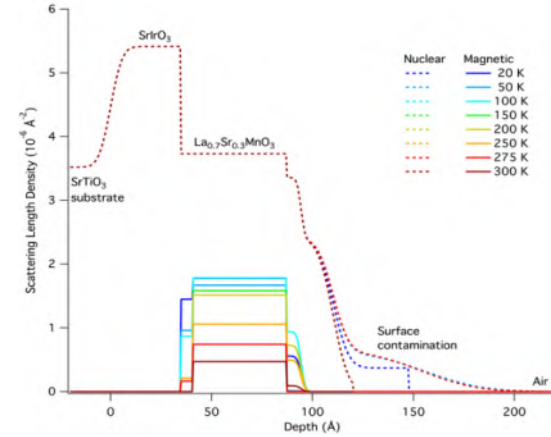
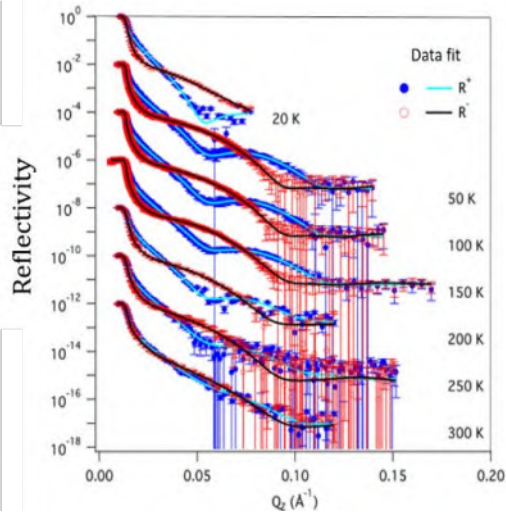
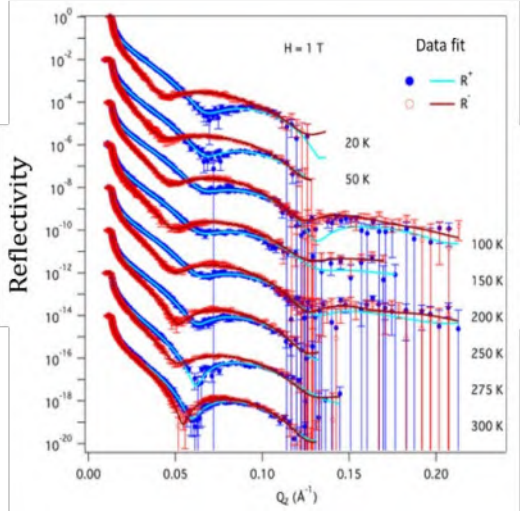
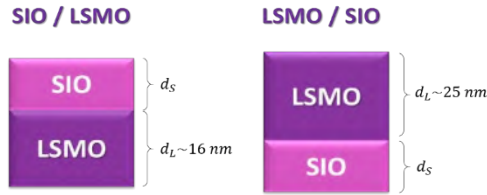
# THE is an interface effect

Topological peak at a wide range of temperature



THE absent in bilayers with inverted layer sequence

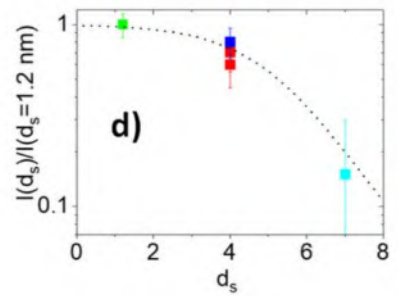
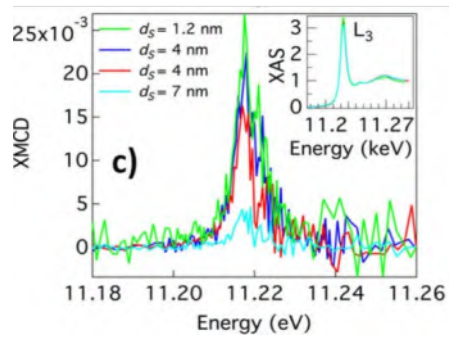
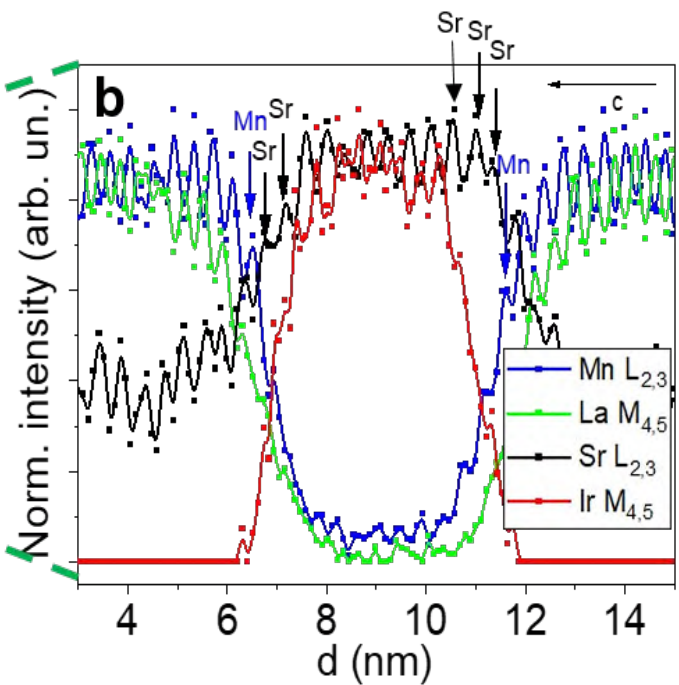
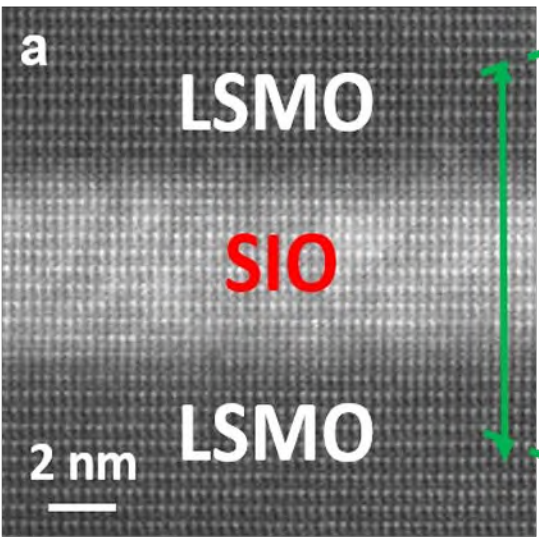
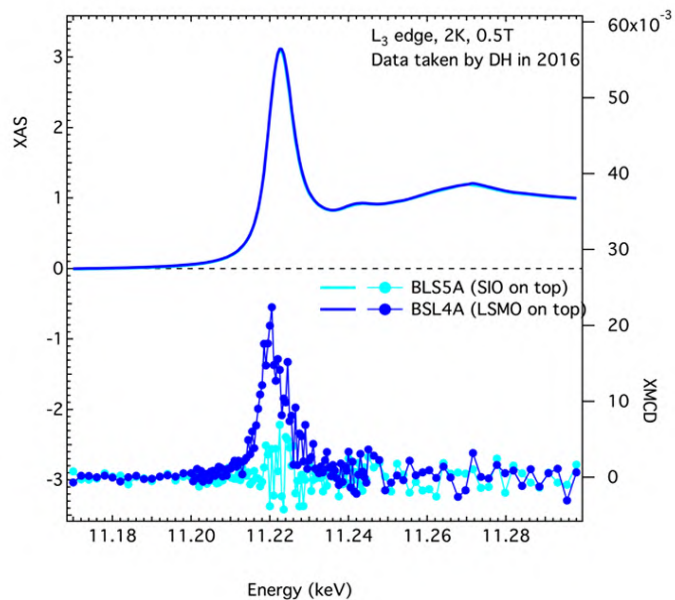




Nature Communications 12 (1), 3283 (2021)

# STEM EELS @ UCM

## M. Cabero

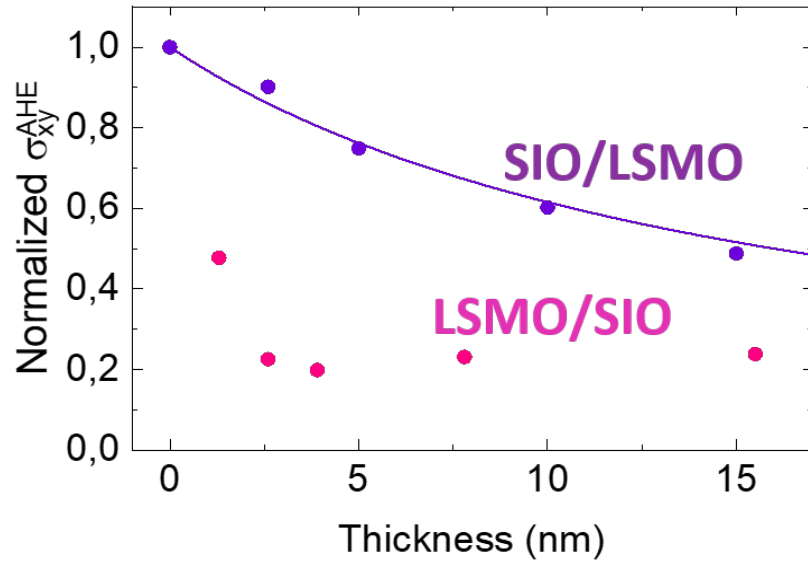
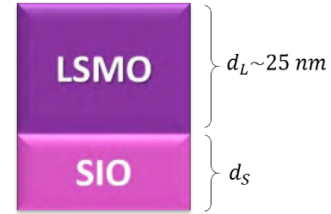


Nature Communications 12 (1), 3283 (2021)

SIO / LSMO

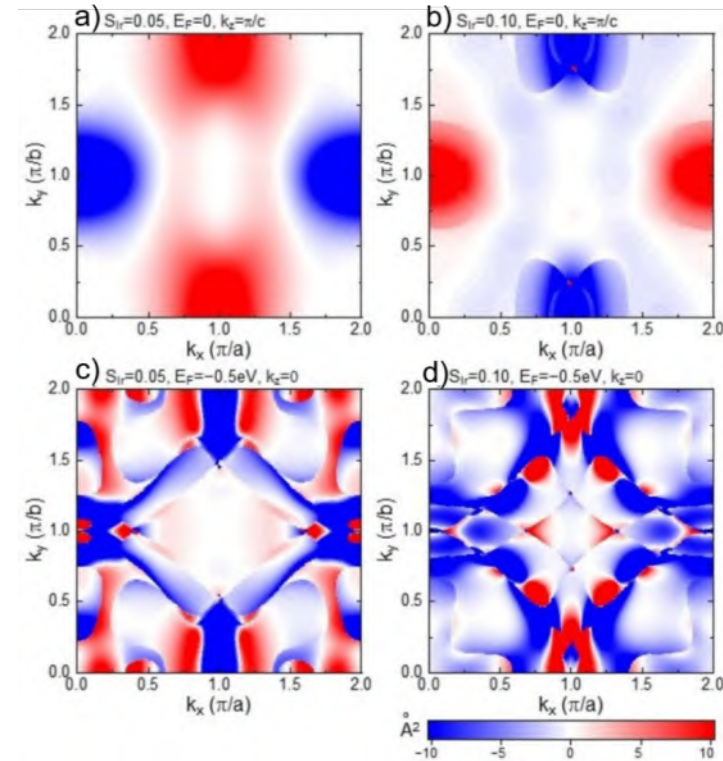


LSMO / SIO



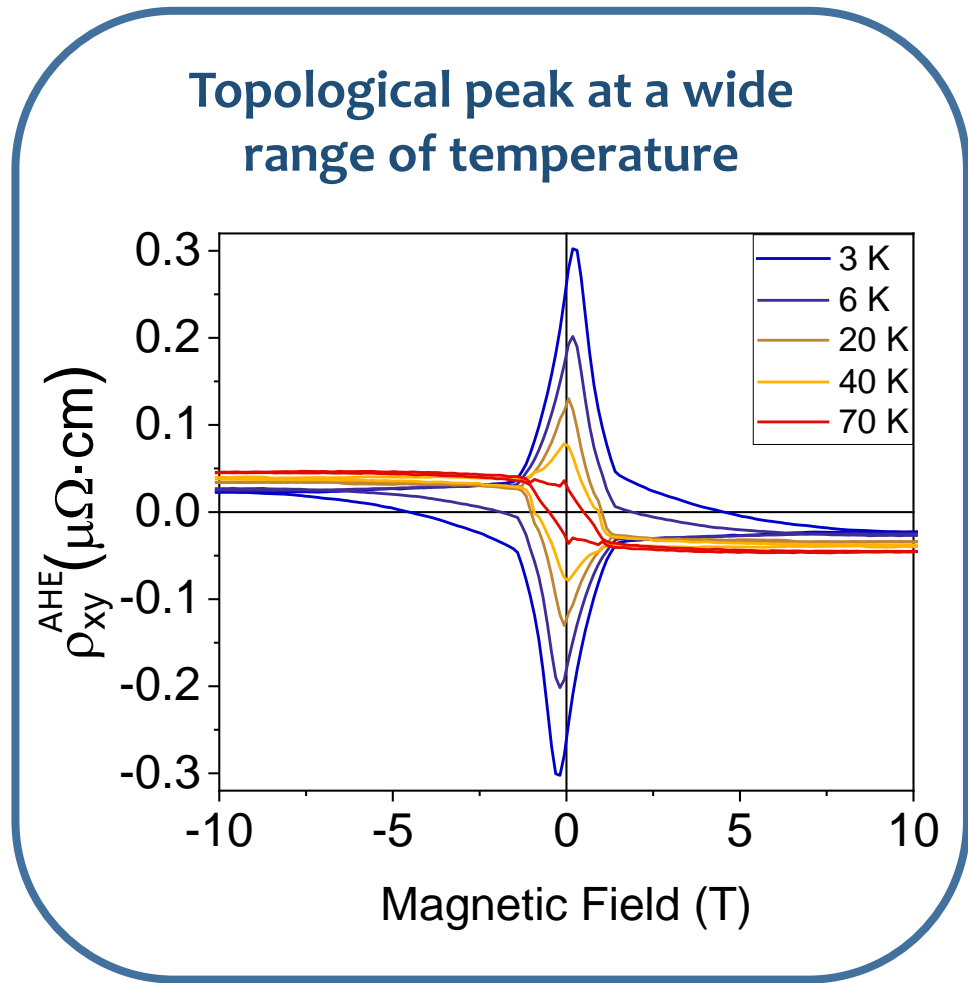
# Berry curvature

S. Okamoto, E. Dagotto @ ORNL

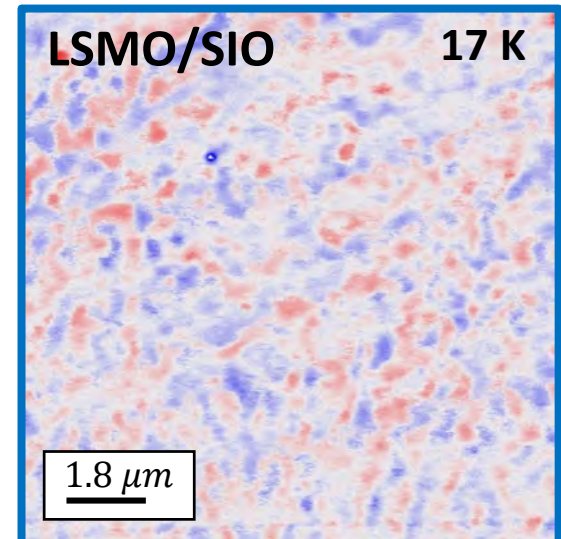
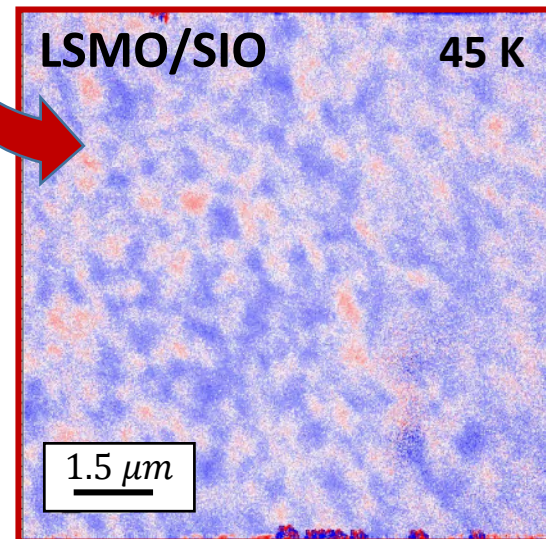
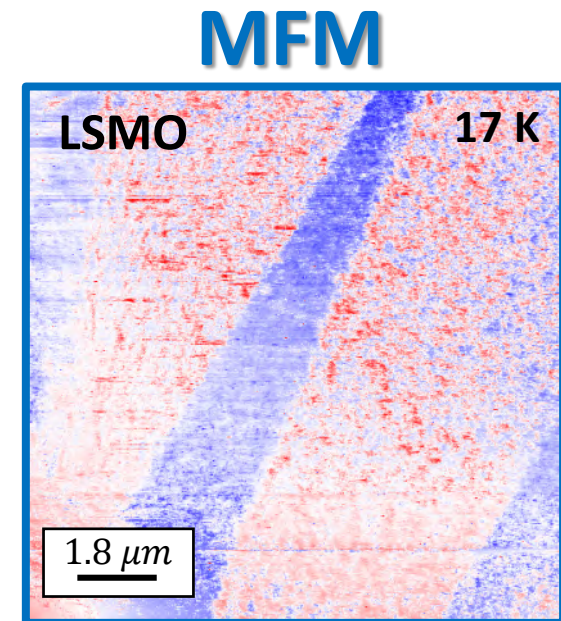
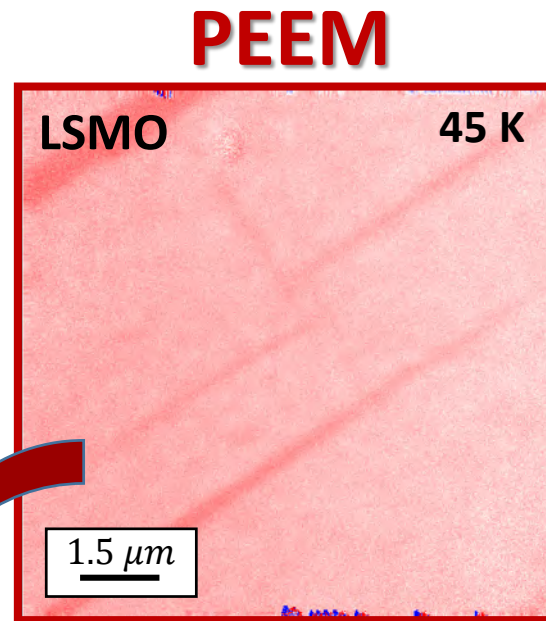


Nature Communications 12 (1), 3283 (2021)

# THE and MFM/PEEM images



Emergence of magnetic textures

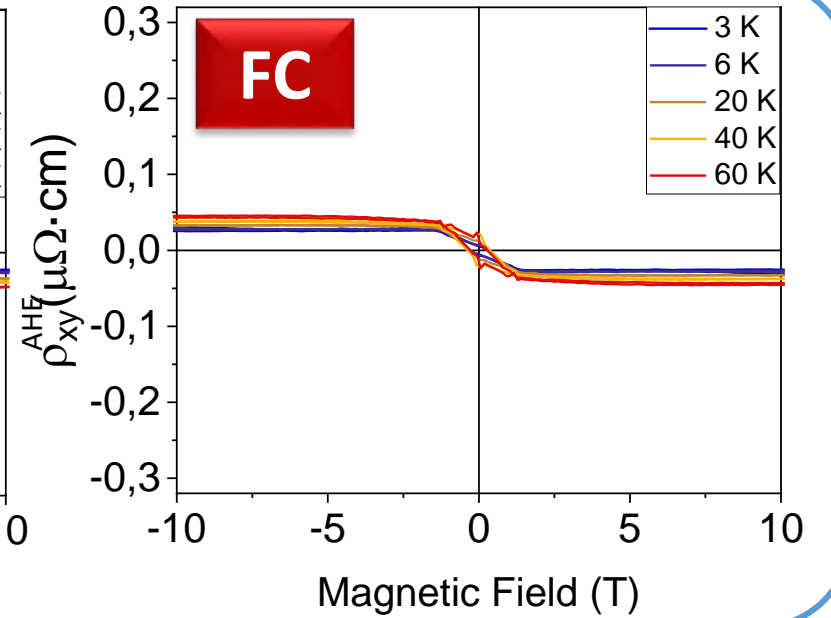
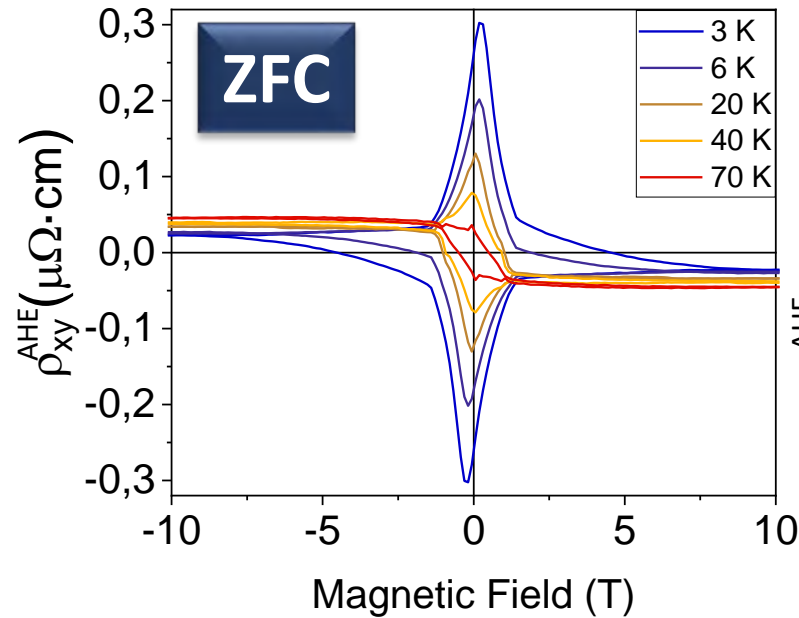


# Zero Field Cool / Field Cool

(ZFC) Zero field cooling -> Cooling from 300 K to 2 K at 0T  
(FC) Field cooling -> Cooling from 320 K to 2 K at 14T

The THE disappear after field cooling (FC)

FC -> Anomalous Hall effect expected in LSMO

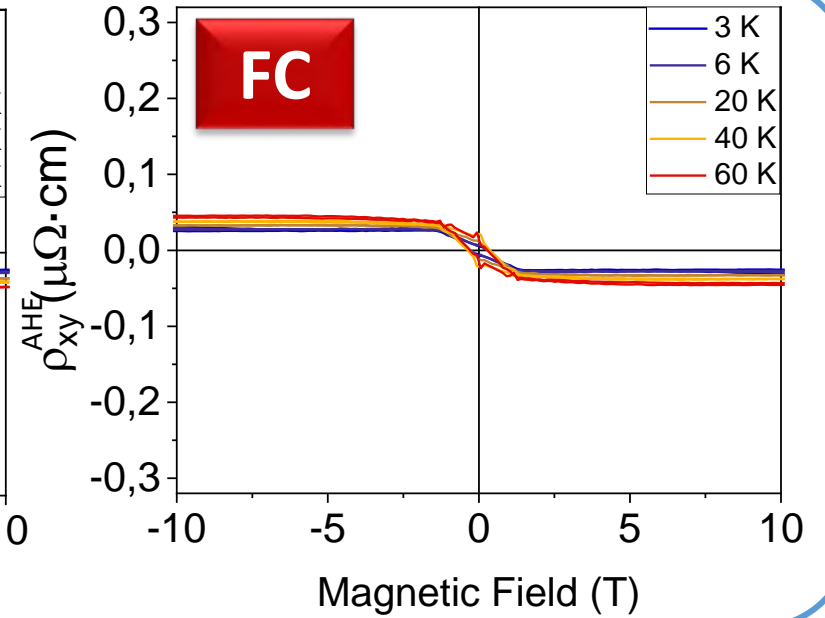
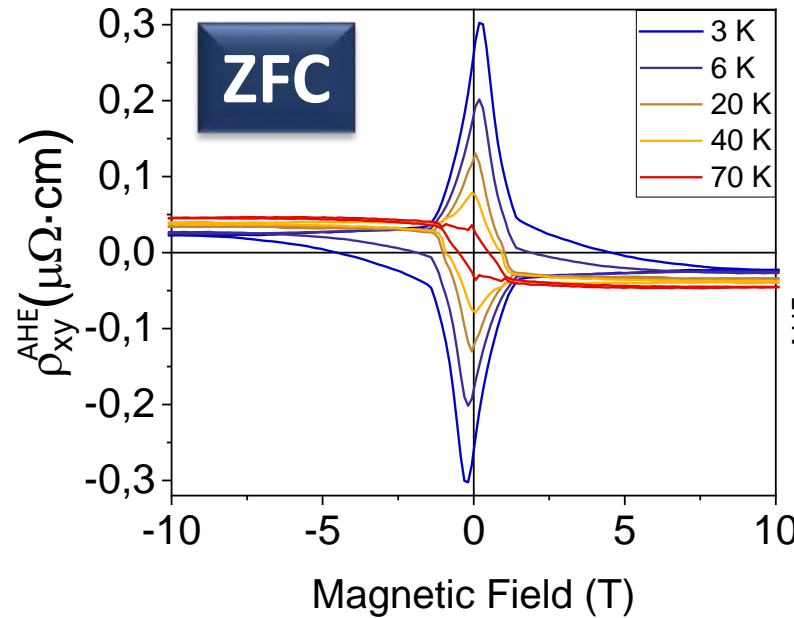


# Zero Field Cool / Field Cool

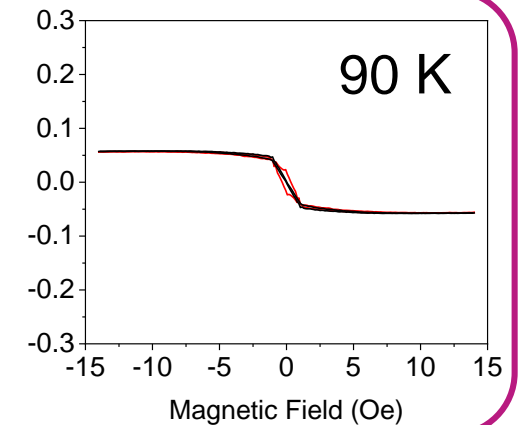
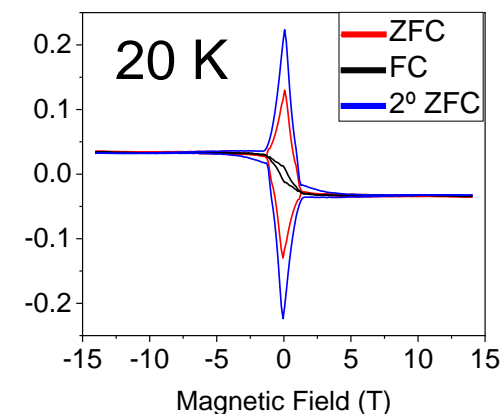
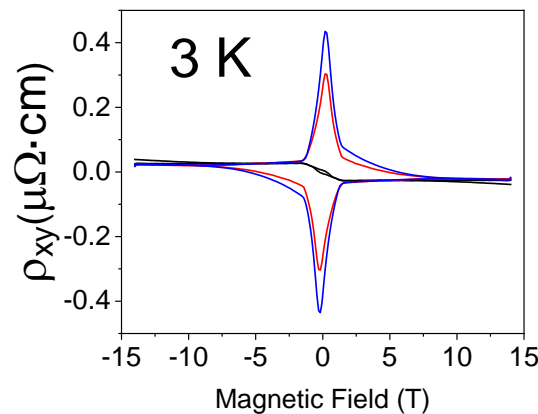
(ZFC) Zero field cooling -> Cooling from 300 K to 2 K at 0T  
(FC) Field cooling -> Cooling from 320 K to 2 K at 14T

The THE disappear after field cooling (FC)

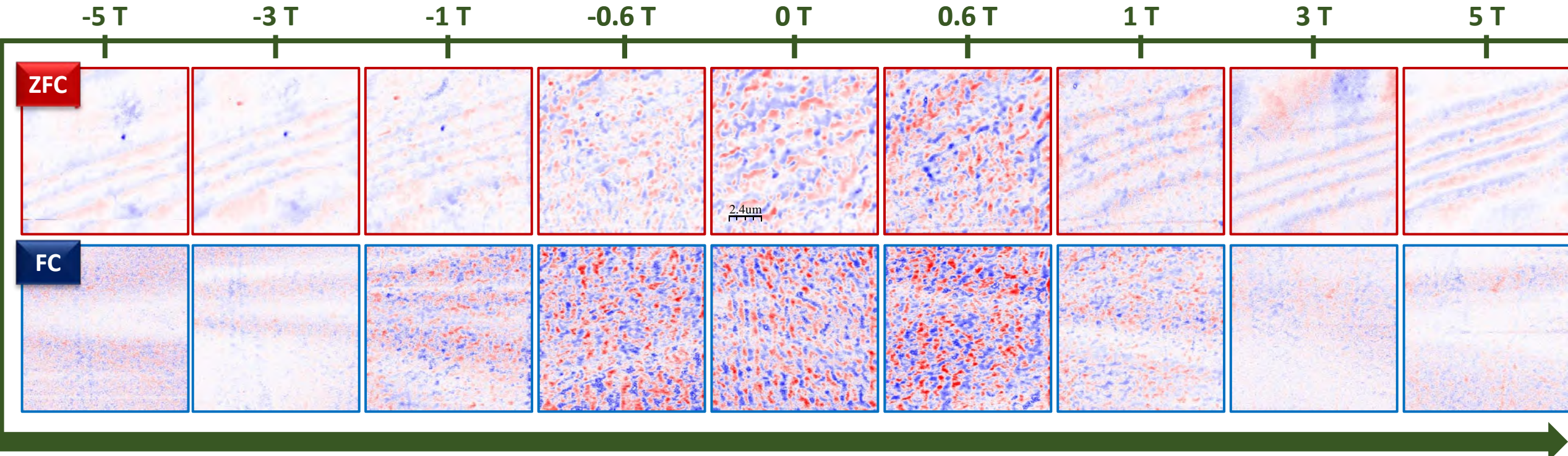
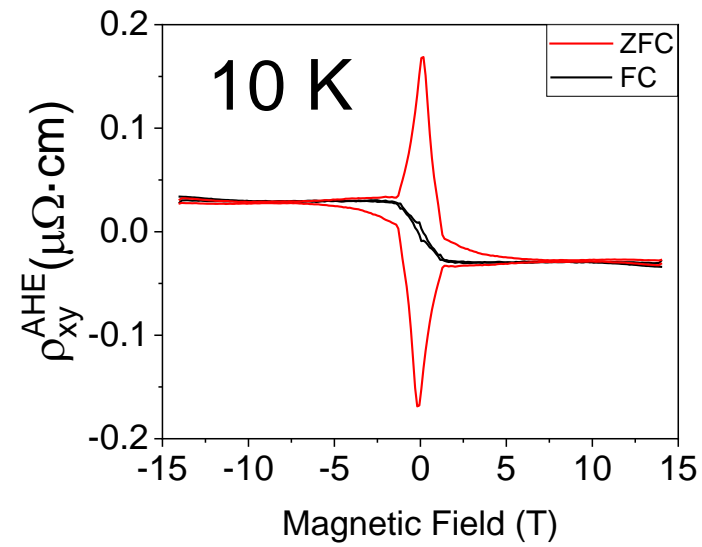
FC -> Anomalous Hall effect expected in LSMO



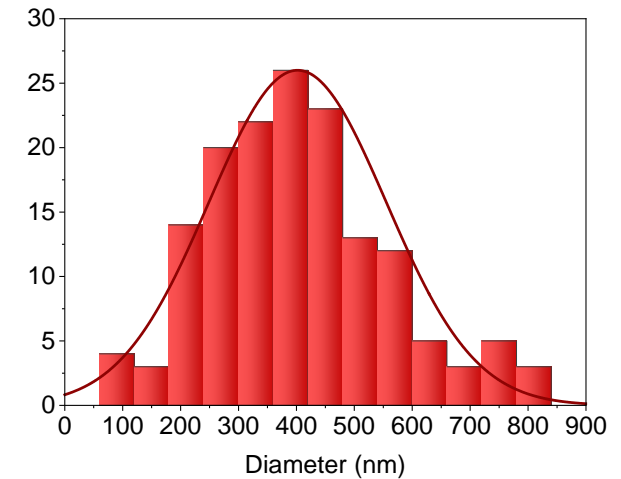
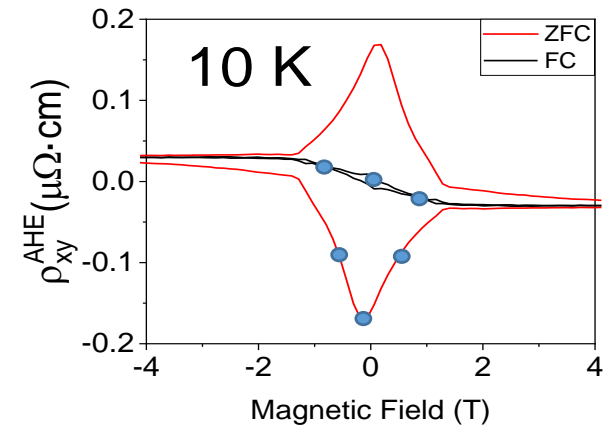
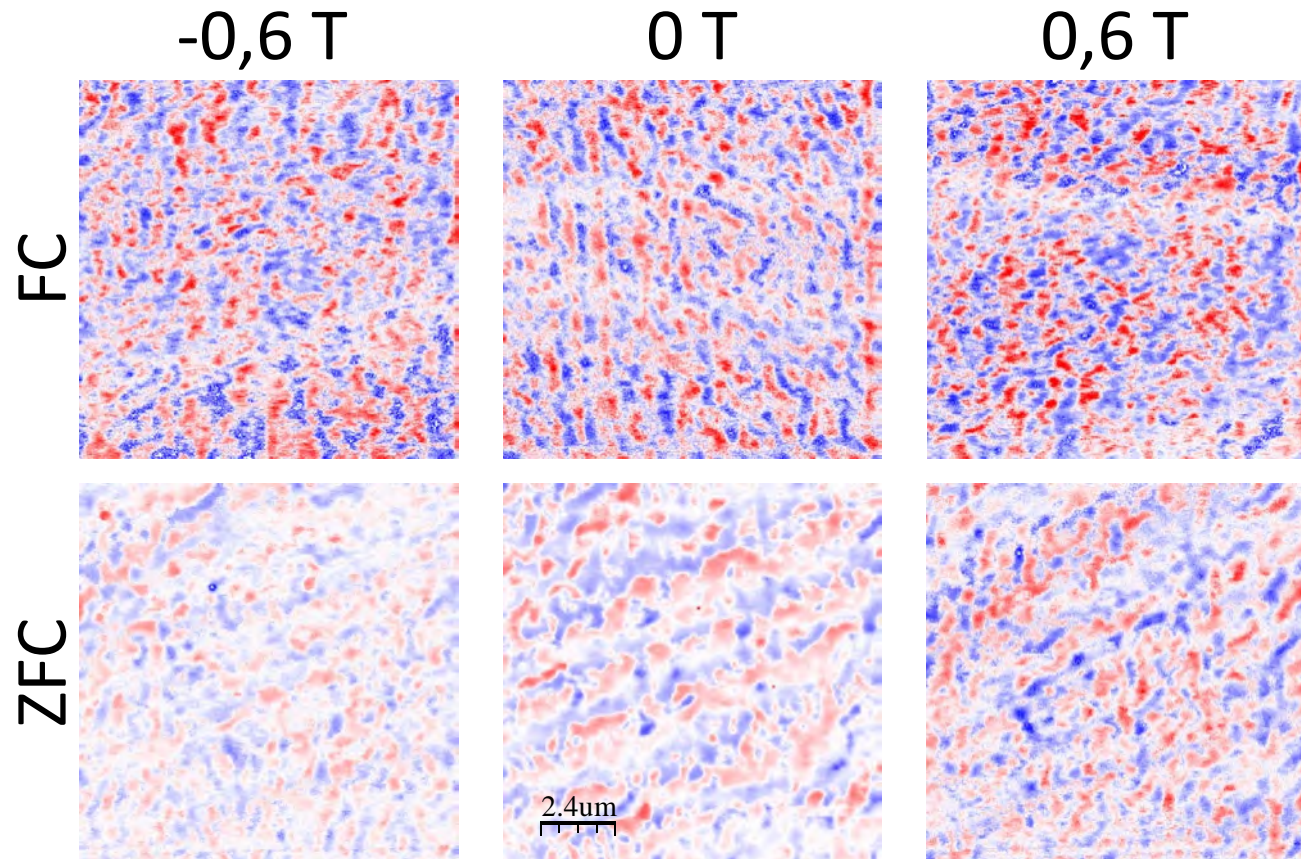
After second ZFC we recover THE



# MFM study in ZFC/FC



# MFM study in ZFC/FC: size analysis



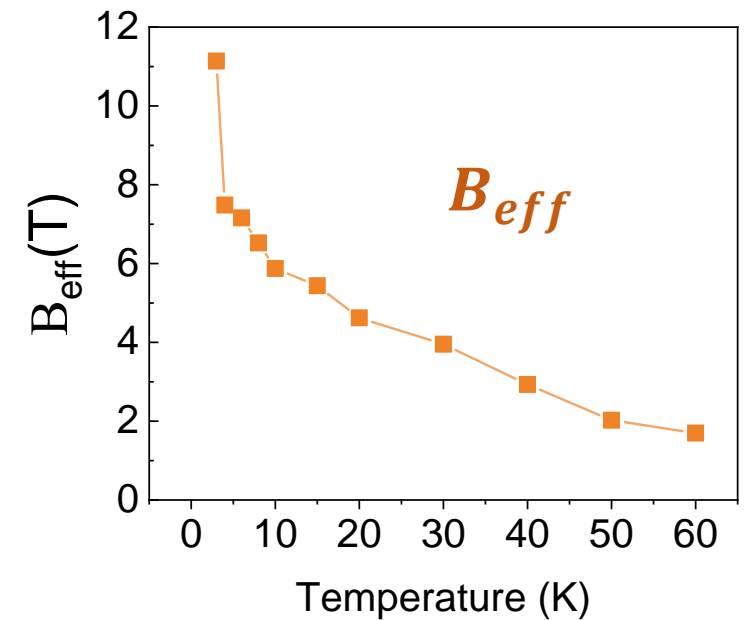
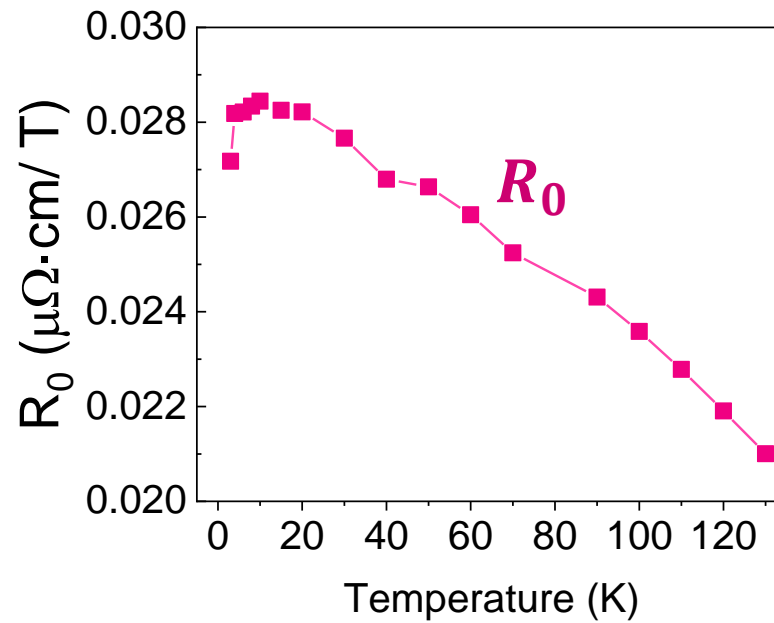
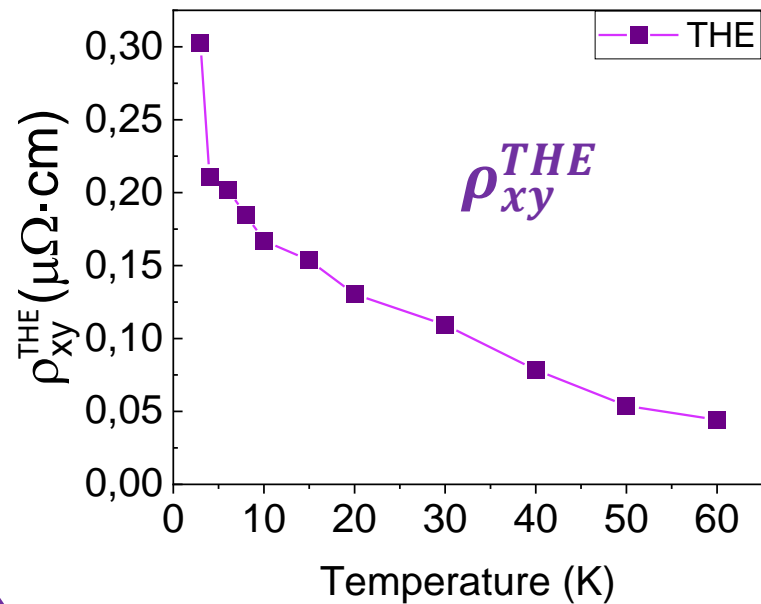
# Transport measurements

Unexpected dependence of the topological peak with the temperature

In the reported skyrmion systems, topological Hall resistivity is temperature-independent

N. Kanazawa et al. Phys. Rev. Lett. **106**, 156603 (2011)

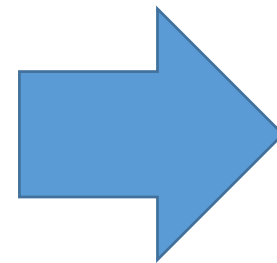
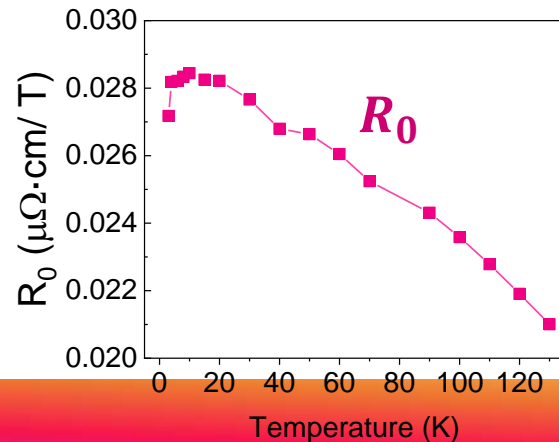
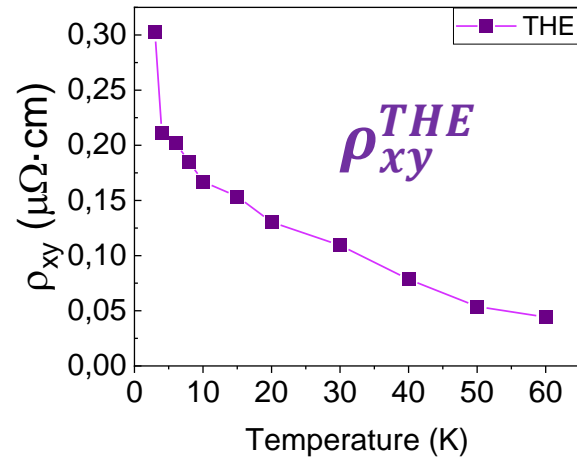
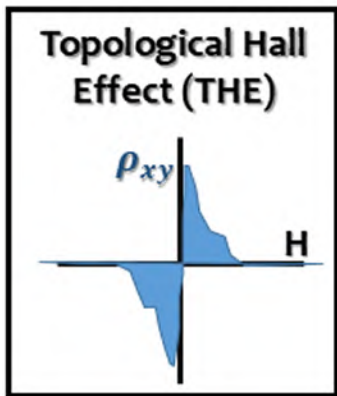
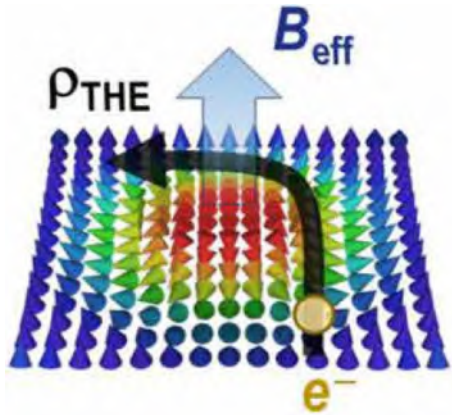
$$\rho_{xy}^{THE} = R_0 \cdot B_{eff}$$



# Skyrmion diameters estimated from THE smaller than actual (MFM) size

$$\rho_{xy}^{THE} = PR_0 B_{eff} = PR_0 n_{sk} \Phi_0$$

P. Bruno, V. K. Dugaev, M. Taillefumier, Phys. Rev. Lett. 93, (2004)

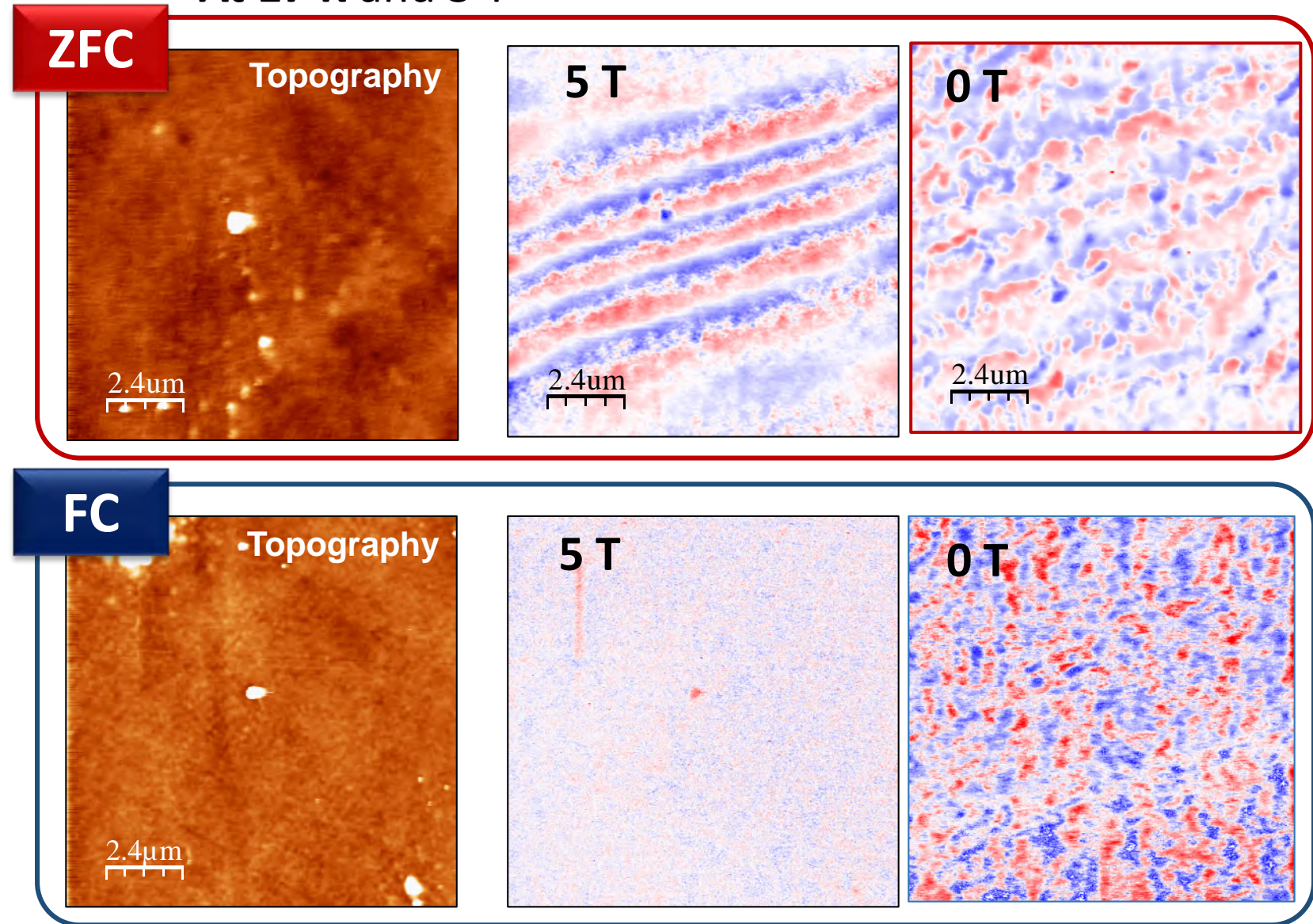
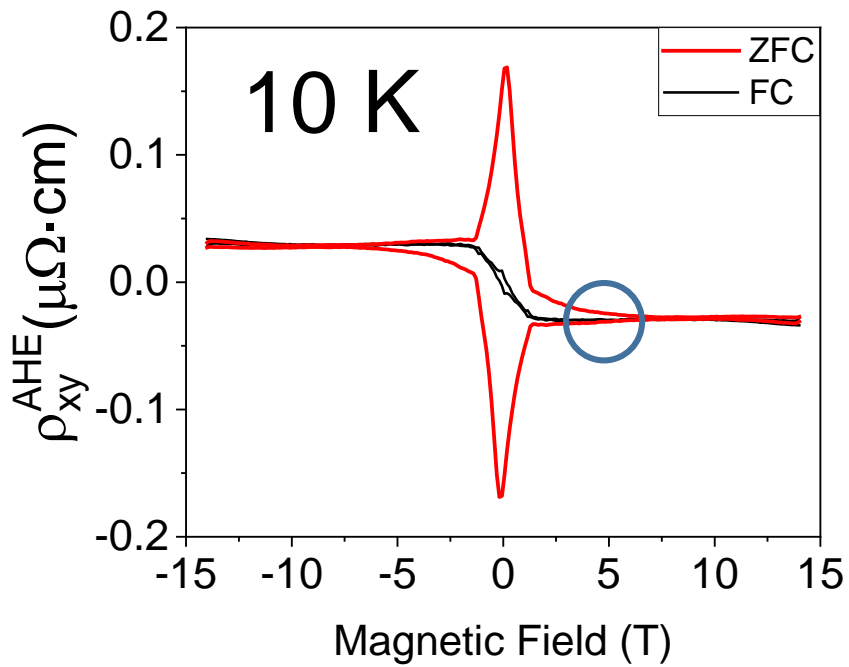


Temperature (K)	Diameter (nm)
3	18
4	22
6	23
8	24
10	25
15	26
20	28
30	31
40	36
50	43
60	47

# MFM study at ZFC/FC

## Spiral features at the origin of THE

At 17 K and 5 T



# Conclusions

- We have found a giant THE in LSMO/SIO bilayers which is tunable with magnetic history (FC/ZFC).
- We propose that the origin of THE are the magnetic textures with chiral boundaries endowed by spin spirals driven by DMI.

# General Conclusions

- TMO can be combined in highly perfect interfaces.
- Variety of different groundstates can be brought into direct contact (**oxitronic effects**): We have shown a long range Josephson effect in a half metallic ferromagnetic weak link which signals a path towards superconducting spintronics
- Spin orbit interaction of 5d oxides couples symmetry breaking electric fields to the electronic structure.
- We have shown interfacial DMI in 3d/5d heterostructures drives the nucleation of chiral domain boundaries yielding very large **THE**.